DISSERTATION

IN VITRO AND IN VIVO CHARACTERIZATION OF RAD51AP1 IN HOMOLOGOUS RECOMBINATION DNA REPAIR

Submitted by

Elena Pires

Graduate Degree Program in Cell and Molecular Biology

In partial fulfillment of the requirements

For the Degree of Doctor of Philosophy

Colorado State University

Fort Collins, Colorado

Fall 2020

Doctoral Committee:

Advisor: Claudia Wiese

Lucas Argueso
Douglas Thamm
Tingting Yao

ABSTRACT

IN VITRO AND IN VIVO CHARACTERIZATION OF RAD51AP1
IN HOMOLOGOUS RECOMBINATION DNA REPAIR

Cancer embodies a large group of diseases that is responsible for illness and deaths in millions of people annually around the world. Many tumors arise due to accumulated, unrepaired damage and alterations to genes, from endogenous or exogenous sources of DNA damage. Among the DNA lesions associated with cancer, DNA double-strand breaks (DSBs) are considered the most dangerous and require coordinated and conserved machinery to prevent unfavorable consequences, such as apoptosis and cancer-causing mutations. One crucial DNA repair pathway for mending DSBs and maintaining genome integrity is homologous recombination (HR) DNA repair. This relatively error-free mechanism employs the RAD51 recombinase and involves the joining of homologous DNA strands to restore lost DNA sequence information at the damage site. RAD51-Associated Protein 1 (RAD51AP1) is a key protein that interacts with RAD51 and stimulates its activities during HR. Nonetheless, there are knowledge gaps in understanding how this HR player functions mechanistically and *in vivo* for protection against DNA damage.

To test our overarching hypothesis that disrupted RAD51AP1 inhibits cellular and organismal protection against spontaneous or induced DNA damage, we assessed the biochemical and biological functions of RAD51AP1 through three main avenues of study: its role in the context of chromatin, the effects of its post translational modifications in cells, and the penalties of its loss in an animal system. This dissertation describes findings from these pursuits that have not been previously characterized and offers new insights into RAD51AP1's functions *in vitro* and *in vivo*.

At the start of this dissertation, our first objective was to define key attributes of RAD51AP1 in the HR reaction by further characterizing the DNA binding properties of recombinant human RAD51AP1. Using the electrophoretic mobility shift assay, we found that RAD51AP1 avidly associates with both naked and chromatinized double-stranded (ds)DNA. Deletional and mutational analyses were used to further define the chromatin-binding region in RAD51AP1, which occurs within its C-terminal DNA binding domain. Two post translational modification (PTM) sites, which undergo phosphorylation at S277 and S282 (in isoform 2) and lie within its C-terminal DNA binding region, were also evaluated and showed decreased affinity to chromatinized dsDNA. These results unveil a novel RAD51AP1 interaction with chromatin DNA.

Next, we further assessed these PTMs in regard to their impacts on RAD51AP1 function and HR capability in cells facing spontaneous or induced DNA damage. Using RAD51AP1 KO cells expressing phosphorylation mimic (S2D) or non-phosphorylatable (S2A) mutants, we found that S2D expressing cells behaved similarly to wild-type expressing cells. Notably, S2A expressing cells were significantly compromised in their growth, cell survival, cell cycle progression, and HR kinetics. The results of these studies provide an important role for PTMs that affect RAD51AP1's functions during HR.

To examine the role of RAD51AP1 in providing protection against DNA damage in an animal system, we utilized a recently available mouse knockout model to evaluate the impacts of *Rad51ap1* deletion from spontaneous DNA damage. Given the role of RAD51AP1 in meiotic HR and its high expression in murine testes, we specifically monitored fertility ratios, spermatogenesis in testes cross sections, and meiosis via synaptonemal complex formation. We found that *Rad51ap1* heterozygous mice do not breed in a Mendelian pattern. Furthermore, while synaptonemal complex formation was not impaired in *Rad51ap1* KO mice, advanced stages of

spermatogenesis were impacted, suggestive of a biological role for RAD51AP1 in maintaining the fidelity of this process.

Collectively, the results of these studies characterizing the *in vitro* and *in vivo* roles of RAD51AP1 provide new insights into this important HR player. For the first time, we reveal a new association between RAD51AP1 and chromatinized dsDNA and propose a model integrating this interaction within the HR reaction, when homology search and hetero-duplex formation after presynaptic filament formation occurs. Additionally, previously uncharacterized PTMs were assessed functionally in cells, and we unveil that the lack of these PTMs negatively impacts cells against spontaneous and induced DNA damage. Lastly, our studies on the biological effects of *Rad51ap1* loss in a recently available *Rad51ap1* KO mouse describe a novel role of *Rad51ap1*/RAD51AP1 during late spermatogenesis in an animal system for the first time. Ultimately, by understanding the mechanisms and biology of this important HR protein, this knowledge can guide the optimization of treatments for cancers that exploit DNA repair factors as well as help us comprehend how this factor protects against DNA damage in mammals.

ACKNOWLEDGEMENTS

I would first like to express my sincere appreciation to my advisor Dr. Claudia Wiese, for funding this research and for making me into the scientist that I have become over the past 4.5 years. It has been quite an honor to be in her lab. This thesis was also made successful with many thanks to my labmates (past and present) Drs. Neelam Sharma and David Maranon, Platon, Noelia, Mollie, and Kriti, for their support and enthusiasm while working alongside me on research projects. I would like to extend my gratitude to my committee members Drs. Lucas Argueso, Doug Thamm, and Tingting Yao, for their valuable time and constructive feedback. Many thanks also to the combined DVM/PhD program for financial support as well as guidance from Drs. Ed Hoover, Sue VandeWoude, Justin Lee, and Dan Regan. Due to their leadership as well as the comradeships with other students in the DVM/PhD program, I have always felt welcome and at home.

Additionally, I'd like to extend my gratitude towards several significant people outside of the CSU community. To my friends (local and across the states), I am thankful for their affection and provision of creative outlets outside of work. To my "salsa family", the Fort Collins Salsa Collective, I am thankful for the confidence gained through dance and for their constant moral support. Exercise through dance really does boost work performance and maintained my spirits.

Finally, I want to acknowledge the cats who "adopted" me during this program, for their comical relief and company (during quarantine) as I wrote my dissertation: Avo and Middz. Lastly and most importantly, I would like to pay special regards to my devoted partner, Troy Cabral, and to my family, most especially my mother Rossana Gumiel-Pires and my brother, Armando Pires, for their constant love, encouragement, and belief in my ability to succeed. My achievements are their achievements, and all the opportunities and experiences I've had are truly thanks to them.

TABLE OF CONTENTS

LIST OF TABLES

LIST OF FIGURES

LIST OF ACRONYMS

BSA	Bovine Serum Albumin
DAPI	4’,6-diamidino-2-phenylindole
DNA	deoxyribonucleoside acid
DSB	Double Strand Break
EMSA	Electrophoretic Mobility Shift Assay
γH2AX	phosphorylated histone subtype H2A isoform X
H&E	Hematoxylin and Eosin
HR	Homologous Recombination
IHC	Immunohistochemistry
IF	Immunofluorescence
IR	Ionizing Radiation
KO	Knockout
MEM	Minimum Essential Media
MMC	Mitomycin C
NCP	Nucleosome Core Particle
PCR	Polymerase Chain Reaction
PFA	Paraformaldehyde
PVDF	Polyvinylidene Difluoride
RAD51AP1	RAD51-associated Protein 1
SCP3	Synaptonemal Complex Protein 3
WT	Wild Type

CHAPTER ONE

Introduction[1]

Summary

The number of cancer diagnoses and deaths due to cancer every year highlights the urgent call for research into its mechanisms and potential therapeutic avenues. The main source of cancer is DNA mutation and loss of genome integrity due to DNA damage. DNA repair mechanisms serve to repair DNA damage and are essential for maintaining genome stability and tumor suppression. DNA repair capacity also determines the efficacy of anticancer therapy. Hence, there is a pressing need to better understand the mechanisms and proteins involved in DNA repair pathways. An emerging player that is critical for homologous recombination (HR) DNA repair is RAD51-associated protein 1 (RAD51AP1). Although much has been learned about the biochemical attributes of this RAD51- and DMC1-interacting protein, the precise molecular role of RAD51AP1 in HR DNA repair is not yet fully understood.

The goal of this introduction is to provide an overview of RAD51AP1, describing its discovery twenty years ago and elaborating on its biochemical profile and biological function, as comprehended so far. This introduction will also provide insights as to how the RAD51AP1 protein may promote cancer development and why it may be a promising new target for therapeutic intervention. This chapter will conclude with the objectives for this thesis about RAD51AP1 as well as elaborate on the specific aims testing the central hypothesis.

---

[1]*This chapter is an adaptation of previously published material. Reference for the full article:* **Pires, E.**, Sung, P., and Wiese, C. 2017 Role of RAD51AP1 in homologous recombination DNA repair. DNA Repair (Amst.) (59) 76-81.

I. The global burden of cancer

Cancer remains one of the leading causes of illness and death worldwide, with approximately 1.8 million new cases projected for 2020 in the United States alone (data by the North American Association of Cancer Registries). The root cause of cancer and many other diseases is DNA mutation and loss of genome integrity. Both can result from DNA lesions of which the DNA double-strand break (DSB) is considered the most deleterious. DSBs are induced exogenously from e.g. exposure to ionizing radiation (IR) or by endogenous sources including reactive oxygen species (ROS) generated during cellular metabolism (SHRIVASTAV *et al*. 2008).

II. DNA repair processes for protection against cancer

Cells respond to DSBs via DNA damage response pathways that activate DNA damage checkpoints and DNA damage repair mechanisms. One such pathway for mending DSBs efficiently is homologous recombination DNA repair (HR), a highly conserved process critical for tumor suppression. In the HR reaction, a homologous template DNA sequence is engaged, allowing for the faithful restoration of lost sequence information at the break site (DALEY *et al*. 2013 and 2014).

HR is catalyzed by the RAD51 recombinase (RICHARDSON 2005), which forms a nucleoprotein filament on resected single-stranded DNA (ssDNA) at the damage site. The RAD51-ssDNA nucleoprotein filament, also called the presynaptic filament, captures duplex DNA and generates a displacement loop (D-loop) upon location of a homologous DNA target. Subsequent DNA synthesis and resolution completes HR DNA repair (MOYNAHAN and JASIN 2010). The repair process requires many mediator proteins that ensure the efficiency of RAD51-ssDNA filament assembly and filament stability; key HR mediators include the human breast cancer

susceptibility gene products BRCA1, BRCA2, and PALB2, and the acidic protein DSS1 (ZHAO *et al*. 2015; MIZUTA *et al*. 1997; DAVIES *et al*. 2001; MOYNAHAN *et al*. 2001a and 2001b; CHEN *et al*. 1998 and 1999; XIA *et al*. 2006). Emerging evidence suggests that these HR mediators may also enhance the activity of the RAD51-related meiotic recombinase DMC1.

III. Role of RAD51AP1 in homologous recombination DNA repair

Besides the aforementioned HR proteins, a key protein that is critical for HR downstream of RAD51 filament formation is RAD51-associated protein 1 (RAD51AP1) (MIZUTA *et al*. 1997; KOVALENKO *et al*. 1997; WIESE *et al*. 2007; MODESTI *et al*. 2007). Much has been learned about the biochemical attributes of this RAD51- and DMC1-interacting protein since its discovery in 1997 (MIZUTA *et al*. 1997; KOVALENKO *et al*. 1997). However, much remains to be learned about the molecular role of RAD51AP1 in the HR reaction, and its impact on cancer initiation and progression remains to be elucidated. Here, we revisit the discovery of RAD51AP1 and review the current understanding of the biochemical and biological functions of this HR factor. We also discuss our view regarding how RAD51AP1 may help to promote cancer development and potentially be a promising new target for therapeutic intervention.

A. Attributes of the RAD51AP1 protein

A.1. Discovery of RAD51AP1 as a RAD51-interacting protein

RAD51AP1 was discovered in 1997 as a RAD51-interacting protein using the yeast two-hybrid (Y2H) system and was originally termed Pir51 and RAB22 for the human and mouse proteins, respectively (MIZUTA *et al*. 1997; KOVALENKO *et al*. 1997). In the Y2H system and in co-immunoprecipitation experiments, RAD51AP1 was shown to interact with RAD51 with high

affinity (MIZUTA *et al*. 1997; KOVALENKO *et al*. 1997; HENSON *et al*. 2006). Follow-up work led to mapping of the RAD51-binding domain onto the C-terminal 26 residues of RAD51AP1 (WIESE *et al*. 2007; MODESTI *et al*. 2007; KOVALENKO *et al*. 2006). Consistent with its role in HR DNA repair, RAD51AP1 foci were shown to co-localize with RAD51 foci spontaneously and after DNA damage induction in CHO-K1 and human cells (MIZUTA *et al*. 1997; WIESE *et al*. 2007; MODESTI *et al*. 2007; OBAMA *et al*. 2008).

The human *RAD51AP1* gene was mapped to chromosome 12p13.1 –13.2 (KOVALENKO *et al*. 1997), a region that shows homology with the distal portion of mouse chromosome 6 and that includes the mouse *Rad51ap1* gene (MIZUTA *et al*. 1997). The RAD51AP1 protein is highly conserved among vertebrates (PARPLYS *et al*. 2014). However, RAD51AP1 orthologs also exist in a number of invertebrates but are absent in model organisms including *D. melanogaster*, *C. elegans*, and *S. cerevisiae* (PARPLYS *et al*. 2014).

The tissue-specific distribution of the human RAD51AP1 transcript is similar to that of RAD51, BRCA1, and BRCA2, being the highest in thymus, bone marrow, spleen, and testis (OBAMA *et al*. 2008), which correlates well with what has been observed in mice (MIZUTA *et al*. 1997). This expression pattern is consistent with a key role of RAD51AP1 and HR in the mitigation of spontaneous DNA damage in proliferating cells. Of the four RAD51AP1 splice variants, two have been shown to code for a functional protein (http://www.proteinatlas.org/). Isoform 1 and isoform 2 are 352 and 335 amino acids in length, respectively, and hydrophilic with a third of their overall composition as aspartic acid, arginine, glutamic acid, and lysine residues (KOVALENKO *et al*. 1997; PARPLYS *et al*. 2014). Both isoforms behave similarly in cell-based and biochemical assays designed to assess HR capacity (WIESE *et al*. 2007; MODESTI *et al*. 2007; DRAY *et al*. 2011; DUNLOP *et al*. 2011 and 2012).

A.2. DNA-binding and HR activity of RAD51AP1

RAD51AP1 binds ssDNA and double-stranded DNA (dsDNA), with a preference for the latter species (KOVALENKO *et al*. 1997; WIESE *et al*. 2007; MODESTI *et al*. 2007). However, RAD51AP1 has the highest affinity for branched DNA substrates and the D-loop, indicative of a role in the formation of DNA intermediates in the HR reaction (WIESE *et al*. 2007; MODESTI *et al*. 2007; PARPLYS *et al*. 2014 and 2015; DUNLOP *et al*. 2012; DRAY *et al*. 2010). Via its DNA binding attribute, RAD51AP1 stimulates the RAD51-mediated D-loop reaction in amounts sub-stoichiometric to that of RAD51 (WIESE *et al*. 2007; MODESTI *et al*. 2007). RAD51AP1 possesses two distinct DNA-binding domains, with one being located within the N-terminal region and the other residing near the C-terminus of the protein (MODESTI *et al*. 2007; DUNLOP *et al*. 2012). Both domains are required for the full activity of RAD51AP1 in protecting cells from DNA damaging agents and in promoting D-loop formation by RAD51 (DUNLOP *et al*. 2012).

In the D-loop reaction, the RAD51 presynaptic filament engages with a dsDNA partner molecule to conduct homology search and synaptic complex formation, in which homologous DNA sequences are aligned to allow for base switching (GUPTA *et al*. 1999; SUNG *et al*. 2003). Interestingly, C-terminally truncated RAD51AP1 (ΔC26) and variants of RAD51AP1 with mutations within the last 26 residues are impaired for RAD51 interaction and for the ability to stimulate D-loop formation (WIESE *et al*. 2007; MODESTI *et al*. 2007; KOVALENKO *et al*. 2006). We surmise that RAD51AP1 bridges the incoming duplex DNA with the presynaptic filament (**Figure 1.1A**), and it is interesting to note that human RAD51AP1 has an elongated configuration, as determined by sedimentation equilibrium and electrospray experiments (MODESTI *et al*. 2007). More mechanistic work will be needed to delineate the spatial and temporal organization of

RAD51AP1 in relation to the presynaptic filament during the duplex engagement, homology search and joint molecule formation steps in the HR reaction.

A.3. RAD51AP1-interacting proteins

PALB2 (Partner and Localizer of BRCA2), a tumor suppressor that assists the recombination mediator BRCA2 in the presynaptic stage of HR (XIA *et al*. 2006), interacts with the N-terminal region of RAD51AP1 (**Figure 1.1B**). PALB2 functions cooperatively with RAD51AP1 in enhancing the recombinase function of RAD51 in the D-loop reaction and during synaptic complex formation (DRAY *et al*. 2010). In spite of the fact that PALB2 and RAD51AP1 can individually promote RAD51-mediated DNA strand invasion, their synergy in this reaction speaks to the intricate crosstalk among the proteins that function in this highly regulated step of HR. Although PALB2-deficient human fibroblasts express RAD51AP1 protein, they cannot assemble RAD51AP1 foci upon treatment with the DNA crosslinking agent mitomycin C (MMC) (DRAY *et al.* 2010), in support of the key role of PALB2 in the recruitment of RAD51AP1 to DNA damage.

In a large-scale proteomic screen (SOWA *et al*. 2009), UAF1-USP1, a complex responsible for the deubiquitylation of mono-ubiquitylated FANCD2 (NIJMAN *et al*. 2005; COHN *et al*. 2007), was found to associate with RAD51AP1. Additionally, the DNA binding activities of UAF1 and RAD51AP1 were shown to be important for FANCD2 deubiquitylation and synaptic complex formation (LIANG et al. 2019 and 2020). A small ubiquitin-like modifier (SUMO)-interacting motif (SIM) in RAD51AP1 (**Figure 1.1B**) was identified and shown to associate with two SUMO-like domains (SLDs) in UAF1 (LIANG *et al*. 2016). RAD51AP1 and UAF1 act synergistically in RAD51-mediated synaptic complex and D-loop formation assays (LIANG *et al*. 2016). Together,

these results have uncovered an association among RAD51AP1, UAF1, and RAD51 at the synaptic stage of HR and suggest the possibility that RAD51AP1 may represent yet another Fanconi Anemia (FA) gene (LIANG *et al*. 2016) that could function downstream (WIESE *et al*. 2007) of FANCD2 mono-ubiquitylation. Both USP1 and UAF1 affect the intracellular stability of RAD51AP1, which appears to be degraded by the proteasome (CUKRAS *et al*. 2016). Cells expressing mutant versions of RAD51AP1 or UAF1 that are compromised for complex formation are hypersensitive to various genotoxic agents including MMC, the topoisomerase I inhibitor camptothecin, and the PARP inhibitor olaparib, and are also impaired for HR (LIANG *et al*. 2016; CUKRAS *et al*. 2016). Similarly, inhibition of the RAD51AP1-UAF1 interaction by viral non structural protein 5A also leads to defective HR in HCV-infected cells (NGUYEN *et al.* 2018). GFP-tagged RAD51AP1 was shown to interact with DNA Ligase 3, PARP1, and the topoisomerases TOP2A and TOP2B in a recent proteomic analysis (WAGNER *et al*. 2016). However, the significance of these interactions remains to be elucidated.

Interestingly, RAD51AP1 also interacts with the meiotic recombinase DMC1 and, similar to its activating ability on RAD51, exerts stimulatory effects on DMC1-mediated duplex DNA engagement, synaptic complex assembly, and D-loop formation (DRAY *et al*. 2011). As with RAD51AP1 and RAD51 (WIESE *et al*. 2007; MODESTI *et al*. 2007), the stimulatory effect of RAD51AP1 on DMC1 is dependent on their physical interaction. In support of the biochemical data, RAD51AP1 co-localizes with a subset of DMC1 foci on meiotic chromatin in mouse spermatocytes (DRAY *et al*. 2011). The DMC1-RAD51AP1 interaction is facilitated by a C-terminal, conserved peptide motif in RAD51AP1 (WVPP), reminiscent of the DMC1-interacting FVPP motif in BRCA2 (THORSLUND *et al*. 2007), which lies directly downstream of RAD51AP1′s C-terminal DNA binding region and does not overlap with its RAD51 interaction domain (DRAY

et al. 2011; DUNLOP *et al*. 2011 and 2012) (**Figure 1.1B**). Consequently, mutant versions of RAD51AP1 that have lost their ability to interact with RAD51 are proficient for DMC1 association (DRAY *et al*. 2011), supporting the notion that in addition to its role in mitotic DSB repair, RAD51AP1 also serves a distinct function in meiotic HR.

A.4. Homology between RAD51AP1 and other proteins

RAD51AP1 shares extensive (28% identical and 11% similar) sequence homology with the NUCKS1 (Nuclear Casein Kinase and Cyclin- dependent Kinase Substrate 1) protein, indicating that these proteins are paralogs (PARPLYS *et al*. 2015). NUCKS1, however, does not harbor any sequence that resembles the RAD51AP1 C-terminal RAD51 interaction domain. Consistent with this observation, NUCKS1 and RAD51 do not physically interact (PARPLYS *et al*. 2015).

The vertebrate-specific RAD51-Associated Protein 2 (RAD51AP2), which is expressed in meiotic tissues only, shares the conserved RAD51 interaction domain found in RAD51AP1 (KOVALENKO *et al*. 2006). However, aside from the RAD51 interaction domain, RAD51AP1 and RAD51AP2 share no further regions of homology (KOVALENKO *et al*. 2006).

A.5. RAD51AP1 protects against DNA damage

In mitotic cells, RAD51AP1 activates the RAD51 recombinase and promotes the repair of DSBs by HR (KOVALENKO *et al*. 1997; WIESE *et al*. 2007; MODESTI *et al*. 2007). Knockdown of RAD51AP1 in human cells or deletion of *Rad51ap1* in chicken DT40 cells increases their sensitivity to the cytotoxic effects of DNA cross-linking agents and to IR (WIESE *et al*. 2007; MODESTI *et al*. 2007; HENSON *et al*. 2006; PARPLYS *et al*. 2014). Knockdown of RAD51AP1 also

leads to increased levels of genome instability and decreased homology-directed repair (WIESE *et al.* 2007; MODESTI *et al*. 2007). Similarly, knockdown of RAD51AP1 in alternative lengthening of telomeres (ALT)-positive cells increased telomere fragility via impaired telomere HR repair, and subsequent addition of RAD51AP1 in RAD51AP1 KO ALT-positive cells rescued telomere length (BARROSO-GONZALEZ *et al.* 2019). Taken together, these findings support the important role of RAD51AP1 in HR DNA repair and in maintaining genome stability.

Several studies investigated if RAD51AP1 expression is altered in response to DNA damaging agents or cell cycle stage in several different cell lines, including HeLa cells, mouse lymphoma cells, human melanocytes, EKT-1 cholangiosarcoma cells, HCT116 cells, and T24 bladder carcinoma cells. Results of these studies show that the RAD51AP1 protein and transcript are regulated in a cell cycle-specific manner, are expressed at higher levels in proliferating cells, and are induced upon exposure to HU or IR (HENSON *et al*. 2006; MULLER *et al*. 2005; FANG *et al*. 2013; OBAMA *et al*. 2008; IWANAGA *et al*. 2006).

A.6. RAD51AP1 maintains replication fork stability

The protection of DNA replication forks and the repair of damaged replication forks are essential for genome stability and cancer avoidance, and the slowing of replication fork progression, commonly referred to as replication stress, has emerged as a significant source of genome instability during early stages of carcinogenesis (HALAZONETIS *et al*. 2008; BARTKOVA *et al*. 2005; GAILLARD *et al*. 2015). Besides ROS-induced DNA-damage, replication stress can result from a variety of other sources, such as nucleotide depletion, conflicts between DNA replication and transcription, and oncogene activation leading to accelerated cell division.

Hormonal signaling and inflammatory processes may exert a similar effect as oncogene activation by coercing cells to undergo high levels of transcription (TUBBS *et al*. 2017).

As demonstrated in DNA combing experiments, loss of RAD51AP1 leads to slowing of DNA replication fork progression and elevated DNA replication stress (PARPLYS *et al*. 2014 and 2015). To resolve these replication abnormalities, RAD51AP1-deficient cells increase their usage of replication origins whereby the timely completion of DNA replication is ensured and further replication stress is minimized (PARPLYS *et al*. 2014 and 2015). These results show that RAD51AP1 is required for replication fork stability and the avoidance of replication stress. These results also may explain why RAD51AP1 transcript and protein increase upon exposure of cells to HU and IR (HENSON *et al*. 2006; OBAMA *et al*. 2008; MULLER *et al*. 2005; FANG *et al*. 2013; GROTH *et al*. 2012).

The cellular response to replication stress is mediated by the Ataxia Telangiectasia and Rad3-related kinase (ATR) which activates the intra S-phase checkpoint (ZEMAN *et al*. 2014). In a quantitative proteomic study to define cellular signaling after replication stress, RAD51AP1 was discovered as a putative target of ATR (WAGNER *et al*. 2016). RAD51AP1 S120 (in isoform 1; **Figure 1.2**) is phosphorylated by ATR upon nucleotide depletion (WAGNER *et al*. 2016), providing more evidence for a role of RAD51AP1 in the replication stress response. To gain further insights into the function of RAD51AP1 during replication stress, Wagner et al. (WAGNER *et al*. 2016) also analyzed the interaction partners of RAD51AP1 after short-term HU treatment. In line with other findings (LIANG *et al*. 2016; SOWA *et al*. 2009; CUKRAS *et al*. 2016), Wagner et al. (WAGNER *et al*. 2016) showed that RAD51AP1 interacts with UAF1-USP1, but also with USP7 and USP11, highlighting important roles in the cellular response to DNA damage and DNA replication stress

(NIJMAN *et al*. 2005; FAUSTRUP *et al*. 2009; ALONSO-DE VEGA *et al*. 2014; WILTSHIRE *et al*. 2010).

A.7. Post translational modifications of RAD51AP1

Further proteomic studies identified RAD51AP1 S120 as a target of ATR or ATM (Ataxia Telangiectasia Mutated serine/threonine-protein kinase) following exposure of 293T cells to IR (MATSUOKA *et al*. 2007). S120 is also phosphorylated after exposure of HeLa, U2OS or GM00130 B-lymphocyte cells to X- or γ-rays (ELIA *et al*. 2015; BELI *et al*. 2012; BENNETZEN *et al*. 2010), and after etoposide treatment in U2OS cells (BELI *et al*. 2012). Furthermore, S19, S20, S294 and S299 (in isoform 1) become phosphorylated after IR exposure (ELIA *et al*. 2015; BELI *et al*. 2012), although the responsible kinases remain to be identified. Interestingly, S294 and S299 lie within the C-terminal DNA binding domain of RAD51AP1 (**Figure 1.2**), and it is tempting to speculate that phosphorylation of these 2 residues regulates the affinity of RAD51AP1 for DNA. RAD51AP1 is also acetylated and ubiquitylated (**Figure 1.2**). However, the phenotypic consequences of these post translational modifications remain to be explored.

B. RAD51AP1 and cancer

B.1. Elevated RAD51AP1 in cancer

Cancer cells and precancerous lesions frequently contain aberrantly regulated DNA repair pathways (BARTKOVA *et al*. 2005; GORGOULIS *et al*. 2005), and high expression of DNA repair genes has been described to be associated with metastasis (KAUFFMANN *et al*. 2008; REDMER *et al*. 2017; MATHE *et al*. 2015; SARASIN *et al*. 2008). With respect to studies on RAD51AP1, its transcript was found to be upregulated in primary hepatocellular carcinoma compared to normal

liver tissue (SONG *et al*. 2004). RAD51AP1 transcript was also found to be elevated in intrahepatic cholangiocarcinomas, and suppression of RAD51AP1 by shRNA resulted in growth suppression of cholangiocarcinoma cells (OBAMA *et al*. 2008). The *RAD51AP1* transcript was shown to be overexpressed in aggressive mantle cell lymphoma compared to indolent small lymphocytic lymphoma (HENSON *et al.* 2006), in HPV-positive squamous cell carcinoma of the head and neck compared to normal oral epithelium (MARTINEZ *et al*. 2007), in ovarian cancer as a consequence of downregulated microRNA hsa-mir-140-3p (MILES *et al*. 2012; SANKARANARAYANAN *et al*. 2015), in ovarian and lung cancers compared to normal tissue (CHUDASAMA *et al.* 2018), and in basal and triple-negative breast cancers compared to normal mammary tissue (MATHE *et al*. 2015; PATHANIA *et al*. 2016). Consistent with a potential role for RAD51AP1 in metastatic disease (KAUFFMANN *et al*. 2008; REDMER *et al*. 2017), high RAD51AP1 expression was found to correlate with reduced time of survival of breast and ovarian cancer patients (SANKARANARAYANAN *et al*. 2015; PATHANIA *et al*. 2016), HBV-related hepatocellular carcinoma patients (XIE *et al.* 2019), triple-negative breast cancer patients (LE *et al.* 2019), and lung adenocarcinoma patients (LI *et al.* 2018). Sporadic cases of childhood papillary thyroid cancer also showed increased RAD51AP1 message (HANDKIEWICZ-JUNAK *et al*. 2016), and the CpG methylation of the RAD51AP1 promoter region appears to be associated with prostate cancer (WANG *et al*. 2005).

Additional interesting observations of RAD51AP1's possible linkage to metastatic disease have been made. Elevated RAD51AP1 transcript was detected in metastatic melanoma compared to metastasis-free melanoma (KAUFFMANN *et al*. 2008; REDMER *et al*. 2017). RAD51AP1 expression was positively linked to expression of the stem cell marker CD271 and to mechanisms of therapy resistance in metastatic melanoma cells (REDMER *et al*. 2017; LEBRAIKI *et al*. 2015).

Elevated expression of RAD51AP1 was also observed in a small set of brain metastasis (REDMER *et al*. 2017). Since RAD51AP1 is involved in mitigating replication stress (WIESE *et al*. 2007; MODESTI *et al*. 2007; PARPLYS *et al*. 2014; WAGNER *et al*. 2016), it is tempting to speculate that its enhanced expression in metastatic tumors may stem from the requirement of metastatic cells to limit replication stress.

B.2. RAD51AP1 as a potential therapeutic target

To date, microarray analyses on gene regulatory networks have led to the discovery of numerous "molecular signatures" associated with specific cancers and additional studies on RAD51AP1 as a potential target have been made. The *RAD51AP1* gene was identified as a differentially expressed gene with higher connectivity after protein-protein interaction analysis in MYCN-amplified neuroblastoma after inhibition of cyclin-dependent kinase 2 (SONG *et al*. 2017), in lung adenocarcinoma (LI *et al.* 2018), and in laryngeal squamous cell carcinoma (CHEN *et al*. 2020), suggesting its potential as a target in these cancers. Additional analyses found high expression of RAD51AP1 protein in cancerous lung tissue compared to normal (WU *et al.* 2019), and upregulated transcript in lung adenocarcinoma and lung squamous cell carcinoma cell lines (WU *et al.* 2019) and in epithelial growth factor receptor mutant cells that contribute to glioblastoma (WANG *et al.* 2019). Furthermore, a retrospective analysis of microarray expression data revealed elevated expression of RAD51AP1 in BRCA1-deficient compared to sporadic breast tumors (MARTIN *et al*. 2007), pointing towards genetic suppression of this breast cancer subtype by high RAD51AP1.

It has become increasingly apparent that lesions generated at DNA replication forks, as introduced by many anticancer drugs, are substrates for HR-mediated DNA repair (HELLEDAY

2010). Hence, HR-deficient tumors are sensitive to many DNA damaging agents that target replication forks. However, there are also many examples of the re- or over-expression of HR genes in tumor tissues, leading to anticancer drug resistance (HELLEDAY 2010; LORD *et al*. 2013 and 2017). As described above, RAD51AP1 could be one such example, and its expression may be linked to tumor resistance in response to anticancer treatment. Knockdown of RAD51AP1 stunts the growth of intrahepatic cholangiocarcinoma cells (OBAMA *et al*. 2008), ovarian and lung cancer cells (CHUDASAMA *et al.* 2018), lung adenocarcinoma and lung squamous cell carcinoma cells (WU *et al*. 2019), as well as significantly inhibited tumor volumes in intracranial mouse glioma models (WANG *et al.* 2019) and suppressed epithelial-mesenchymal transition and metastasis in xenograft mice with non-small cell lung cancer (WU *et al*. 2019), thus revealing a promising therapeutic avenue in RAD51AP1 inhibition. Similarly, treatment of breast cancer stem cells with 5-azacytidine plus butyrate reduces RAD51AP1 and cell proliferation (PATHANIA *et al*. 2016), and the addition of selenium in chemotherapy of gynecologic cancer downregulated RAD51AP1 and correlated with better prognosis (SONG *et al.* 2018). Future work on RAD51AP1 should focus on determining whether its downregulation or inhibition would improve the efficacy of cancer therapy. In this regard, targeting the RAD51 interaction domain on RAD51AP1 may provide new avenues of therapeutic intervention.

C. Summary and Knowledge Gaps

Since the discovery of RAD51AP1 20 years ago (MIZUTA *et al*. 1997; KOVALENKO *et al*. 1997), we have made significant progress towards a better understanding of its biochemical and cell biological attributes. However, we still lack knowledge of the precise molecular mechanisms by which RAD51AP1 carries out the HR reaction in cells, and how post translational modifications

affect the activities and biology of RAD51AP1. Refined *in vivo* model systems using *Rad51ap1* knockout mice are also needed to better understand the organismal consequences of *Rad51ap1* deletion and the relevance of its overexpression in specific tissues. Filling the knowledge gaps in the aforementioned areas will lead to a better understanding of the complexities associated with the HR reaction and will also enhance the knowledge and prospects for targeted therapies of cancers with high RAD51AP1.

IV. Hypothesis and Specific Aims

When considering the need to better understand DNA repair mechanisms to enhance cancer prevention and targeted therapies, and given the importance of RAD51AP1 in HR DNA repair, the overarching objective of this dissertation was to characterize the *in vitro* and *in vivo* traits of RAD51AP1 in regards to the HR reaction. The central hypothesis of this dissertation is that disruption of RAD51AP1 in HR inhibits cellular and organismal protection against spontaneous or induced DNA damage. To test this hypothesis, the biochemical and biological functions of RAD51AP1 in HR were assessed in the context of chromatin and its post translational modifications in cells as well as the penalties of its loss in an animal system. The following dissertation chapters will explore and describe, for the first time, RAD51AP1's mechanistic functions in HR in the context of its interaction with chromatinized DNA, the impacts of two of its post translational modifications on DNA binding and HR capability in cells, and the consequences of its loss on meiotic HR in a novel mouse knockout model. The specific aims designed to examine the hypothesis are summarized below and in **Figure 1.3**.

Specific Aim 1: Characterize the biochemical attributes of mutant RAD51AP1 impaired in DNA interaction in the context of chromatin.

Hypothesis 1.1: RAD51AP1 possesses two DNA-binding domains, at its N- and C- terminus. We hypothesize that one or both of these DNA-binding domains are essential for RAD51AP1's interaction with chromatinized DNA, relevant to its function in HR DNA repair.

Experiments 1.1: Define the mechanistic relationship between RAD51AP1 and chromatin through testing of mutant RAD51AP1 variants in EMSAs and pull-down assays.

Specific Aim 2: Characterize the biochemical and cellular attributes of post translational modifications of RAD51AP1.

Hypothesis 2.1: Upon exposure to DNA damaging agents, RAD51AP1 obtains post translational modifications (PTMs), and two modification sites of interest lie within its C-terminal DNA-binding domain. We hypothesize that modification of these residues regulates the binding of RAD51AP1 to DNA substrates.

Experiments 2.1: Characterize these modified residues' impacts on RAD51AP1 function through use of mutant variants of RAD51AP1 that mimic these PTMs in EMSAs and duplex capture assays assessing HR capability.

Hypothesis 2.2: We hypothesize that modification of these residues in cells monitors affinity of RAD51AP1 for DNA and in turn regulates the capacity of cells to repair spontaneous or induced DNA damage.

Experiments 2.2: Describe the impacts on cellular function of PTM RAD51AP1 with ectopically expressed variants of PTM RAD51AP1 in the face of spontaneous and induced DNA damage, through cell survival, growth, and immunofluorescent assays.

Specific Aim 3: Evaluate the biological impacts of RAD51AP1 loss in a novel mouse knockout model.

Hypothesis 3.1: RAD51AP1 interacts with DMC-1, a protein involved in meiosis, a process that employs HR to produce our sex cells. Given this fact and that there is documented evidence of high expression of RAD51AP1 in murine testes, we hypothesize that loss of RAD51AP1 will demonstrate a mouse phenotype altering reproductive biology and meiotic HR parameters in male mice.

Experiments 3.1: Characterize the organismal consequences of *Rad51ap1* loss in mice in regards to meiotic HR and reproductive parameters, assessing fertility, Mendelian ratios, and germ cell development via spermatogenesis.

Figures

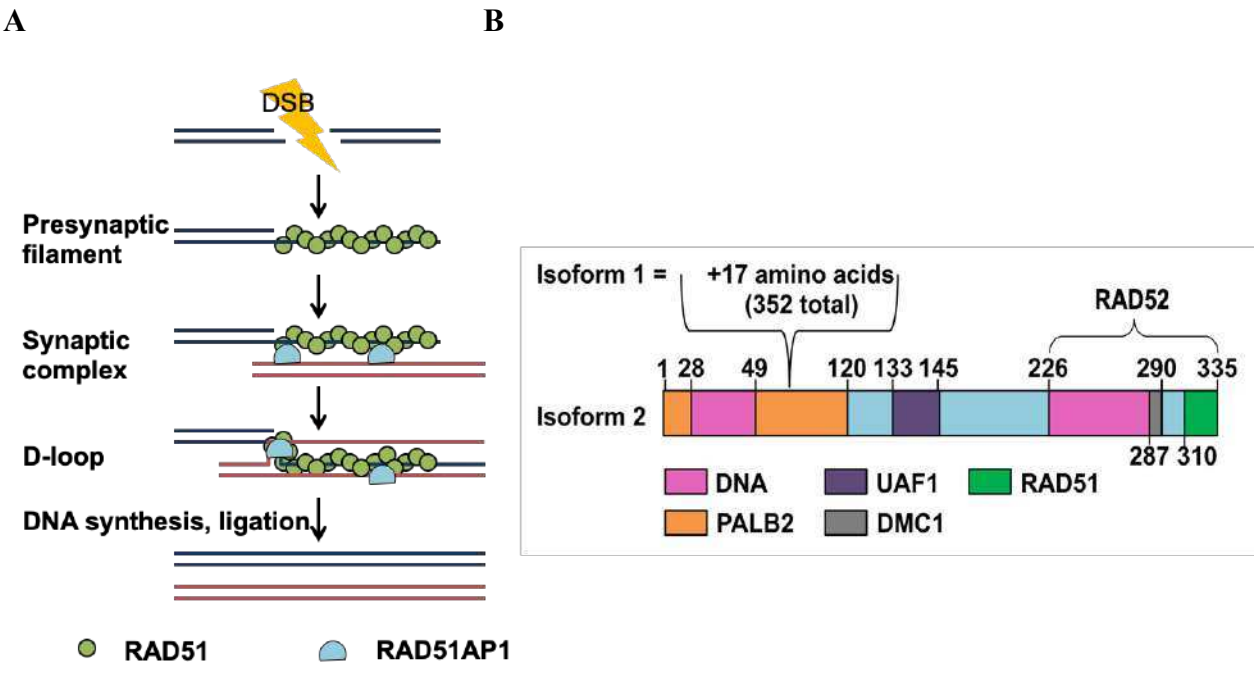

Figure 1.1. RAD51AP1 in HR DNA repair and functional domains

This figure depicts a succinct schematic of RAD51AP1 and its (A) involvement HR DNA repair and (B) its mapped functional domains. (A) The involvement of RAD51AP1 in the HR reaction is confined to synaptic complex formation and strand-invasion, HR stages downstream of presynaptic filament formation. (B) The mapped domains of the DNA and protein interactions with RAD51AP1 are indicated as comprehended so far. For details, see text (section A.2-A.3).

Figure 1.2. Post translational modifications of RAD51AP1

This figure depicts the ClustalW sequence alignment of the two prevalent isoforms of RAD51AP1 (http://www.proteinatlas.org/) with identified residues for post translational modification (WAGNER *et al*. 2016; MATSUOKA *et al*. 2007; ELIA *et al*. 2015; BELI *et al*. 2012; BENNETZEN *et al*. 2010) highlighted, as follows: phosphorylation (green), acetylation (red), and ubiquitinylation (blue). Asterick on K123 (isoform 1) indicates that this residue is either acetylated or ubiquitylated in response to DNA damage (ELIA *et al*. 2015). The N-terminally located and the 2 identified parts (DNA (I) and DNA (II) of the C-terminally located DNA-binding domains (DUNLOP *et al.* 2012) are underlined by a solid line. The RAD51 interaction domain (very C-terminus 26 residues) is also underlined.

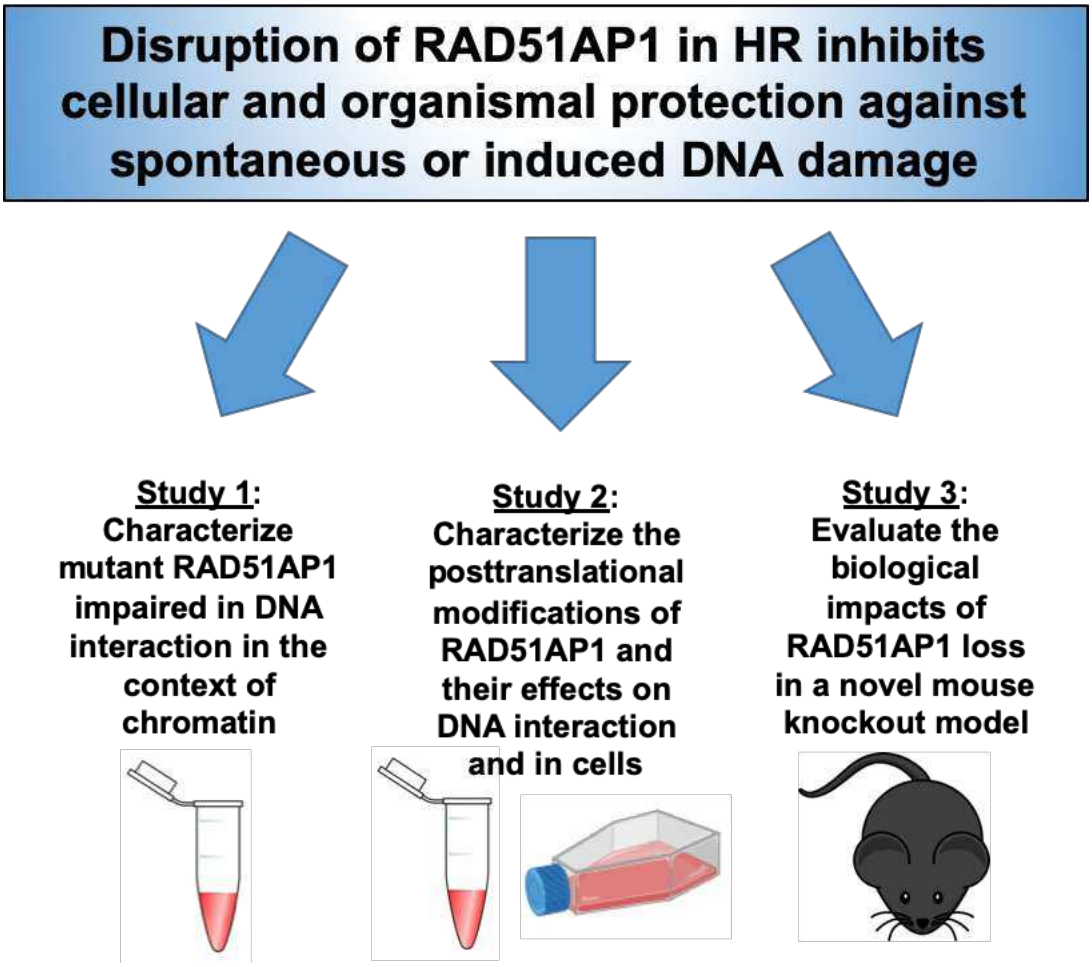

Figure 1.3. Overarching hypothesis and workflow for examining the *in vitro* and *in vivo* traits of RAD51AP1 for protection against spontaneous or induced DNA damage

CHAPTER TWO

RAD51AP1 mediates HR DNA repair in chromatin[2]

Summary

RAD51-associated protein 1 (RAD51AP1) is a key homologous recombination (HR) DNA repair protein, so named due to its ability to bind RAD51 and enhance RAD51 activity through formation of the synaptic complex and subsequent D-loop. RAD51AP1 binds to various DNA substrates via two DNA-interaction domains, located within its N- and C- termini, respectively. Upon induction by DNA damage, RAD51AP1 receives post translational modifications, which reflects its functional diversity. To date, research on RAD51AP1 has explored several of its biochemical and cell biological traits. However, no studies have yet investigated its role in HR in the context of chromatin or its post translational modifications (PTMs), which likely are a crucial aspect for regulating HR DNA repair in the cellular environment.

This chapter will focus on *in vitro* studies that assess the affinity of RAD51AP1 towards different DNA substrates as well as evaluate two post translational modifications located within its C-terminal DNA-binding domain. The results of our efforts show a novel association of RAD51AP1 with chromatinized double-stranded (ds)DNA, which occurs strictly through its C-terminal DNA-binding domain. Our findings also indicate that two post translational modification sites within its C-terminal DNA-binding region have decreased affinity to chromatinized dsDNA *in vitro* and play a role in cell survival against spontaneous and induced DNA damage. By understanding the mechanistic and cellular function of this important HR protein, we expect to have direct clinical relevance via the optimization of targeted cancer therapies.

---

[2]*A version of this chapter will be submitted as a manuscript.*

Introduction

Genome integrity is constantly challenged by a variety of endogenous and exogenous DNA-damaging agents, which can lead to a variety of DNA lesions (SHRIVASTAV *et al*. 2008). Among these lesions, the double-strand break (DSB) is the most lethal to DNA, and if not repaired or repaired incorrectly, creates mutations that may predispose cells to carcinogenesis. DNA repair processes are crucial for mending DSBs, maintaining genome integrity, and preventing mutations leading to cancer (SCULLY *et al*. 2019). One major DNA repair process is homologous recombination DNA repair (HR), a process that requires the recruitment the RAD51 recombinase to align homologous DNA sequences and allow faithful repair of lost sequence information (DALEY *et al*. 2013 and 2014; LAURINI *et al*. 2020).

It is now extensively documented that the packaging of genomic DNA into chromatin deeply affects nuclear processes, including DNA repair and recombination (HAUER *et al*. 2020). At the first level of chromatin organization is the nucleosome core particle (NCP), which consists of nearly two turns of double-stranded DNA (147 base pairs in length) wrapped around a histone octamer core consisting of two copies each of the four core histone molecules: H3, H4, H2A, and H2B (HAUER *et al*. 2020; LUGER *et al*. 1997). Higher organizational levels of chromatin consist of these nucleosome core particles connected by linker DNA of variable length, nucleosomes, and other unidentified architecture. In the context of HR DNA repair, this wrapping of DNA into nucleosomes in chromatin is quite inhibitory to the central activity of RAD51 in aligning homologous DNA sequences (SORIA *et al*. 2012; SEEBER *et al*. 2013). To overcome this nucleosome barrier, factors must assist in chromatin disassembly, assembly, and remodeling. An example factor is the HR factor RAD54, an ATP-dependent protein that possesses homology-driven chromatin-remodeling activity and stimulates the RAD51-ssDNA complex to promote

homologous pairing (ALEXEEV *et al*. 2003; ALEXIADIS *et al*. 2002; JASKELIOFF *et al*. 2003; ZHANG *et al*. 2007).

Similar to RAD54, RAD51-associated protein 1 (RAD51AP1) is a key HR protein that is vital for enhancing RAD51 activity via stimulation of synapsis and the D-loop reaction during HR (WIESE *et al*. 2007; MODESTI *et al*. 2007; DUNLOP *et al*. 2012). RAD51AP1 is also required for protecting human cells from the DNA damaging effects of mitomycin C (MMC) and ionizing radiation exposure and for facilitating DNA replication fork progression and stability (WIESE *et al*. 2007; MODESTI *et al*. 2007; HENSON *et al*. 2006; PARPLYS *et al*. 2014). RAD51AP1 binds DNA and possesses two DNA-binding domains to achieve this: one at its N-terminus and another at its C-terminus (**Fig. 1.1B**). Both DNA-binding domains play roles in protein function and for DNA damage resistance of cells (MODESTI *et al*. 2007; DUNLOP *et al*. 2012).

In response to damage, several DNA damage-induced post translational modifications (PTMs) occur in RAD51AP1: acetylation, phosphorylation, ubiquitylation, and SUMOylation (ELIA *et al*. 2015; BELI *et al*. 2012; WAGNER *et al*. 2016; BARROSO-GONZALEZ *et al.* 2019). Two sites of modification lie by its C-terminal DNA binding domain: phosphorylation at Ser-277 and Ser-282 (in isoform 2; **Fig. 2.4A**). Intriguingly, these two phosphorylation sites lie directly next to crucial DNA binding residues Lys-283, Lys-284, Lys-286, and Trp-287 in the C-terminal DNA-binding domain (in isoform 2; DUNLOP *et al*. 2012), prompting conjecture that phosphorylation of Ser-277 and/or Ser-282 may regulate binding of RAD51AP1 to DNA. While these PTMs are induced by DNA damage, it is not yet clear how they regulate RAD51AP1 function in HR DNA repair.

As reported by our studies here, we have uncovered a novel interaction between RAD51AP1 and NCP. The goals of our studies were to further analyze this interaction and advance

knowledge of the mechanism of action of RAD51AP1 in HR DNA repair. We further find that phosphomimetic mutants at S277 and S282 impacts binding of RAD51AP1 to NCP and that the non-phosphorylatable mutants compromises cell survival against spontaneous and induced DNA damage. Based on these findings, we propose a model in which the modified states of RAD51AP1 may guide homology search and hetero-duplex formation after RAD51 filament formation in the HR reaction. These observations are notable as no assessment to date has found an association of RAD51AP1 to chromatin, and no mechanistic studies have evaluated its PTMs.

Materials and Methods

Transformations

Competent cells for either plasmid preparation or protein expression were taken out of the -80°C freezer and thawed on ice. Agar plates containing the appropriate antibiotic (ampicillin at 100 μg/mL or kanamycin at 50 μg/mL) were removed from storage at 4°C and warmed up in a 37°C incubator. DNA of interest (10ng for DH5a cells or 20 ng for Rosetta cells) was mixed in 50 μl of competent cells in a microcentrifuge tube for 30 minutes on ice with gentle mixing via tube flicking every 10 minutes. Tubes were then placed in a heated water bath at 42°C for 45 seconds and then returned on ice for 5 minutes. SOC media (950 μl; Thermo Scientific) was added to each tube, and tubes were then taped sideways in a 37°C rotating incubator for gentle mixing for 1 hour. Afterwards, 50-100 μl of the transformation was plated onto an agar plate, and plates were incubated overnight at 37°C.

Plasmid Preparation

Amplification of cloned full-length human RAD51AP1 and its variants was achieved with plasmids transformed in *Escherichia coli*. Freshly transformed E. coli cells (DH5a; Invitrogen) were grown on LB plates containing ampicillin (100 μg/mL) or kanamycin (50 μg/mL) at 37°C. After an overnight incubation, colonies were collected and inoculated into LB medium (5 mL) containing ampicillin (100 μg/mL) or kanamycin (50 μg/mL), and the cultures were grown overnight before miniprep and sent for sequencing by Genewiz. Full-length human RAD51AP1 and variants either contained an N-terminal maltose-binding protein (MBP) and C-terminal His_6 tag, an N-terminal FLAG protein and C-terminal His_6 tag, or an N-terminal His_8 tag and C-terminal Strep-tag II. Constructs, protein tags, and expression vectors are listed in **Table 2.1**. Point mutations, such as in the S2A and S2D mutants, were generated with the NEB site-directed mutagenesis kit (# E0554S). The phosphorylation mimic, S2D, was achieved with substitutions of Serines 277 and 282 to aspartic acid. The non-phosphorylatable mutant, S2A, was achieved with substitutions of these serine sites to alanine. Primers used for site-directed mutagenesis kit are listed in **Table 2.2**.

Protein Induction

To prepare pellets for protein purification, plasmids were transformed in Rosetta cells (EMD Chemicals, Inc.; product no. 71403 Rosetta 2(DE3)pLysS Competent Cells). Freshly transformed Rosetta cells were grown on LB plates containing ampicillin (100 μg/mL) or kanamycin (50 μg/mL) at 37°C. After a 16h incubation, colonies were collected and inoculated into LB medium (5 mL) containing ampicillin (100 μg/mL) or kanamycin (50 μg/mL). Colonies were grown at 37°C in 1L LB broth (Alfa Aesar H26676) until the A600 reached 0.4-0.6, at which

point 400 μM IPTG was added to induce protein expression, and cultures were grown for 4 more hours at 37°C before centrifugation and storing of pellets at -80°C.

Protein Purification

Purification of full-length RAD51AP1 and its variants was achieved using affinity purification methodologies. Ni-NTA agarose beads (Invitrogen R901-15) were used for affinity purification of His_6-tagged proteins, Streptavidin agarose (Qiagen 1057978) was used for affinity purification of Strep-tagged proteins, and FLAG resin (Sigma F2426) was used for affinity purification of FLAG-tagged proteins. For tandem affinity purifications of MBP-His_6-tagged proteins and FLAG-His_6-tagged proteins, proteins were first purified via their His_6-tag and then further purified via either their Strep-tag or FLAG-tag. A frozen cell pellet in a Falcon tube (50 ml from 1L cell culture) that was stored at -80°C was thawed at room temperature and resuspended in 5 ml lysis buffer (50 mM Tris-HCl pH 7.5, 300 mM KCl, 1 mM EDTA, with Protease Inhibitor Mixture [Thermo Scientific]) and subject to sonication to prepare crude lysate. After centrifugation (10,000 rpm, 10 min), the clarified lysate was transferred to a 15 ml Falcon tube containing 500 μl Ni-NTA agarose beads. The mixture was subjected to gentle rotation at 4°C for 2 h. The resin was then washed three times with 10 ml of buffer (50 mM Tris-HCl pH 7.5, 300 mM KCl, 1 mM EDTA, 50 mM Imidazole), before elution of bound protein by 500 μl elution buffer (50 mM Tris-HCl pH 7.5, 300 mM KCl, 1 mM EDTA, 300 mM Imidazole). The eluate was then mixed with Streptavidin agarose or FLAG resin for tandem purification, following manufacturers' instructions. All eluted proteins after tandem purification underwent overnight dialysis in dialysis buffer (50 mM Tris-HCl at pH 7.5, 3M KCl, 0.5M EDTA, 2M DTT, 20% glycerol, 0.01% NP-

40). Final concentrations of proteins ranged between 1-3 mg/ml and were frozen in aliquots by liquid nitrogen and stored at -80°C.

DNA Substrates

The naked double-stranded DNA substrate used in the DNA electrophoretic mobility shift assay was 147 base pairs in length (CSU: The Histone Source), consisting of sites for nucleosome positioning (LOWARY *et al*. 1998; GOTTESFELD *et al*. 2001). The nucleosome core particle (NCP) used in the binding assays consisted of this 147bp DNA substrate and human histone octamer (CSU: The Histone Source) mixed together in a reaction containing 1M NaCl. The NCP was then assembled via stepwise salt dilution by 1X TE buffer, as established previously (DYER *et al*. 2004), to a final NaCl concentration of 0.1M. Each dilution step was incubated for 30 minutes at 4°C with gentle rotation. The final assembled NCP was stored at 4°C on ice for up to a month in 1X TE buffer.

Electrophoretic Mobility Shift Assay

The purified RAD51AP1 protein or variants (0.05-0.6 μM) were incubated with 1-2 μM of dsDNA or NCP in 10 μl of reaction buffer (buffer composition: 40 mM Tris-HCl at pH 7.5, 100mM NaCl) on ice for 30 minutes, before adding 20% sucrose (in nanopore water) to the reaction. The reactions were then loaded on native 5% PAGE gels at 4°C and run at 150 volts for 1 hour in 0.2% TBE buffer. Gel staining was achieved with ethidium bromide (brand/catalog number) for 15 minutes, before having images captured and optical densities analyzed (BioRad Molecular Imager ChemiDoc XRS+ with Image Lab software version 3.0).

Duplex Capture Assay

This procedure was performed as previously described (DRAY *et al*. 2011). Briefly for 5 min at 37°C, the presynaptic filament was formed via incubation of 5 μl magnetic beads containing 5'-biotinylated 80-mer ssDNA (5 μM) with RAD51 (700 nM) in buffer A (25 mM HEPES (pH 7.5), 50 mM Tris-HCl (pH 7.5), 2 mM ATP, 1 mM DTT, 0.2 mM B-mercaptoethanol, 2% glycerol, 35 mM NaCl, 45 mM KCl, 1 mM MgCl2, 0.16 mM EDTA, 0.4 mM Mercaptoethanol, 0.01% NP-40, and 100 μg/ml BSA). The supernatant was removed, and the beads were re-suspended in buffer A and incubated with FLAG-tagged RAD51AP1 (400 and 800 nM) for 5 min at 37°C. The supernatant was removed, and the beads were re-suspended in 10 μl of this buffer containing either 147bp dsDNA (1 μM) or NCP (1 μM; see above on assembly of NCP) and incubated for 10 min at 37°C. The supernatant was saved, and beads were washed 4 times with 200 μl of buffer A. Beads and supernatant were treated with Proteinase K (2.4 mg/ml) containing 0.2% SDS, and the reaction was incubated for 15 min at 37°C. The supernatant and bead-bound DNA were analyzed via 1% agarose gel in 1X TBE. Visualization of DNA occurred via staining with ethidium bromide, and DNA bands were quantified using ImageJ software.

Affinity Pull-Down Assays

FLAG pull-downs were performed with anti-FLAG resin (catalog), as described by the manufacturer. Resin was equilibrated in binding buffer containing 50 mM Tris-HCl (pH 7.5), 150 mM NaCl, 0.25% Triton X-100, and 100 μg/ml BSA. Purified FLAG-tagged RAD51AP1 (50 nM) was incubated with 50 μl resin for 1 h at 4°C with gentle rotation in binding buffer. Supernatant containing unbound protein was removed, and H2A/H2B histone dimer or H3/H4 histone tetramer was added and further incubated for 2 h at 4°C with gentle rotation in 20 μl binding buffer. After

binding, resin was washed three times with 200 µl of binding buffer. Elution of proteins from the resin was achieved with 20 µl binding buffer containing 150 ng/µl 3X FLAG peptide. Proteins were resolved by 10% SDS-PAGE and western blot analysis.

Nickel pull-downs were performed with Ni-NTA agarose beads (Invitrogen R901-15). Purified His_6-tagged RAD51AP1 (6 µM; 12 µg) was mixed with Ni-NTA agarose beads (25 µl, 50% slurry) in 25 µl buffer consisting of 20mM Tris-HCl (pH 8.0), 100 mM NaCl, 30 mM imidazole, and 2% BSA. After an incubation at 4°C with gentle rotation for 1 h, the beads were centrifuged, and supernatant containing unbound protein was removed. H3/H4 histone tetramer (3.5 µM; CSU: The Histone Source) was then added in 25 µl buffer of 20mM Tris-HCl (pH 8.0), 100 mM NaCl, 30 mM imidazole, and 2% BSA. After an incubation of 2h at 4°C with gentle rotation, the beads were washed five times with 200 µl of 20mM Tris-HCl (pH 8.0), 200 mM NaCl, 50 mM imidazole, and 0.2% Tween 20. Elution of protein from the beads occurred after a 15-minute incubation on ice in 30 µl buffer containing 500 mM imidazole. Total eluate volume collected was 30 µl, and 10 µl of this eluate (with 2 µl of loading buffer) was analyzed by 10% SDS-PAGE and western blot staining.

Western Blotting

Proteins for western blot analysis resolved by either Native-PAGE or SDS-PAGE gels were transferred onto a PVDF membrane at 4°C in transfer buffer (1X Tris Glycine buffer containing 25 mM Tris-Cl, 250 mM glycine, 0.1% SDS, and 10% methanol) running at 35V overnight. After transfer, membrane was blocked in 5% milk (1X TBST with 5% nonfat dry milk) at room temperature for 20 min with gentle rotation. The membrane was then incubated with primary antibodies for 2 h, washed three times in 1X TBST (Tris-buffered saline with 0.1%

Tween-20), and incubated with secondary antibodies for 45 minutes. The membrane then was washed six times with 1X TBST before analysis by chemiluminescence (Thermo Scientific catalog #34580 or #34095). Antibodies and concentrations used are listed in **Table 2.4**.

Far Western Blotting

After native PAGE, RAD51AP1 and NCP were transferred onto a PVDF membrane, as described for western blot analysis. The membrane was soaked at room temperature for 2 h in buffer B containing 10 mM KH2PO4 (pH 7.4), 150 mM KCl, 15 mg/ml BSA, 2 mM 2-mercaptoethanol and 0.05% Tween 20. Then the membrane was incubated with 3 μg/ml RAD51 in 4 ml buffer shaking at 4°C overnight. The next day, the membrane was washed in 10 ml buffer three times before incubation with primary and secondary antibodies to RAD51, washes, and chemiluminescence as described for western blotting. Antibodies and concentrations used are listed in **Table 2.4**.

Cell Culture

HeLa cells and cell lines used in these studies were grown in Minimum Essential Medium (Earle's) supplemented with 10% fetal bovine serum (Sigma) and antibiotics (Invitrogen). Cells were maintained in a humidified incubator at 37°C with 5% CO2.

Generation of wild-type- and mutant-complemented RAD51AP1 KO cell lines

RAD51AP1 KO cells were described previously (LIANG et al. 2019). Expression of RAD51AP1-WT, RAD51AP1-S277D and S282D (S2D), RAD51AP1-S277A and S282A (S2A), RAD51AP1-S277A, and RAD51AP1 S282A in RAD51AP1 KO cells occurred by transduction

with lentivirus, as previously described (CAMPEAU *et al*. 2009). A FLAG-tagged RAD51AP1 ORF cloned into the entry vector pENTR1a was available in our lab, and this vector was subjected to site-directed mutagenesis, as described above, to mutagenize S2D, S2A, S277A, and S282A. In the presence of the LR clonase (Thermo Fisher), a recombination reaction allowed transfer of the insert from the entry vector into a destination vector. Replication-incompetent lentiviral particles were produced after transfection of HEK 293T cells with viral packaging mix (Invitrogen) and in the presence of 6ug/ml polybrene. RAD51AP1 KO cells were transduced with 0.5 ml supernatant containing lentiviral particles, and clonal isolates were initially selected by antibiotic resistance to G418 (2 mg/ml). Subsequent single clonal isolates were selected by plating the G418-resistant cells on a 96-well plate. The expression level of RAD51AP1 for ~20 clones per construct were confirmed via western blot, and final clones were selected on the basis of complementation of phenotype and expression of identical levels of the RAD51AP1 protein.

Growth Curve Analysis

Cells were plated onto 6-well plates at 12,000 cells/well and were incubated in a humidified chamber at 37°C with 5% CO2 and monitored for growth under unperturbed conditions. Over the course of 9 days, the medium was removed, and cells were washed once, trypsinized, and harvested daily. Trypsinized cells were washed twice with 1X PBS, suspended in 10 ml growth media, and counted.

Mitomycin C Exposure

Cells were plated in T25 flasks at 250,000 cells/flask. After 48 h, cells were exposed to an acute dose of mitomycin C (Sigma) for 1 hour in growth media at the following concentrations:

0.5 μM, 1 μM, 1.5 μM, 2 μM, and 3 μM. After exposure, the medium was removed, and cells were washed once with 1X PBS, trypsinized, harvested, and counted. For colony formation assays, Trysinized cells were then washed twice with 1X PBS, suspended in 10 mL growth media, and counted. Cells were then plated and incubated in regular growth medium at 37°C for 12 days. After 12 days, cells were fixed and stained with crystal violet to visualize colonies.

Cell Cycle Analysis

RAD51AP1-WT, RAD51AP1-S2D, and RAD51AP1-S2A expressing RAD51AP1 KO cells and HeLa cells ($2.5x10^5$) were seeded into T-25 flasks, incubated for 48 hours, and treated for 2 hours with mitomycin C (0.5 μM) or mock-treated. Cells were washed with warm PBS for three times, fresh media was added, and cells were incubated for indicated recovery times: A pulse of EdU (10 μM) for 20 minutes was given prior to cell harvest, and cells were then trypsinized, harvested via centrifugation at 1100 RPM for 6 minutes, washed once with PBS, fixed with 70% chilled ethanol, and stored at 4°C until further processing. Before processing, cells were rehydrated with 1X PBS for 1 hour, permeabilized with 0.5% Triton X-100 in PBS, washed with 1% BSA in 1X PBS. Cells were processed using the Click-iT Cell Reaction kit (Thermo Fischer) using manufacturer's instructions, suspended in PBS containing 0.25 μl/ml Sytox AADvanced and 80 μg/ml RNaseA, incubated at 4°C overnight in the dark to allow the cell cycle dye to saturate, and analyzed by flow cytometry with a 3-laser CyAn flow cytometer and FlowJo 10.7 software.

DNA Fiber Assay

This assay was performed as previously described (PARPLYS *et al*. 2015). Briefly, exponentially growing cells were pulse-labeled with CIdU (0.025 mM; catalog) for 20 minutes.

After, cells were washed twice with warm PBS and further incubated for 5 hours with sham or HU treatment (2 mM, catalog?). Then, cells were washed twice with warm PBS and incubated with IdU (0.25 mM, catalog?) for 20 minutes. After, cells were washed twice with ice-cold PBS and harvested via scraping on ice. Cells were adjusted to 5x10^5/ml and prepared for DNA fiber spreads. A 2 µl droplet of cells was placed per slide and gently mixed with 7 µl spreading buffer for 2 minutes before tilting of slides to allow spreads. Slides were fixed in 3:1 methanol/acetic acid for 10 minutes, air-dried, and stored at 4°C until staining. For staining, slides were rehydrated in 1XPBS twice for 5 minutes. And then denatured in HCl (2.5 M) at room temperature for 50 minutes. Slides were washed in PBS and blocked with block buffer (5% BSA, 1X PBS, 0.1% Triton X-100) for 1 h. Primary antibodies to detect CIdU or IdU were added, and slides were incubated for 1 h before three washes each in 1X PBS and block buffer. Secondary antibodies were added, and slides incubated for 1 h before subsequent washes in 1X PBS, block buffer, and water. Slides were mounted with Prolong Antifade, cover-slipped, and stored overnight at 4°C before imaging the next day. Images were taken using a 63x oil objective and a Zeiss Axio-Imager.Z2 microscope. Analyses of images occurred through ImageJ software. Second pulse replication tracts (elongation) green tracts were measured and plotted after conversion of tract lengths to elongation rates (kilobases per minute). A conversion factor for the length of a labeled track of 1 µm = 2.59 kb was used (JACKSON *et al*. 1998). At least 100 individual fibers were analyzed per condition.

Immunofluorescence

Cells of interest were seeded at appropriate densities (20, 000 cells/chamber) on 4-well chamber slides 48 hours prior to IR treatment (8 or 20 Gy, at a dose rate of ~2.9 Gy/min). Following irradiation or sham treatment, cells were fixed at 4h, 8h, and 24h at room temperature

in pre-extraction buffer for 3 minutes and 2% paraformaldehyde for 15 minutes, washed with 0.5% and 0.25% glycerol in PBS for 10 and 5 minutes respectfully, and permeabilized in 0.25% Triton X-100 in PBS for 15 minutes. Cells were blocked in 1% BSA in PBS for 30 minutes before staining with rabbit anti-RAD51 antibody (Santa Cruz Biotechnology) overnight at 4°C, to monitor RAD51 foci as a readout for HR DNA repair capability and formation/resolution kinetics. AlexaFluor-488 goat anti-rabbit were used for secondary antibody staining the following day, with 45-minute incubation followed by nuclei labeling with DAPI. Image capture of RAD51 foci occurred using 20 Z-stack section images taken per sample using a 63x oil objective and a Zeiss Axio-Imager.Z2 microscope. Analysis of images was done on ImageJ after collapse of the Z-stacks down to maximum intensity projections. Nuclei counted as foci-positive if > 5 foci were identified per nucleus. Experiments were carried out in triplicate, and significances were determined using two-way ANOVA analysis with $P \leq 0.05$ considered significant.

Statistics

Statistical analyses were performed using Prism 8 GraphPad on the data from at least three independent experiments for each condition, with the exception of the DNA fibers analysis of one experiment and cell cycle distributions and growth curves of two experiments. Densitometric analyses of gels and Western blots were performed using ImageJ (NIH) with appropriate background correction. Statistical significance between three or more groups was determined using two-way ANOVA, and multiple comparisons were corrected using Tukey's multiple comparisons test. A p-value <0.05 between control and tested condition (i.e. wild type versus mutants; wild-type versus truncations; S2D vs. S2A) was deemed statistically significant.

Results

RAD51AP1 associates with the nucleosome core particle and histones through its C-terminus

Following incubation of RAD51AP1 protein with the nucleosome core particle (NCP) as dictated by our schematic (**Fig. 2.1A**), we observed DNA mobility shifts on native PAGE gels by ethidium bromide staining (**Fig. 2.1B** lanes1-5, **Fig. 2.1C** lanes 1-4, **Fig. 2.1D** lanes 1-3) and Imperial staining (**Fig. 2.1B** lanes 6-8). This indicated that an interaction between RAD51AP1 and NCP occurred, and this is the first documentation of RAD51AP1 associating with chromatinized dsDNA. RAD51AP1 as well as histone components of NCP, H2A and H3, were found within the mobility shifts (**Fig. 2.1C-D**), further supporting the existence of a likely intact RAD51AP1-NCP complex. Notably, RAD51AP1 was only able to enter the gel when bound to NCP and not by itself (**Fig. 2.1B**, lane 11). This interaction between RAD51AP1 and NCP was also confirmed with recombinant RAD51AP1 protein engineered with different tags (His_6-Strep tagged and His_6-FLAG tagged).

After confirming the novel association between RAD51AP1 and NCP, we were prompted to address which DNA-binding domains were responsible for this interaction. RAD51AP1 possesses two distinct DNA-binding domains, one within its N-terminus and another within its C-terminus. Each DNA-binding domain has been previously shown to have different affinities towards various non-chromatin DNA substrates (DUNLOP *et al*. 2012). We generated fragments of RAD51AP1 (**Fig. 2.2A**) that isolated the DNA-binding domains. We found that RAD51AP1-F3 was the only fragment capable of causing a mobility shift (**Fig. 2.2B-C**, lanes 7-8), whereas RAD51AP1-F1 and -F2 were devoid of any shift (lanes 4-5), confirming that the interaction between RAD51AP1 and NCP occurs via within residues 187-335 of the protein containing the C-terminally located DNA-binding domain. To assess the possibility of a direct interaction between

RAD51AP1 and the H3/H4 histone tetramer independent of DNA, affinity pull-down assays with H3/H4 histone tetramer were performed. Results confirmed that the novel interaction between NCP and RAD51AP1 can occur via binding with H3/H4 (**Fig 2.2D-E**), and this association mainly occurred through RAD51AP1-F3 (**Fig. 2.2E**, lane 10). An interaction with H2A/H2B also occurred with F.L. RAD51AP1 (data not shown), although weaker than with H3/H4 tetramer.

Division of the F3 fragment and its DNA binding domain (**Fig S2.2A**) into F4 and F5 fragments impaired its interaction with NCP as indicated by reduced mobility shifts (**Fig. S2.2B-C**), suggesting that all DNA binding residues within F3 need to be present for the interaction. kD assays (data not shown) reveal less affinity by RAD51AP1 towards NCP, compared to its avid affinity to naked dsDNA (WIESE *et al*. 2007; MODESTI *et al*. 2007; PARPLYS *et al*. 2014 and 2015; DUNLOP *et al*. 2012; DRAY *et al*. 2010).

The RAD51AP1-NCP complex is capable of RAD51 interaction

Since our results confirmed that the interaction between RAD51AP1 and NCP stems from its C-terminus, we next questioned whether the RAD51AP1 in the RAD51AP1-NCP complex was capable of retaining its interaction with RAD51. To this end, we conducted a Far Western experiment in which we first incubated RAD51AP1 and NCP together to form the RAD51AP1-NCP complex and ran this complex on an EMSA for its mobility shifts, before transferring shifts to a membrane to be incubated with RAD51 protein and probed for RAD51 via Western blot. Results from the Far Western assay (**Fig. 2.3A**) showed that RAD51 associated with RAD51AP1-NCP (**Fig. 2.3A**, lane 8), suggesting that NCP-bound RAD51AP1 is able to interact with RAD51. In contrast, RAD51 alone is unable to associate with the NCP as determined by EMSA (data not shown), eliminating the possibility that the association of RAD51 to RAD51AP1-NCP is via the

NCP. Our studies here confirm that the RAD51AP1, while bound to NCP, is capable of interacting with RAD51, supporting the notion that RAD51AP1 may able to stimulate the RAD51 presynaptic filament during the D-loop reaction in the context of chromatin.

RAD51AP1 stimulates duplex capture of both naked and chromatinized dsDNA

During RAD51-mediated D-loop reaction, the RAD51 presynaptic filament captures the duplex DNA partner, followed by a search for DNA homology that then forms the synaptic complex, an HR intermediate that aligns homologous DNA molecules. Earlier reports on RAD51AP1 show its ability to stimulate duplex capture in the context of naked dsDNA, an activity that RAD51 alone struggles to perform without RAD51AP1 (WIESE *et al*. 2007; MODESTI *et al*. 2007; PARPLYS *et al*. 2014 and 2015; DUNLOP *et al*. 2012; DRAY *et al*. 2010). Here, we tested the ability of RAD51AP1 to promote capture of chromatinized dsDNA via the NCP. First, we assembled RAD51 filaments on biotinylated ssDNA which we then incubated with RAD51AP1. We then offered the 147 bp dsDNA fragment or the NCP and purified captured dsDNA or NCP through streptavidin beads mediated by the biotin-ssDNA-RAD51 nucleoprotein filament (schematic of the assay shown in **Fig. 2.3.B**). In accordance with earlier reports (DRAY *et al*. 2010; LIANG *et al*. 2016 and 2020), RAD51AP1 stimulated duplex capture of dsDNA (**Fig. 2.3B**, lanes 3-4). RAD51AP1 also stimulated capture of the NCP (**Fig. 2.3C**, lanes 7-8). Quantitative analysis from three independent experiments shows that RAD51AP1 more avidly promotes the reaction with the NCP than with naked dsDNA. (**Fig. 2.3D**). These results suggest further that RAD51AP1 functions during HR in the context of chromatin and highlight the multi-faceted role of RAD51AP1 in associating with chromatin and non-chromatin DNA substrates during duplex capture.

RAD51AP1 mutants compromised in binding with the nucleosome core particle

Previous studies (DUNLOP *et al*. 2012) have documented critical DNA-binding residues for the C-terminal DNA-binding domain in RAD51AP1 that if mutated to a neutral charge lead to an impairment in DNA interaction. To test against the context of NCP interaction, we constructed two of these mutants in the setting of the F3 fragment via site-directed mutagenesis: K4A (K231A, K232A, K234A, K236A) and K3WA (K283A, K284A, K286A, W287A) (**Fig. S2.2D**) and found that both mutants were impaired in NCP binding, as expected (**Fig. S2.2E**, lanes 4-5). We also generated additional mutant variants: K4A1 (K231A, K232A), K4A2 (K234A, K236A), K3WA1 (K283A, K284A), and K3WA2 (K286A, W287A) to assess which residues may be most crucial to NCP interaction. We found that these mutants did exhibit diminished NCP binding (data not shown) but were not as compromised in binding compared to K4A and K3WA. These findings demonstrate that these previously identified critical DNA binding residues in the C-terminal DNA binding domain are also important for the interaction between RAD51AP1 and NCP.

In response to damage, several DNA damage-induced post translational modifications (PTMs) occur in RAD51AP1: acetylation, phosphorylation, and ubiquitylation (ELIA *et al*. 2015; BELI *et al*. 2012; WAGNER *et al*. 2016). Intriguingly, two phosphorylation sites (S277 and S282) are highly conserved in mammals (**Fig. 2.4A**) and lie directly next to crucial DNA binding residues K283, K284, K286, and W287 in the C-terminal DNA-binding domain (DUNLOP *et al*. 2012), prompting conjecture that phosphorylation of S277 and/or S282 may regulate binding of RAD51AP1 to DNA. We sought to test this hypothesis via generation of phospho-mutants mimicking phosphorylation through aspartic acid residues: F3-S2D and FL-S2D (S277D, S282D). We utilized the EMSA assay to examine mobility shifts of these mutants towards dsDNA or NCP.

Compared to the F3 fragment and F.L. controls, F3-S2D and F.L.-S2D exhibited decreased mobility shift ability with NCP (**Fig. 2.4B-C**). Interestingly, F3 and F3-S2D showed no apparent difference in binding to naked dsDNA (**Fig. S2.3A**).

To further characterize these residues, each Serine was further evaluated individually via S277D and S282D single mutants and showed no apparent impairment for dsDNA binding compared to F3 control (**Fig. S2.3A**). Given that one additional Serine lies between S277 and S282 at S279, we speculated that the impaired NCP binding exhibited by S2D may be further amplified via a phospho-mimic for all three serine residues: S3D (S277D, S279D, S282D). After generating S3D, EMSA testing did show diminishment of mobility shift activity by S3D compared to F.L. control; however, S2D still remained the most compromised in NCP binding (**Fig. S2.3B**, lanes 5-6), highlighting the unique importance of these two residues.

Cell growth and survival against spontaneous and induced DNA damage is impaired in S2A-expressing cells

To interrogate the biological relevance of the S277 and S282 post translational modifications of RAD51AP1, we utilized HeLa cells that are deleted for *RAD51AP1* (KO) and expressed in these cells either *RAD51AP1* wild-type (WT), *RAD51AP1*-S2D (S277D, S282D), or *RAD51AP1*-S2A (S277A, S282A). We chose clones for our experiments that expressed the ectopic RAD51AP1 proteins at similar levels (**Fig. 2.5A**). We then assessed these clones' cellular growth over the course of 9 days. Expression of RAD51AP1-S2D exhibited similar growth characteristics as WT protein and as parental RAD51AP1 KO cells. However, stable expression of the RAD51AP1-S2A protein in RAD51AP1 KO cells led to diminished cell growth that did not reach the levels of the WT and S2D expressing clones and of RAD51AP1 KO cells (**Fig. 2.5B**). By Day

4, there was a significant difference in growth among these cell lines due to the growth lag exhibited by RAD51AP1-S2A expressing cells.

To assess the effects of induced DNA damage, we subjected these cell lines to toxicity assays that tested cell survival after exposure to mitomycin C (MMC), a DNA cross-linking drug that is often used in chemotherapies and whose mechanism of action induces inter-strand crosslinks leading to DSBs. Previous publications show that RAD51AP1 knockdown or deletion in human or chicken cells leads to increased cellular sensitivity to DNA damaging agents (WIESE *et al*. 2007; MODESTI *et al*. 2007; HENSON *et al*. 2006; PARPLYS *et al*. 2014). As expected, KO cells were more sensitive to MMC compared to HeLa cells and RAD51AP1 KO cells ectopically expressing the RAD51AP1 protein (**Fig. 2.5D**). RAD51AP1 KO cells expressing the RAD51AP1-S2D protein mimicked the response of cells expressing the wild type protein. In contrast, RAD51AP1 KO cells expressing the RAD51AP1-S2A protein were significantly more sensitive to the cytotoxic effects by MMC exposure (**Fig. 2.5D**).

Cells respond to DNA damage by delaying the G2/M transition in order to prevent damaged chromosomes from being segregated during the cell cycle. When evaluating cell cycle progression, all cell lines exhibited similar completion of G1, S, and G2 phases without treatment (**Fig. 2.5C**). Upon treatment with MMC, cells expectedly exhibited extended G2 arrest, with S2A expressing cells showing the most prominent accumulation in G2 phase (**Fig. 2.5C**). Together, these results suggest that RAD51AP1-S2A expressing cells encounter higher and more lethal levels of DNA damage by MMC exposure compared to wild type and RAD51AP1-S2D expressing cells.

When dealing with DSBs, HR is the preferred cellular repair pathway in terms of fidelity (SCULLY *et al*. 2019). Cells defective in HR may display perturbed DNA replication as dictated

by stalled replication forks. Previous studies found that RAD51AP1 is essential for maintenance of DNA replication fork progression. Here, we sought to assess the role of S277 and S282 under perturbed DNA replication through utilization of the DNA fiber assay. We labeled exponentially growing cells with CIdU (red label), then HU-treated cells for 5 hours, and lastly switched cells with IdU-labeling (green) before cell lysis. We measured replication restart (green-labeled fibers) after HU treatment in each cell line. Preliminary results from one experiment showed that S2D and S2A expressing cell lines exhibited a degree of decreased elongation after HU treatment (**Fig. 2.5E**). There was also a significant difference between these cell lines before and after HU treatment, with S2A expressing cells having decreased elongation rates on both regards compared to S2D expressing cells. This is suggestive that the phosphorylation status of these residues may play a role in maintaining DNA replication forks.

To determine if the phenotype of RAD51AP1-S2A expressing cells was due to the combined effects of both S277A and S282A or due to mutation of one of these serines, we evaluated S277 and S282 individually through generation of cell lines expressing either S277A or S282A. Initial colony formation assays after chronic treatment with MMC revealed that the single mutants had no valuable effect against the cells' ability to form colonies (**Fig. S2.3C**). These findings further highlight the importance of these two residues jointly.

RAD51 and RAD51AP1 foci kinetics are altered in S2A expressing cells

To further investigate the role of S277 and S282 in HR, we tested if S2A and S2D would affect the formation or resolution of RAD51 foci, as a readout for HR capability. To this end, we treated WT, KO, S2A, and S2D cells with 8 Gy IR after 48 hours of growth on chamber slides.

We fixed cells that were non-treated at 4 h and also at 4 h, 8 h, and 24 h after IR treatment and then assessed their level of RAD51 foci via immunofluorescence. In terms of RAD51, neither RAD51AP1 variant affected the formation of RAD51 foci, highlighting that RAD51AP1 functions downstream of RAD51 presynaptic filament formation. Regarding downstream HR effects, deletion of RAD51AP1 in HeLa cells does delay RAD51 resolution (**Fig. 2.6A**, gray bars), as previously described (WIESE *et al*. 2007) and depicted by elevated RAD51 foci signals 24h after IR treatment, when WT-expressing cells (blue bars) have resolved RAD51 back to untreated control levels. Note that S2D expressing cells behaved like WT expressing cells (**Fig. 2.6A**, green bars) in terms of formation and resolution of RAD51 foci. In contrast, S2A expressing cells displayed kinetics comparable to KO cells, with more nuclei with RAD51 foci remaining at 24 h post exposure (**Fig. 2.6A**, red bars). These results show that S2A expressing cells, which lack phosphorylation ability at S277 and S282, exhibit an impairment of delay in the resolution of RAD51 foci.

We also evaluated RAD51AP1 foci, as an additional HR parameter. To induce RAD51AP1 foci, we treated WT, S2A, and S2D cells after 48 hours of growth on chamber slides with 20 Gy IR, a dose previously published to induce RAD51AP1 foci in HeLa cells (MODESTI *et al*. 2007) and ETK-1 cells (OBAMA *et al*. 2008). Our efforts to induce RAD51AP1 foci with 8 Gy IR were unsuccessful in our WT, S2D, and S2A expressing cells (but not HeLa cells) and may stem from lower RAD51AP1 protein expression by our WT, S2D, and S2A expressing cells compared to HeLa cells. We monitored formation of RAD51AP1 foci in non-treated cells at 8 h and in treated cells at 8 and 24 h after IR treatment. In sham-irradiated cells, RAD51AP1 foci levels were relatively similar, with about 20% of cells having more than 5 foci per nucleus (**Fig. 2.6B**). In treated cells at 24 h, both WT and S2D expressing cells (blue and green bars) formed RAD51AP1

foci, nearly doubling the number of cells with over 5 foci per nucleus (**Fig. 2.6B**). On the other hand, while S2A expressing cells (red bars) were able to form RAD51AP1 foci, foci levels remained considerably lower than in WT expressing cells and at levels similar to non-treated samples (**Fig. 2.6B**). These results highlight how lack of phosphorylation of these residues causes an impairment in the formation of RAD51AP1 foci upon DNA damage insult.

Discussion

Previous studies have provided clear evidence that RAD51AP1 possesses DNA binding activity towards various non-chromatin DNA substrates, with DNA interaction domains located in its N- and C-terminal regions that are crucial for D-loop formation and HR function (WIESE *et al*. 2007; MODESTI *et al*. 2007; PARPLYS *et al*. 2014 and 2015; DUNLOP *et al*. 2012; DRAY *et al*. 2010). Here, our studies show new associations of RAD51AP1 with a chromatin DNA substrate, mimicked by the NCP, and with histone H3 that mainly occur by interaction through its C-terminal domain. Importantly, while bound to NCP, RAD51AP1 remains capable of interacting with RAD51 (also through its C-terminus). Additionally, we have found in this study that RAD51AP1-RAD51 is proficient in the duplex capture of chromatinized DNA. Our findings are in line with past reports that support the importance of the C-terminus of RAD51AP1 during the HR reaction in stimulating the D-loop. An association between NCP and RAD51AP1 provides new insights into how this important HR player may be functioning during synapsis and D-loop steps of HR, where chromatin presents as a barrier on the intact sister chromatid that serves as the template for homologous pairing and heteroduplex formation. Our findings support the idea that RAD51AP1 provides a bridging function between the chromatinized dsDNA template and the RAD51 presynaptic filament, and this may help alleviate the chromatin barrier to maintain HR.

Furthermore, our efforts have elucidated two RAD51AP1 residues within its C-terminal domain that are important for the *in vitro* interaction with the NCP: S277 and S282. We show that mutations of these two residues that mimic phosphorylation compromise the NCP binding ability of RAD51AP1. Interestingly, while our biochemical assays assessing DNA interaction of the phospho-mimic S2D mutant revealed mildly decreased binding towards NCP, S2D-expressing cells did not exhibit an overt phenotype and behaved much like WT-expressing cells. This could be primarily attributed to the divergent settings of these experiments, in which the EMSAs were performed using isolated components of purified protein and NCP, in contrast to the cellular environment that contains not only these components but a slew of other HR players, cellular signaling factors, and complex pathways at work. The organization of DNA in cells is also not normally isolated as NCP substrates but is rather organized in higher order structures that further compact chromatin into the cell nucleus. Thus, the subtlety that we observed of the reduced NCP interaction by S2D may explain the lack of a cellular phenotype in our studies.

Another explanation about the lack of a phenotype in S2D-expressing cells could be related to proper cellular signaling and response when facing DNA damage. In the case of S2D, the affected residues mimic phosphorylation, and this phosphorylation status could serve the RAD51AP1 protein best for proper DNA damage response and HR pathway signaling and may potentially allow S2D-expressing cells to manage DNA damage passably. Previous studies that have identified these residues as phosphorylation sites that are induced upon specific types of DNA damage exposure support this view (ELIA *et al*. 2015; BELI *et al*. 2012). The loss in ability to phosphorylate these residues in S2A-expressing cells clearly demonstrate a strong phenotype that negatively impacts cells' ability to grow under unperturbed conditions, repair induced DSBs, proceed through the cell cycle, resolve RAD51 in a timely manner after induced DNA damage,

and form RAD51AP1 foci adequately in response to induced DNA damage, when compared to cells expressing the WT or phosphorylation mimic (S2D) protein. Collectively, our results indicate that the ability of RAD51AP1 to be phosphorylated at S277 and S282 is significant for its proper function and stability in HR and DNA damage responses in cells, to both spontaneous and induced DNA damage.

We note that S2A-expressing cells, like RAD51AP1-deficient cells, show no defect in the formation of RAD51 foci upon IR treatment (**Fig. 2.6A**). Rather, the defect occurred during resolution of foci, in which foci remained elevated at 24 h. Additionally, we see that S2A-expressing cells are able to form RAD51AP1 foci but were unable to induce foci after IR treatment, compared to WT- and S2D-expressing cell levels (**Fig. 2.6B**). To test for protein folding impacts, we performed co-immunoprecipitation experiments and found that S2A in cells was able to associate with proteins that interact with WT and S2D (data not shown), suggesting that protein folding is not the root issue that explains the detrimental effects by S2A expression in cells. Altogether, these findings suggest that the phosphorylation of these residues plays a crucial late role in regulating the protein's activities in the HR reaction after pre-synaptic filament formation. Additionally, given the implications of RAD51AP1's involvement in other cellular processes, it may be possible that suppressing the affinity of RAD51AP1 to the chromatinized DNA template via phosphorylation affects other functions of this protein beyond the scope of our studies presented here.

Despite the critical cellular role unveiled of phosphorylating these two residues in RAD51AP1, much remains to be learned about the responsible kinases. Previous proteomic studies have showed that RAD51AP1 gets phosphorylated at S120 by ATR or ATM kinases (MATSUOKA *et al*. 2007), which are involved in the DNA damage response. The cyclin-dependent kinases

(CDKs) are other potential kinases that regulate cell division and progression through the cell cycle as well as have been shown to participate in the DNA damage response and regulate important HR players. The kinase CDK1 phosphorylates BRCA1 at multiple sites, and its depletion in cancer cells has been shown to render cells HR-defective and sensitive to PARP inhibition (JOHNSON *et al*. 2012). In the yeast model system, Rad51 was shown to be activated by CDK1-dependent phosphorylation, and phosphorylation regulated the binding of Rad51 to DNA (LIM *et al*. 2020). *In situ* phosphorylation has also identified RAD54, a protein with largely overlapping roles as RAD51AP1 in HR, as a target of the kinase CDK2, and direct CDK2 phosphorylation of RAD54 was confirmed with immunoprecipitation methodology from HEK293 cells (CHI *et al*. 2020). Additionally, phosphorylation of RAD54 at CDK2 consensus sites inhibited its ability to oligomerize to perform its translocating activity and branch migration of Holliday junctions but did not prevent its ability to stimulate RAD51 (GOYAL *et al*. 2018). CDKs phosphorylate proteins in a proline-directed fashion on either serine or threonine, and it is believed that SP or TP motifs represent the minimal CDK consensus motif. S277 in RAD51AP1 does adhere to an SP motif (underlined: 277-**SP**SAES-282), leading us to presume that CDKs may be involved in the phosphorylation of this region as well as in the regulation of the activities of RAD51AP1.

In summary, our findings unveil new mechanistic and cellular functions of the RAD51AP1 protein, regarding its interaction with NCP and the significance of two of its phosphorylation sites in impacting NCP interaction and HR capability in cells. Our models that depict the binding of the RAD51AP1 protein with naked dsDNA, chromatinized dsDNA, and RAD51 during intermediate HR stages as well as how the modified states of RAD51AP1 affect HR function are illustrated and described in **Chapter 4**.

Figures

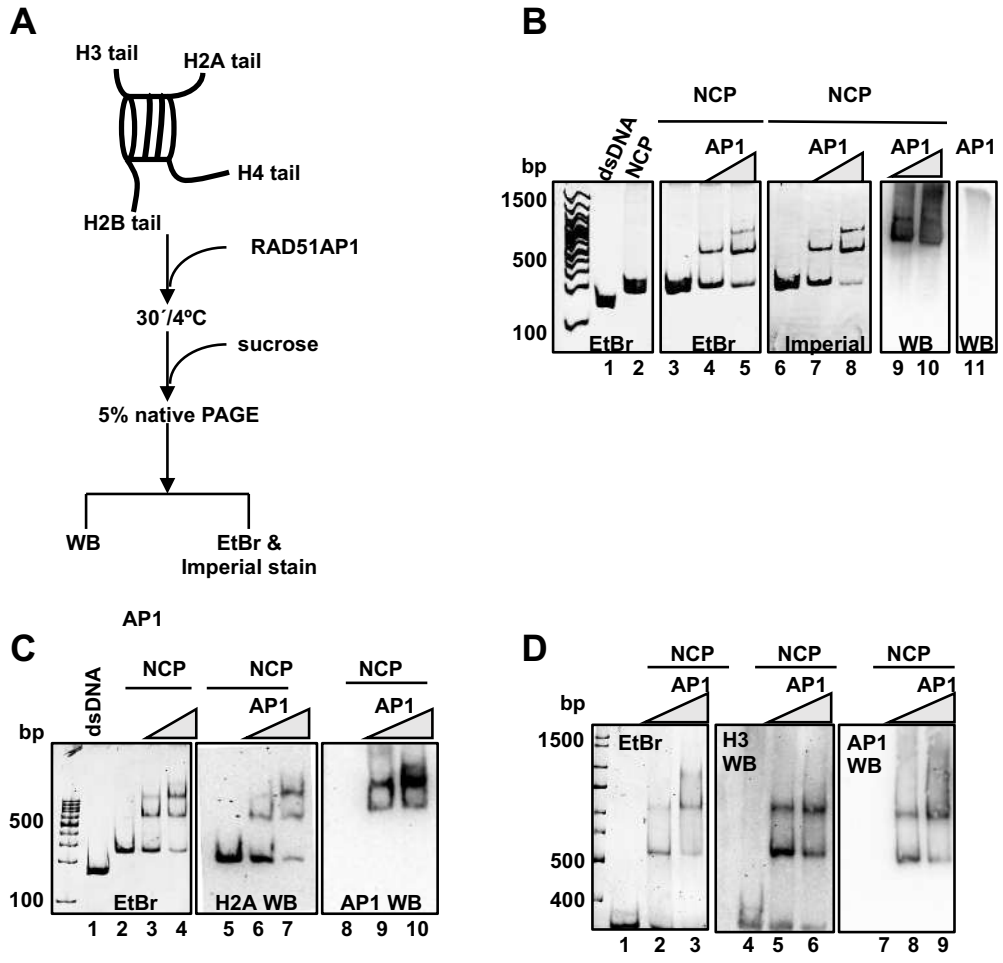

Figure 2.1 RAD51AP1 interacts with the nucleosome core particle (NCP)

(A) Schematic of NCP and the EMSA protocol. (B-D) Native-PAGE gels and western blots of EMSAs. In Panel B, results of the EMSA involving NCP and RAD51AP1 (0.1 and 0.2 uM) are visualized by ethidium bromide (EtBr) and Coomasie (Imperial) staining. The western blots show the presence of RAD51AP1 entering the gel only when bound to NCP (lanes 9 and 10), not alone (lane 11). In Panels C and D, results of the EMSA involving NCP (0.4 uM) and RAD51AP1 (Flag-His tagged; 0.476 and 0.952 uM) are visualized by ethidium bromide (EtBr). Western blot analyses indicate the presence of NCP components (H2A and H3) and RAD51AP1 at the mobility shifts (in C - lanes 6, 7, 9, and 10; in D - lanes 5, 6, 8, and 9).

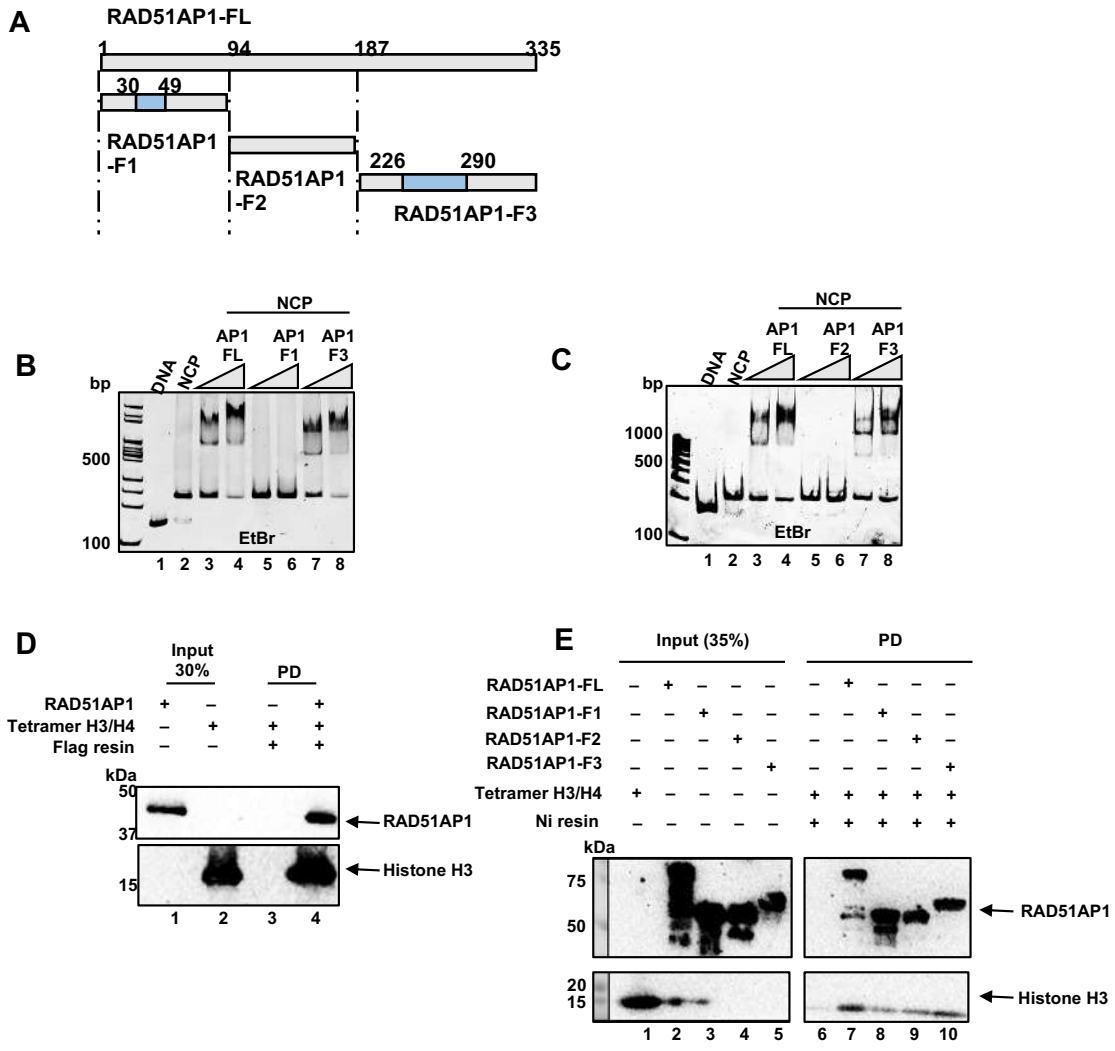

Figure 2.2 The interaction between RAD51AP1 and NCP and histones occurs at its C-terminal DNA-binding domain

(A) Schematic of the RAD51AP1 fragments (F1, F2, and F3) generated for studying individual DNA-binding domains (regions indicated in blue boxes). (B-C) RAD51AP1 variants (0.1 and 0.2 uM) were incubated with NCP (0.2uM; as described in **Fig 2.1A**), and mobility shifts were observed, with full-length (F.L.) as positive control (lanes 3-4). Binding of NCP with F1 or F2 did not result in a mobility shift (lanes 5-6), while F3 did (lanes 7-8). (D-E) Nickel and FLAG pull-down assays between RAD51AP1 variants and H3/H4 histone tetramer. Tetramer mostly bound to F.L. and F3 (in D – lanes 7 and 10; in E – lane 4). [Panel D data by Neelam Sharma]

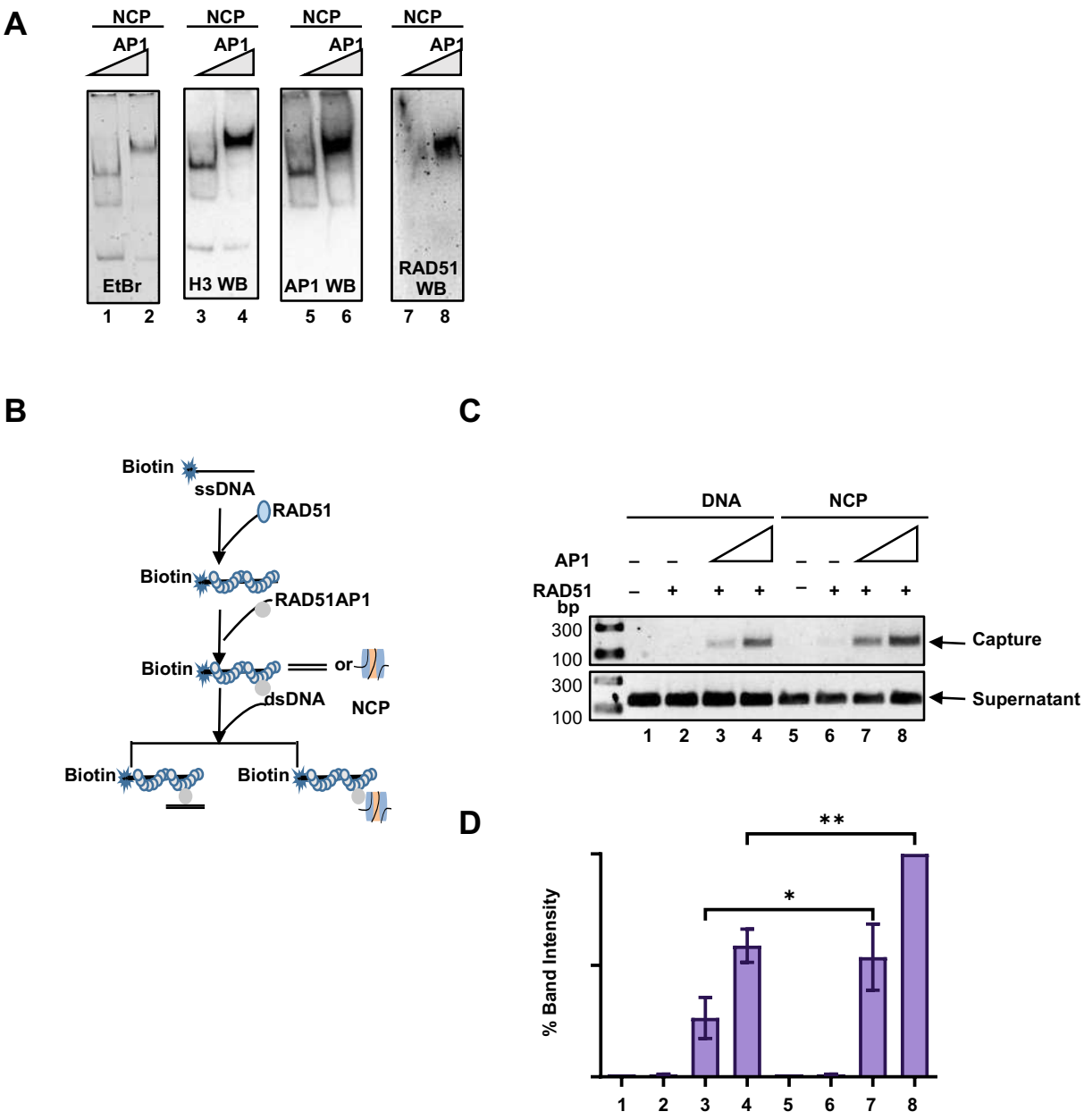

Figure 2.3 Function of RAD51AP1 in binding RAD51 and chromatinized dsDNA duplex capture

(A) Western blots after RAD51AP1-NCP EMSA to examine components of mobility shifts and Far Western analysis (lanes 7-8) to examine RAD51AP1-NCP for RAD51 interaction. (B) Schematic of duplex capture assay. (C-D) Agarose gel and O.D. analysis of duplex capture by RAD51AP1-RAD51 for dsDNA and NCP. Bars are the means from three experiments: $\pm$ 1SEM; *, $P < 0.05$; **, $P < 0.01$; two-way ANOVA analysis. [Panels C-D data by Neelam Sharma]

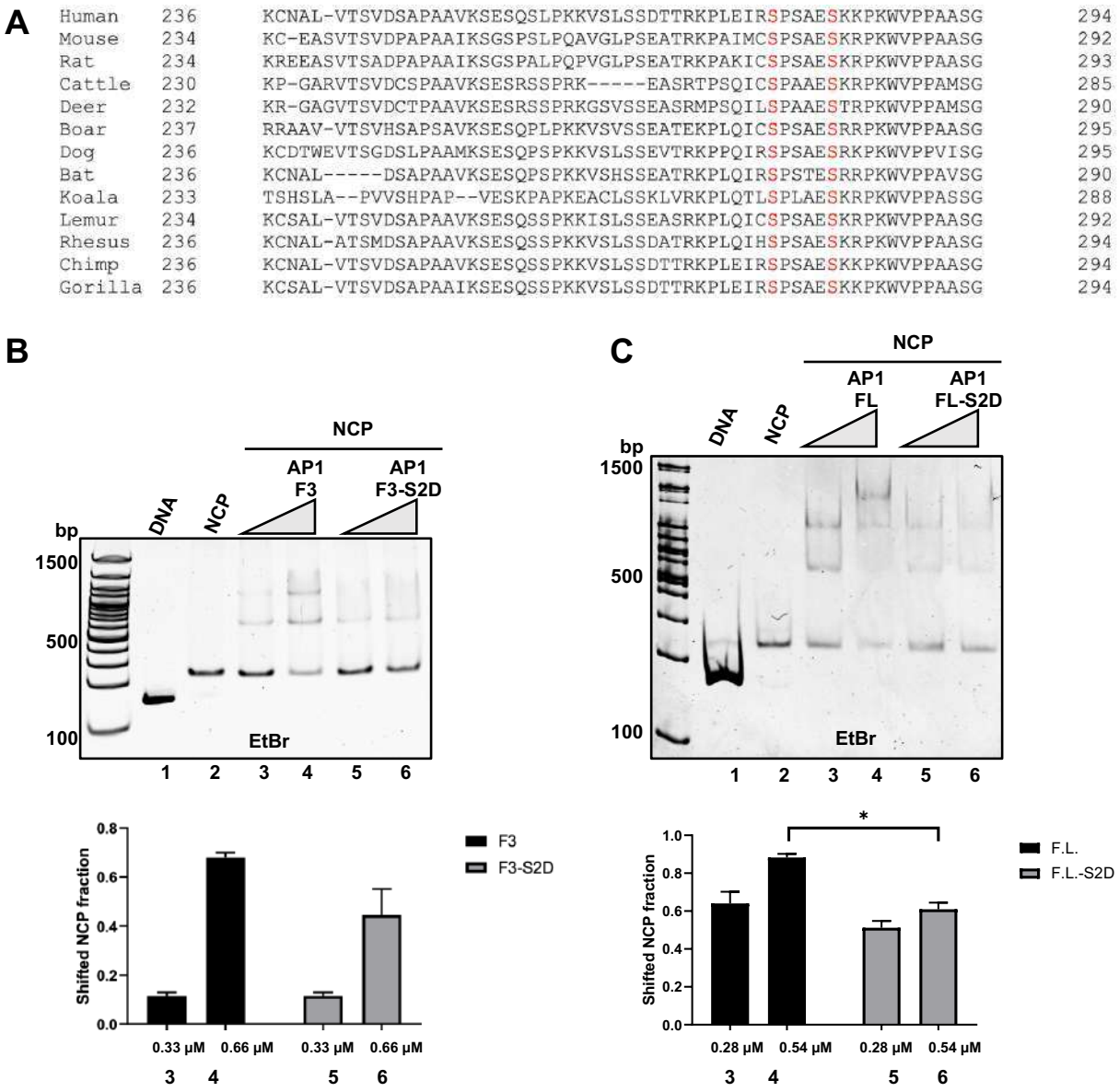

Figure 2.4 RAD51AP1 mutants attenuated in binding with NCP

(A) ClustalW sequence alignment of human and other mammalian RAD51AP1, with S277 and S282 residues conserved and shown in red. (B-C) NCP was incubated with RAD51AP1 and variants; F3 or F.L. were positive controls (lanes 3-4), and F3-S2D or F.L.-S2D were tested mutants (lanes 5-6). Native-PAGE gel and O.D. analyses of NCP mobility shifts are shown. Bars are the means from two (B) and three (C) experiments $\pm$ 1SEM; *, $P < 0.05$; two-way ANOVA analysis.

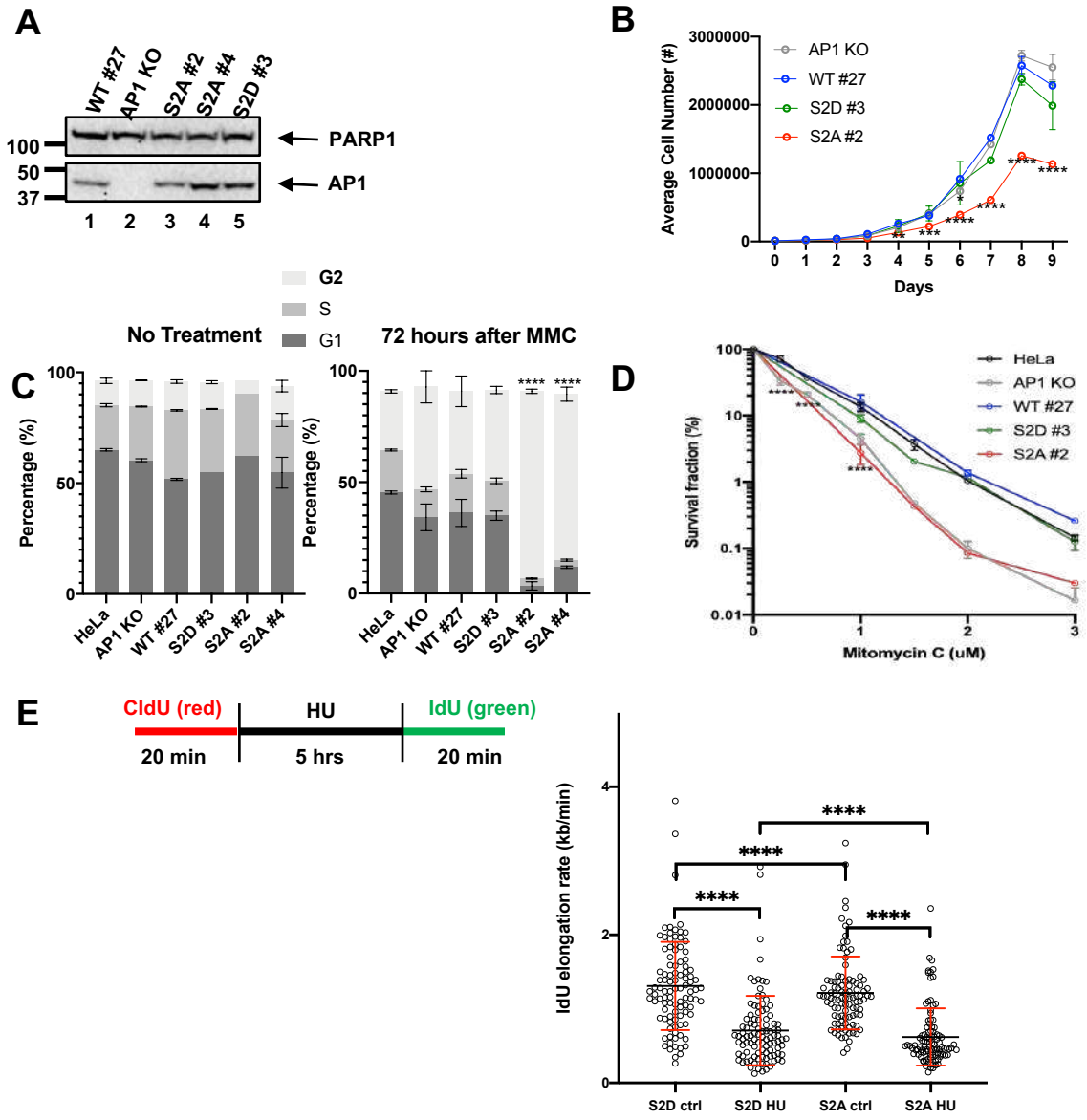

Figure 2.5 Characterization of RAD51AP1-S2A- and S2D-expressing derivatives of HeLa RAD51AP1 KO cells

(A) Western blot to indicate expression levels of RAD51AP1 in cell lines utilized for our studies; PARP1 served as the loading control. (B) Cell growth analysis of the aforementioned cell lines in regular growth medium over the course of 9 days. Data from two independent experiments +/- 1SEM; ****, $P < 0.0001$; two-way ANOVA analysis. (C) Cell cycle progression after MMC treatment via flow-cytometry analysis. Data from two independent experiments +/- 1SEM; *, $P <$

0.05; ***, $P < 0.001$; ****, $P < 0.0001$; two-way ANOVA analysis. (D) Results from MMC cell survival assays. The percentage of surviving cells are shown as the mean from three independent experiments +/- 1SEM; ****, $P < 0.0001$; two-way ANOVA analysis. (E) Schematic of the DNA labeling protocol used for the DNA fibers assay and subsequent graph of IdU measurements in un-treated controls and HU-treated samples; the data plotted are the measurements of 100 fibers per group from one experiment; ****, $P < 0.0001$; Tukey's multiple comparisons test. [Panels A-D data by Neelam Sharma and Platon Selemenakis; Panel E data is by Claudia Wiese, Neelam Sharma, and Elena Pires]

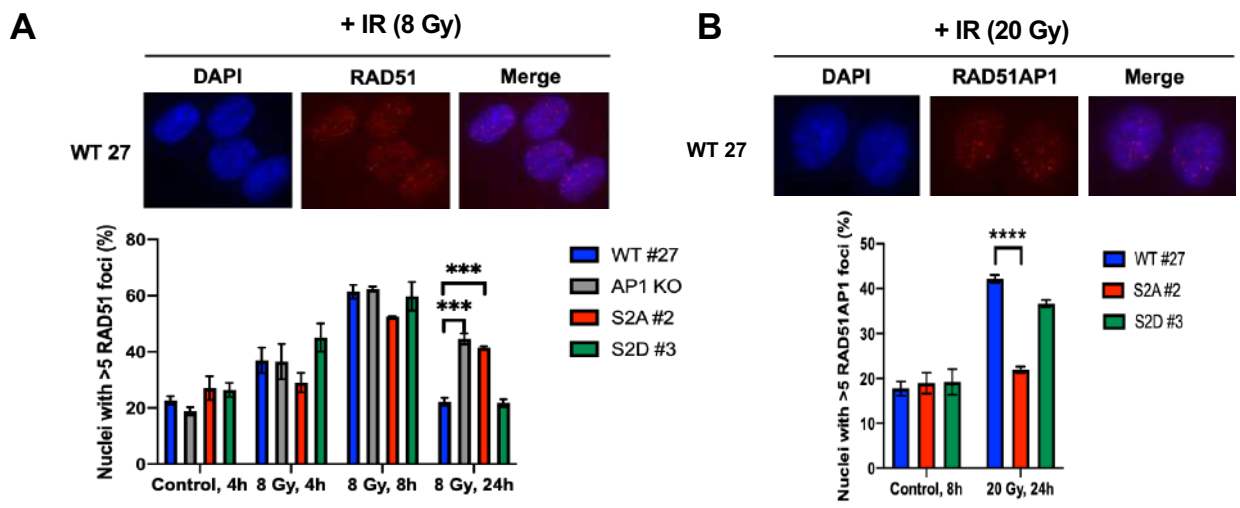

Figure 2.6 Role of RAD51AP1-S2A and S2D in cellular foci kinetics of HR markers

(A) Representative micrographs of RAD51AP1 WT-expressing RAD51AP1 KO nuclei 8 h after 8 Gy, DAPI (blue) and RAD51 (red). Quantification of RAD51 foci: bars are the means from three independent experiments ± 1SEM; ***, $P < 0.001$; two-way ANOVA analysis. (B) Representative micrographs of RAD51AP1 WT-expressing RAD51AP1 KO cells 24 h after 20 Gy, DAPI (blue) and RAD51AP1 (red). Quantification of RAD51AP1 foci: bars are the means from three independent experiments ± 1SEM; ****, $P < 0.0001$; two-way ANOVA analysis.

Tables

Table 2.1 List of constructs used for protein expression and isolation from *E. coli*

#	Expression Vector	Protein Tags	Construct
1	pET24a	N-terminal MBP C-terminal 6xHis	FL, F1, F2, F3, C60, F3-S2D, F3-K4A, F3-K4A1, F3-K4A2, F3-K3WA, F3-K3WA1, F3-K3WA2, F3-K1Q, F3-S2D, F3-S2D1, F3-S2D2
2	pQE-TriSystem His-*Strep* 2	N-terminal 8xHis C-terminal Strep-tag II	FL, F3, F3-S2D, F3-N88, C60, F3-S3D
3	pQE-80L	N-terminal 6xHis C-terminal FLAG	FL, FL-S2D

Table 2.2 List of oligonucleotides used as primers for site-directed mutagenesis

#	Construct	Primer Name	Primer Sequence (5'-3')
1	F3-S2D, FL-S2D	S2D Forward	gctgaagacAAGAAACCTAAATGGGTC
2		S2D Reverse	tgaaggatcGCGTATTTCTAATGGTTTC
3	F3-S2D1	S2D 1 Forward	gctgaaagcAAGAAACCTAAATGGGTC
4		S2D Reverse	tgaaggatcGCGTATTTCTAATGGTTTC
5	F3-S2D2	S2D Forward	gctgaagacAAGAAACCTAAATGGGTC
6		S2D 2 Reverse	tgaaggactGCGTATTTCTAATGGTTTC
7	F3-S3D	S2D Forward	gctgaagacAAGAAACCTAAATGGGTC
8		S3D Reverse	atcaggatcGCGTATTTCTAATGGTTTC
9	S2A	S2A Forward	gctgaagccAAGAAACCTAAATGGGTC
10		S2A Reverse	tgaaggagcGCGTATTTCTAATGGTTTC
11	S2A1	S2A1 Forward	gctgaaagcAAGAAACCTAAATGGGTC
12		S2A1 Reverse	tgaaggagcGCGTATTTCTAATGGTTTC
13	S2A2	S2A2 Forward	gctgaagccAAGAAACCTAAATGGGTC
14		S2A2 Reverse	tgaaggactGCGTATTTCTAATGGTTTC
15	K1Q	K1Q Forward	AGCACGAGTTcaaCCTTTGCATC
16		K1Q Reverse	AATCTGGACAAGCCGAGG
17	K3WA	K3WA Forward	tgcagcgGTCCCACCAGCGGCATCT
18		K3WA Reverse	ggtgccgcGCTTTCAGCTGAAGGACTGC
19	K3WA1	K3WA 1 Forward	AGCTGAAAGCgcggcaCCTAAATGGGTCC
20		K3WA 1 Reverse	GAAGGACTGCGTATTTCTAATG
21	K3WA2	K3WA 2 Forward	CAAGAAACCTgcagcgGTCCCACCAGC
22		K3WA 2 Reverse	CTTTCAGCTGAAGGACTG
23	K4A	K4A Forward	gcatccgcaTGTAATGCTTTGGTGACTTC
24		K4A Reverse	agatgccgcCTCTTTCTTTTCTACTGGGG
25	K4A1	K4A 1 Forward	AAAGAAAGAGgcggcaTCTAAATCCAA ATGTAATGC
26		K4A 1 Reverse	TCTACTGGGGATTTTACC
27	K4A2	K4A 2 Forward	cgcaTGTAATGCTTTGGTGACTTC
28		K4A 2 Reverse	gatgcAGATTTCTTCTCTTTCTTTTCTAC

These primers were generated with NEBasechanger (nebasechanger.neb.com). Mutated or inserted nucleotides are written in lower case characters.

Table 2.3 List of oligonucleotides used as primers for generating protein fragments

#	Tags	Construct	Primer Name	Primer Sequence (5'-3')
1	HS	F3	F3-HS2 Forward	TAAGCAGGATCCTGATTCTGAGGAT GATTCTGATTTTTGTGAGAG
2			F3-HS2 Reverse	TAAGCAAAGCTTGGTGCTAGTGGCA TTTGGATGCAAAGGTTTAA
3	HS	C60	C60-HS2 Forward	TAAGCAGGATCCTCGCAGTCCTTCA GCTGAAAGCAA
4			F3-HS2 Reverse	TAAGCAAAGCTTGGTGCTAGTGGCA TTTGGATGCAAAGGTTTAA
5	HS	F3-N88	Updated N88 Forward	TAAGCAGGATCCTGATTCTGAGGAT GATTC
6			New F3-N88 Reverse	TAAGCAAAGCTTTATTTCTAATGGTT TCCTAGT
7	HF	FL	Forward	ATCGGGATCCGTGCGGCCTGTGAGA CATAAGAAACC
8	HF	FL	Reverse	CGATGTCGACTCATTTATCGTCATCG TCTTTGTAATCACCGGTGCTAGTGGC ATTTGGATGCAAAGG

HS = N-terminal His_8, C-terminal Strep-tag II
HF = N-terminal His_6, C-terminal FLAG tag

Table 2.4 Antibodies and concentrations used in this study

Antibody	Species	Brand	Application	Concentration
Anti-RAD51	Rabbit	Millipore (cat. PC130)	Immunofluorescence Western Blot	1:1000 1:4000
Anti-RAD54	Mouse	Santa Cruz (cat. 374598)	Immunofluorescence	1:500
Anti-RAD51AP1	Rabbit	Novus (cat. NBP2-13197)	Immunofluorescence	1:5000
Anti-H2A	Rabbit	GeneTex (cat. GTX12918)	Western Blot	1:10,000
Anti-H2B	Rabbit	Millipore (cat. 07-371)	Western Blot	1:500
Anti-H3	Rabbit	Abcam (cat. 1791)	Western Blot	1:10,000
Anti-FLAG	Mouse	Sigma (cat. A8592)	Western Blot	1:2,000
Anti-HA	Mouse	BioLegend (cat. MMS-101P)	Western Blot	1:1,000
Anti-His6-HRP	Mouse	Sigma (cat. 91K4885)	Western Blot	1:2,000
Anti-PARP1	Rabbit	Abcam	Western Blot	1:5,000
Anti-rabbit Alexa Fluor 594	Goat	Invitrogen (cat. A21121)	Immunofluorescence	1:750
Anti-mouse Alexa Fluor 488	Goat	Invitrogen (cat. A11037)	Immunofluorescence	1:750
Anti-rabbit IgG, HRP-conjugated	Goat	Jackson ImmunoResearch Laboratories (cat. 111-035-045)	Western Blot	1:10,000
Anti-mouse IgG, HRP-conjugated	Goat	Jackson ImmunoResearch Laboratories (cat. 115-035-062)	Western Blot	1:10,000

Table 2.5 List of buffers used in this study

Buffer	Application	Composition
Lysis buffer	Protein Purification	50 mM Tris-HCl pH 7.5, 300 mM KCl, 1 mM EDTA, with Protease Inhibitor Cocktail
Wash buffer	Protein Purification	50 mM Tris-HCl pH 7.5, 300 mM KCl, 1 mM EDTA, 50 mM Imidazole
Elution Buffer	Protein Purification	50 mM Tris-HCl pH 7.5, 300 mM KCl, 1 mM EDTA, 300 mM Imidazole
Dialysis Buffer	Protein Purification	50 mM Tris-HCl at pH 7.5, 3M KCl, 0.5M EDTA, 2M DTT, 20% glycerol, 0.01% NP-40
Reaction Buffer	EMSA	40 mM Tris-HCl at pH 7.5, 100mM NaCl
Buffer A	Duplex Capture Assay	25 mM HEPES (pH 7.5), 50 mM Tris-HCl (pH 7.5), 2 mM ATP, 1 mM DTT, 0.2 mM B-mercaptoethanol, 2% glycerol, 35 mM NaCl, 45 mM KCl, 1 mM MgCl2, 0.16 mM EDTA, 0.4 mM Mercaptoethanol, 0.01% NP-40, and 100 μg/ml BSA
Binding Buffer	FLAG Pull-down	50 mM Tris-HCl (pH 7.5), 150 mM NaCl, 0.25% Triton X-100, and 100 μg/ml BSA
Eluting Buffer	FLAG Pull-down	50 mM Tris-HCl (pH 7.5), 150 mM NaCl, 0.25% Triton X-100, and 100 μg/ml BSA, 3X FLAG peptide (150 ng/ul)
Ni Binding Buffer	Ni Pull-down	20mM Tris-HCl (pH 8.0), 100 mM NaCl, 30 mM imidazole, and 2% BSA
Ni Wash Buffer	Ni Pull-down	20mM Tris-HCl (pH 8.0), 200 mM NaCl, 50 mM imidazole, and 0.2% Tween 20
Ni Elution Buffer	Ni Pull-down	20mM Tris-HCl (pH 8.0), 200 mM NaCl, 50 mM imidazole, and 0.2% Tween 20, 500 mM Imidazole
Transfer Buffer	Western Blot	25 mM Tris-Cl, 250 mM glycine, 0.1% SDS, and 10% methanol

TBST	Western Blot	Tris-buffered saline with 0.1% Tween-20
Buffer B	Far Western Blot	10 mM KH2PO4 (pH 7.4), 150 mM KCl, 15 mg/ml BSA, 2 mM 2-mercaptoethanol and 0.05% Tween 20
Block Buffer	DNA Fibers Assay	5% BSA, 1X PBS, 0.1% Triton X-100

CHAPTER THREE

Effects of Rad51ap1 loss on murine fertility and spermatogenesis: implications for meiotic HR[3]

Summary

RAD51AP1 is an important factor in homologous recombination (HR) DNA repair, a significant cellular process employed in both mitosis and meiosis. While much has been learned about the function of RAD51AP1 in HR biochemically and in the context of mitotic cells, the impacts of *Rad51ap1* loss on tissue homeostasis remains to be characterized in an animal model. Unfortunately, orthologs of RAD51AP1 do not present in a number of common laboratory model systems such as *D. melanogaster*, *C. elegans*, or *S. cerevisiae*, causing impediment in assessing its biological function at the whole-animal level. Most recently, a *Rad51ap1* KO mouse (*Rad51ap1*$^{tm1.1(KOMP)Vlcg}$) has become accessible. Remarkably, this mouse is viable and fertile, allowing for the study of its phenotype and consequences of *Rad51ap1* deletion, which is crucial for assessing impacts of the HR process in mammals.

This chapter will focus on the study of a novel *Rad51ap1* mouse knockout model and will expose, for the first time, the biological impacts of its loss on mammalian health, with particular focus on reproductive parameters and meiotic HR. Given the interaction between RAD51AP1 and the meiotic recombinase DMC-1 during meiosis as well as the elevated expression of RAD51AP1 in murine testes, we hypothesized that loss of *Rad51ap1* in mice would lead to compromised male fertility and impaired spermatogenesis. Histology and immunohistochemical analyses of mutant testes revealed that, while fertility and meiosis progression endured, loss of *Rad51ap1* impacted late spermatogenesis in mice.

---

[3]*A version of this chapter will be submitted as part of a manuscript.*

Introduction

The success of species in relation to fertility and offspring health primarily depend on the production of gametes with intact genomes. Germ cells must preserve genomic integrity in order to ensure that intact genetic information is passed onto future generations. Particularly important to this process is the proper synapsis and segregation of chromosomes during Prophase I, the first meiotic division, which relies heavily on homologous recombination (HR), a high-fidelity DNA repair process of complex DNA damage, such as double-strand breaks (DSBs) (DALEY *et al*. 2013 and 2014; KREJCI *et al*. 2012; JACKSON *et al.* 2009). Errors in HR may lead to severe meiotic phenotypes such as aneuploidy, a state of having abnormal chromosome numbers in a cell, often due to nondisjunction. Consequences of aneuploidy in meiosis are a major cause of infertility, miscarriage, and congenital birth defects, such as Down syndrome (trisomy of chromosome 21) and cancer (DURRBAUM *et al.* 2015; LAMB *et al.* 2005; HOLLAND et al. 2012; GORDON et al. 2012).

During meiosis, HR is initiated by SPO11-induced DSBs (KEENEY *et al.* 1997) and is mediated by RAD51 and DMC-1, recombinases that are orthologs of bacterial RecA. Like RecA, RAD51 and DMC-1 form a recombinase-ssDNA nucleoprotein filament (presynaptic filament), that accommodates incoming duplex DNA in the search for homology and facilitates homolog pairing and synapsis (HUNTER 2006; PAGE *et al.* 2003). Synaptonemal complexes (SCs), tripartite proteinaceous structures with zipper-like morphology, assist in connecting homologous chromosomes along their lengths as they pair (ZICKLER 2006; YANG et al. 2009; QIAO *et al*. 2012). This pairing of homologous chromosomes is believed to stabilize their interactions and promote the exchange of genetic information via crossover events, which are critical for proper meiotic chromosome segregation and which also give rise to the valuable genetic diversity of species

(MARTINEZ-PEREZ *et al.* 2009; HUNTER 2006). These complex processes of meiosis occur during Prophase I, further sub-divided into leptotene, zygotene, pachytene, diplotene, and diakinesis phases (BELLVE *et al.* 1977; GUNES *et al.* 2015), and the progression of these phases can be visualized with markers for SCs (**Fig. 3.4A**).

A variety of RAD51 and DMC-1 recombinase-interacting proteins that enhance the HR reaction have been identified and include RAD51-associated protein 1 (RAD51AP1). Studies on RAD51AP1 exposed its ability to enhance the D-loop reaction with both RAD51 and DMC-1 filaments (DRAY *et al*. 2011; DUNLOP *et al*. 2011). Mutagenic protein studies using spliced and mutant variants of RAD51AP1 revealed that its interaction and cooperation of the D-loop reaction with RAD51 and DMC-1 occur via separate binding regions on RAD51AP1, further highlighting its unique function in meiotic HR (DUNLOP *et al*. 2011).

The *RAD51AP1* gene belongs to the RAD52 epistasis group and is highly conserved among mammals (PARPLYS *et al*. 2014). Since RAD51AP1 is a mostly vertebrate-specific protein (**Fig 3.1**), it is not present in common laboratory animal models, such as *D. melanogaster*, *C. elegans*, or *S. cerevisiae*, making assessment of its biological function challenging. However, a novel *Rad51ap1* KO mouse (*Rad51ap1*$^{tm1.1(KOMP)Vlcg}$) has become recently available and is viable and fertile, allowing for studies on its phenotypic traits and consequences of *Rad51ap1* loss. Studies in wild-type mice reveal that the RAD51AP1 transcript is elevated in multiple organs and has the highest expression in murine testes (MIZUTA *et al.* 1997), which correlates with what has been shown in humans (OBAMA *et al*. 2008). Given the embryonic lethality associated with disruption of *Rad51* and other HR players in the RAD52 epistasis group in mice (RICHARDSON 2005), exploring the effects of a disrupted *Rad52* epistasis group gene in a viable mouse is advantageous towards better understanding the biological impacts of the HR process in mammals.

Since RAD51AP1 expression is highly abundant in testes and enhances the D-loop reaction with meiotic recombinase DMC-1, we speculated that RAD51AP1 has an essential function in meiotic HR, and its loss would lead to some detrimental effect to male reproductive biology. Hence, we sought to investigate this hypothesis via study of male *Rad51ap1* KO mice. To test if *Rad51ap1* is required for HR and/or synapsis during meiosis, we analyzed the assembly of the synaptonemal complex in prophase spermatocytes of wild-type control and mutant *Rad51ap1* KO mice, by immunostaining surface-spread spermatocytes for the axial/lateral element SCP3 as well as for DSB marker γH2AX. To note appropriate maturation, progression, and phenotype of male germ cells (**Fig. S3.1**), we also analyzed hematoxylin and eosin (H&E)-stained cross sections of testes. Determining these biological attributes of the *Rad51ap1* mouse knockout model will unveil the relevance of RAD51AP1 in HR processes within a viable animal system.

Materials and Methods

Generation of Rad51ap1-deficient Mice

The *Rad51ap1*$^{tm1.1(KOMP)Vlcg}$ mouse has been the product of the efforts of the Jackson Lab and the NIH Knockout Mouse Project at University of California Davis and are of a pure C57BL/6N genetic background. The Wiese lab has been able to purchase these mice and intercross them to obtain desired genotypes: wild-type, heterozygous, and knockout. Breeding results of this intercross are stated in **Table 3.1**. Cohorts and ages of male mice used in this study are described in **Table 3.2**. Mice were genotyped with tail and/or ear punch samples by PCR, using a primer set designed to detect the wild-type specific product and a primer set designed to detect the mutant-specific product (**Fig. 3.2A**).

Histology and Staining

For H&E staining, testes were dissected and fixed in neutral buffered formalin before being sectioned and stained by the CSU Diagnostic Medical Center. Images were analyzed with a Zeiss Axio-Imager.Z2 microscope by 20X lens and EVOS Cell Imaging System by 20X lens. Testes were evaluated for their spermatogenic index (SI) by Johnson's score (Johnson *et al.* 1970). A score from 1 to 10 was given to each tubule cross section, according to the range from no cells to complete spermatogenesis. Mutant testes were additionally evaluated for abnormalities observed in tubule cross sections, following a severity grading scale recommended by the OECD (Organization for Economic Co-operation and Development).

Meiotic Chromosome Surface Spreads from Mouse Spermatocytes

Testes were prepared for study of meiosis via chromosome surface spread methodology (DIA *et al.* 2017) that yields nuclei undergoing substages of Prophase I. Briefly, isolated testes with the tunica removed had their weights recorded before 1 hour incubation in 10mL cold HEB buffer (30 mM Tris-Cl at pH 8.2, 50 mM sucrose, 17 mM Trisodium citrate dihydrate, 5 mM EDTA, 0.5 mM dithiothreitol, 0.1 mM phenylmethylsulfonyl fluoride), to allow hypotonic swelling of meiotic cells. During incubation, clean slides were labeled and placed in fixative solution (1% paraformaldehyde, 0.15% Triton X-100, pH 9.2). After incubation, seminiferous tubules of the testis were separated into 3 mm clumps, which were then soaked in 23 µl of 100 mM sucrose solution. The tubules were minced until the solution became cloudy, before another 23 µl addition of the sucrose solution. After gentle pipetting of the mixture, 20 µl of the sucrose cell suspension was added at the bottom corner of a prefixed slide, and careful tilting of the slide allowed the droplet to spread the cell suspension across the length of the slide. Slides were

incubated in a covered chamber at room temperature for 2.5 hours as well as an additional 30 minutes uncovered, to allow slides to dry before two 5-minute washes in 1X PBS solution. Dried slides were stored in -80°C or processed immediately for immunostaining.

Immunocytochemistry of Meiotic Chromosomes

For staining of slides, slides were first brought to room temperature and washed one time with 1X PBS solution. Slides were then blocked for 30 minutes at room temperature in 1X PBS buffer containing 1% BSA. Primary antibodies were diluted in 1X PBS solution containing 1% BSA. To each slide, 150 µl of primary antibody solution was added before use of coverslip and overnight incubation in a humidified chamber at 4°C. The following morning, slides were washed twice in 1X PBS solution and incubated with secondary antibodies diluted in 1X PBS solution for 45 minutes. After incubation, slides were washed twice in 1X PBS before mounting with DAPI. Visualization and analysis of Prophase I phases on slides were done with a Zeiss Axio-Imager.Z2 microscope by 63X oil lens. Antibodies and concentrations used are described in **Table 3.4**.

Statistics

To evaluate the variance in the expected and observed Mendelian inheritance after mice breeding, P-values of the Mendelian ratios were calculated with the Chi-square (X) test and were either significant if $p < 0.05$ or not significant (n.s). To evaluate the significance of changes between wild-type and *Rad51ap1* knockout groups after Johnson SI scoring, student's t-test was used. All statistical tests were performed on Prism 8 software.

Results

Rad51ap1-deficient mice are viable, and heterozygous intercross breeding displays a non-Mendelian ratio

Interbreeding heterozygous *Rad51ap1* mutant mice resulted in a non-Mendelian ratio at weaning, with a decrease in both wild-type and *Rad51ap1* knockout mice (**Fig. 3.2**). There were no obvious phenotypic abnormalities observed in these mice. All mice were viable and exhibited similar weights, sizes, and activity. Additionally, *Rad51ap1* knockout male and female mice were fertile (refer to **Table 3.1** for breeding distribution), and their offspring also had no observable phenotypic abnormalities.

Loss of Rad51ap1 in mice impacts spermatogenesis

Histological analyses of mutant testes showed abnormal elongated spermatids, compared to the intact tails of wild-type animals at 77-days-old (**Fig. 3.3**). Phenotypic alterations within the seminiferous tubules of *Rad51ap1* knockout mice showed evidence of dysplastic spermatogenesis, marked by decrease in mature spermatids, irregular or lack of spermatid tails, and the presence of immature cells and proteinaceous material within the lumens of the seminiferous tubules, which may indicate unusual secretion of spermatozoa (**Fig. 3.3B-E**). Additionally, multi-nucleated cells and hyper-eosinophilic apoptotic, globular bodies were noted, although rare, in mutant mice (**Table 3.3**). Abnormalities observed and measured in the testes cross sections of mutant mice are further detailed in **Table 3.3**. In addition, a reduction in the spermatogenic index (Johnson *et al.* 1970) was significant in knockout mice ($p<0.0001$). Taken together, loss of *Rad51ap1* relatively impacted spermatogenesis in mice.

Synaptonemal complex formation of mouse spermatocytes does not require Rad51ap1

Given the apparent histologic abnormalities observed in *Rad51ap1*-deficient mice and the interaction between RAD51AP1 and the meiotic recombinase DMC-1, we next sought to evaluate meiotic progression by immunocytological analyses of meiotic chromosomes, using markers of synaptonemal complex formation during Prophase I. All phases of Prophase I (leptotene, zygotene, pachytene, diplotene) were visualized in both wild-type and knockout mice at 77-days-old (**Fig. 3.4B**). At this age, mice are post-pubertal, and as expected, most meiotic cells in these mice consisted of late stages of Prophase I: pachytene and diplotene.

Discussion

Here, we analyzed the consequences of *Rad51ap1* deletion in a novel mouse model, with a particular focus on meiotic HR and reproductive parameters. The viability and fertility of these mice enabled us to examine Mendelian inheritance, and we found that heterozygous intercross breeding did not produce genotypes in a Mendelian ratio and yielded less knockout mice (**Table 3.1, Fig. 3.2B**), indicating that the *Rad51ap1* gene may be required for embryonic or neonatal development. Less wild-type mice were also an outcome and may be explained by the ability of the heterozygote females to carry litters to term. Comparing observed and expected littered mice with wild-type and KO groups did show no significant difference in wild-type mice but a significant difference in the KO group. Despite this non-Mendelian pattern, offspring of all genotypes appeared phenotypically normal and fertile. Initial murine phenotypic studies performed by the International Mouse Phenotyping Consortium (IMPC) also determined fertility to not be a significant factor affected by the KO mutant genotype. However, their studies on heterozygous breeding outcomes reveals a normal Mendelian inheritance, which differs from our

findings presented here. This discrepancy may be explained by the different amounts of mice produced: n=60 by the IMPC and n=173 by our lab. In terms of KO mutant mice, the IMPC generated 13 mice, while we produced 25 mice. The data collected by the IMPC did show less female than male KO mice produced (males=8; females=5), as did our data (**Fig. 3.2B**; males=16; females=9).

Although expression of RAD51AP1 is substantially increased in murine testes (MIZUTA *et al*. 1997), *Rad51ap1*-deficient male (and female) mice were able to produce offspring. A possible explanation as to why *Rad51ap1*-deficient mice display intact fertility may be due to the redundancy of the functions of HR DNA repair factors. A possible factor that may be compensating for *Rad51ap1* function in murine meiosis and fertility is *Rad54*, a factor involved in HR DNA repair that stabilizes the RAD51 filament and is involved in similar steps of the HR reaction: synapsis and D-loop formation (MAZIN *et al*. 2003; ALEXIADIS *et al*. 2002). Although *Rad54*-deficient mice are viable and fertile (ESSERS *et al*. 1997; RUSSO *et al*. 2018), *Rad54* was found to be required for a normal distribution of RAD51 on meiotic chromosomes despite affecting meiotic HR just mildly (MESSLAEN *et al*. 2013; WESOLY *et al*. 2006), and thus it may be a potential factor supporting progression of meiosis and fertility sustainment in *Rad51ap1*-deficient mice.

Despite having intact fertility, additional analyses of *Rad51ap1*-deficient mice showed distinct effects on spermatogenesis, a process involving mitotic and meiotic divisions to produce haploid spermatozoa (GUNES *et al*. 2015). Assessments of aging and growth in male mice revealed that the total duration of spermatogenesis is about 35 days (BELLVE *et al*. 1977), with elongated spermatids as the majority cell type by day 45 (GOMEZ-MONTOTO *et al*. 2012). When looking at H&E stained cross sections of testes in age-matched wild-type and knockout mice at 77-days-old, progression of all cell types involved in spermatogenesis were present in normally shaped

seminiferous tubules, but the tubules of *Rad51ap1*-deficient mice clearly exhibited abnormalities (**Table 3.3; Fig. 3.3B-E**). These abnormal findings of marked decrease of mature spermatids were also evident in the testes of younger *Rad51ap1*-deficient mice at 50-days-old, despite being at a post-pubertal age, and may indicate a possible delay in maturation.

Taken together, these findings show a role of *Rad51ap1* for timely progression and proper maturation of spermatogenesis in male mice. Indeed, this postponement of meiotic HR may induce delay during the programmed chromatin remodeling that occurs in elongating spermatids (GUNES *et al*. 2015; LEDUC *et al.* 2008a). On the other hand, our findings indicate that it may be possible that *Rad51ap1* has a distinct role during spermiogenesis (**Fig. S3.1A**), the last phase of spermatogenesis when the spermatids develop into mature spermatozoa (BELLVE *et al.* 1977). During this process, the spermatids undergo morphological changes and form the acrosomal head, mid connecting piece, and tail of spermatozoa, and DNA repair mechanisms play a vital role in maintaining genome integrity during spermiogenesis (LEDUC *et al.* 2008b). A role of *Rad51ap1* during spermiogenesis may be unlikely in the context of its HR function given the haploid nature of elongating spermatids where HR cannot be utilized (AHMED *et al*. 2015), but a role during spermiogenesis or in the repair of DNA damage in sperm via another pathway cannot be rejected completely.

After meiosis, other DSB repair pathways outside of HR serve as mechanisms to combat DNA damage, since sperm are highly susceptible to accumulated damage (MARCHETTI *et al*. 2005 and 2008). These mechanisms primarily include error-prone non-homologous end-joining (NHEJ) pathways (canonical and alternative; AHMED *et al*. 2015; LEDUC *et al.* 2008b), where broken DNA ends are ligated. A form of the alternative NHEJ pathway, otherwise known as microhomology-mediated end-joining (MMEJ), aligns micro-homologous sequences internal to the broken DNA

ends. MMEJ requires the activity of PARP-1 and the ligation action of DNA ligase III, the latter of which plays a major role in MMEJ (AUDEBERT *et al.* 2004; WANG et al. 2005a). Interestingly, both factors have been identified as interacting partners of RAD51AP1 via proteomic analysis (WAGNER *et al.* 2016), although the functional relevance of these interactions remains to be elucidated. While a role of RAD51AP1 in NHEJ/MMEJ has not been identified, it may be worth pursuing whether these interactions with PARP-1 and/or DNA ligase III may contribute to adequate spermiogenesis in mice, in light of our findings here.

During spermiogenesis, round spermatids undergo complex changes in chromatin remodeling and formation of the acrosome and tail, leading to mature spermatozoa (**Fig. S3.1A**). This process involves the removal of histones from the DNA, to be replaced by transition proteins and then by protamines. In **Chapter 2**, we show a novel association of RAD51AP1 for the nucleosome core particle via the histone core, so in this regard, we speculate a potential involvement of RAD51AP1 with histones during spermiogenesis. Additionally, these chromatin changes during spermiogenesis are associated with transient DNA strand breaks, in order to promote topological changes to the DNA, mediated by topoisomerase II beta (TOP2B) (LEDUC *et al.* 2008a). An interaction between RAD51AP1 and TOP2B has been acknowledged (WAGNER *et al.* 2016), although the functional meaning behind this association remains to be uncovered. The presence and significant contributions of TOP2B and PARP-1 during late spermatogenesis in the spermiogenesis phase have been characterized in the mouse. TOP2B functions during chromatin condensation in murine spermiogenesis via interactions with PARP-1 and PARP-2 (MEYER-FICCA *et al*. 2011), and it may be interesting to elucidate whether RAD51AP1 associates with these proteins during late spermatogenesis.

During spermiogenesis, autophagy plays a critical role in allowing spermatids to modify their morphology and content into mature spermatozoa (OZTURK *et al*. 2017). Our histologic findings in *Rad51ap1*-deficient mice of proteinaceous material in the lumens of seminiferous tubules (**Table 3.3**; **Fig. 3.3B** and **D**; black asterisks) may indicate an autophagic process at work. In a recent study, a connection between RAD51AP1 and autophagy was shown (BARROSO-GONZALEZ *et al*. 2019). Deletion of RAD51AP1 in alternative lengthening of telomere cancer cells prevented telomere HR, and an autophagy pathway became activated to allow these cells to survive instead of undergoing apoptosis (BARROSO-GONZALEZ *et al*. 2019). In that regard, it would be interesting to infer that autophagy may be mis-regulated during spermiogenesis in the absence of *Rad51ap1*, which could impact the progression of spermatids.

Although Fanconi anemia (FA) proteins are mainly involved in the repair of inter-strand DNA crosslinks and in overcoming replication stress (LONGERICH *et al.* 2014; KEE *et al.* 2010), studies on the assembly of FA proteins in the mouse revealed that some components of FA protein complexes are expressed at certain periods during male germ cell development, including advanced stages of spermatogenesis in round and elongated spermatids (JAMSAI *et al*. 2015). Among these proteins is *Fancj* (alias BRIP1), which interacts with BRCA1. PALB2, an interacting partner of RAD51AP1, also interacts with BRCA1, and disruption of the PALB2-BRCA1 interaction led to reduced male fertility and histologic defects in male mice similar to what we observed in *Rad51ap1*-deficient mice: marked decrease of elongated spermatids and disorganized spermatogenesis as well as tubules with normal cellularity and spermatozoa, despite normal meiotic formation and clearance of DMC1/RAD51 foci and sustained, although reduced, male fertility (SIMHADRI *et al*. 2014). Since RAD51AP1 has implications in FA, and certain FA

components are expressed during spermiogenesis, RAD51AP1 may similarly play a role during late spermatogenesis in the DNA damage repair that occurs during chromatin condensation.

Overall, our findings suggest that *Rad51ap1* may play a role in the DNA repair and/or progression of late spermatogenic cells. At this time, it is undocumented if the seminiferous tubules of *Rad51ap1*-deficient mice eventually matured to proper physiologic levels compared to wild-type mice. It is also unclear whether defects in meiosis occurred in the context of abnormal RAD51 and DMC-1 localization and distribution on chromosomes, despite having seemingly normal meiotic progression and maturation into round spermatids. Given that *Rad51ap1*-deficient male mice at 4- and 7-months of age were able to breed and produce healthy, viable litters, we expect that chromosome abnormalities were not an issue and that normal histology eventually was reached, to explain their sustained fertility. On the other hand, continued sub-fertile male mice still have some potential to be fertile and reproduce with able female mice. After all, the maternal DNA repair machinery during the early phases of mammalian development contributes to the genome integrity of the zygote and is able to repair damage in both parent genomes (BRANDRIFF *et al.* 1981; ASHWOOD *et al.* 1996). Nonetheless, more studies are needed on the mechanisms and factors involved in these timely events.

Figures

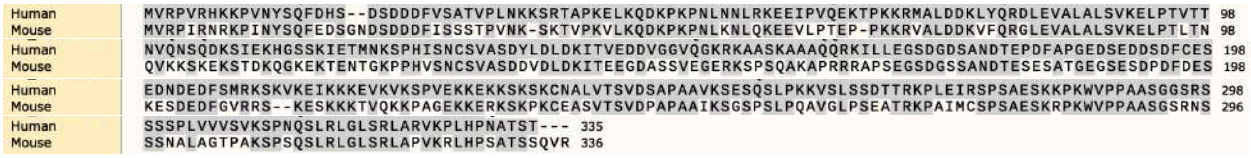

Figure 3.1. RAD51AP1 is highly conserved between humans and mice

Shown here is a ClustalW alignment as viewed on SnapGene Viewer of the RAD51AP1 protein comparing human and mouse protein sequences. Amino acids highly conserved between human and mouse are highlighted in gray.

A

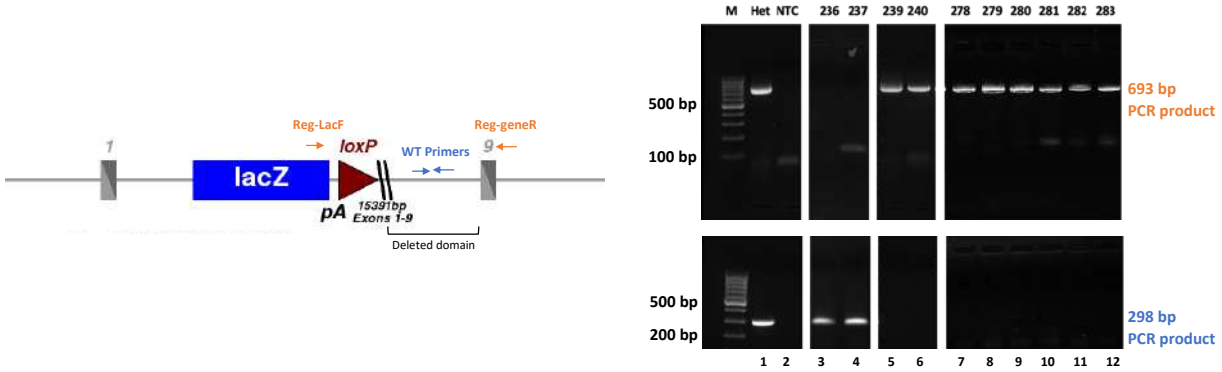

B

Rad51ap1 heterozygous x heterozygous (23 litters, 173 mice)		
Genotype	**Expected no. (%)**	**Observed no. (%)**
WT	43 (25%)	37 (21%)
Heterozygous	87 (50%)	111 (64%)
KO	43 (25%)	25 (15%)
Chi-square (df 2, N = 173) = 8.124, p 0.0172		
	Male	**Female**
WT	17	20
Heterozygous	53	58
KO	16	9(n.s.)

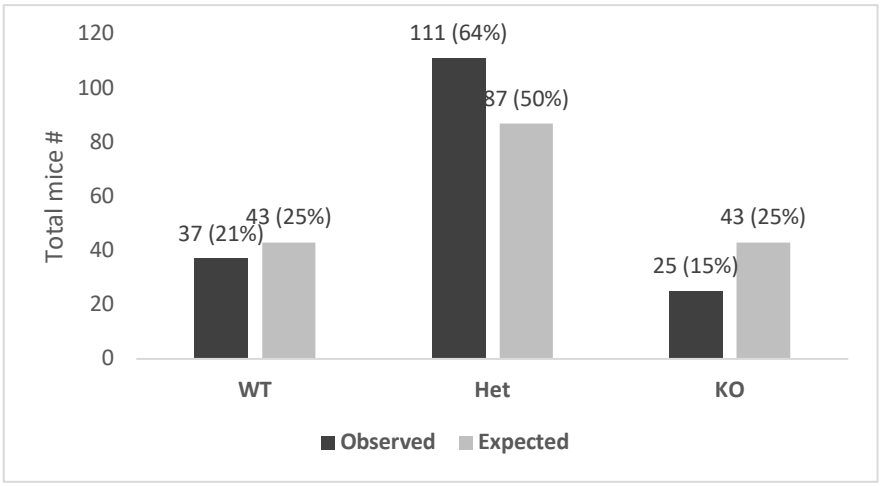

Figure 3.2. *Rad51ap1* heterozygous mice do not breed at predicted Mendelian ratios

In Panel A, the genotyping schematic and placement of PCR primers are shown, along with agarose gels confirming the genotypes of mice used in this study (lanes 3-12). Reg-LacF and Reg-

geneR give a 693 bp mutant-specific product, and the WT Primers give a 298 bp wild-type specific product. A heterozygous mouse and non-template control (NTC) were used as controls (lanes 1-2). In Panel B, the number and percentages of various genotypes obtained by the *Rad51ap1* heterozygous intercrosses is shown. The expected number of mice was calculated according to the total number of mice born (n = 173). Mice were not born at the expected Mendelian ratio, with decreased numbers of both wild-type and *Rad51ap1* knockout mice. The Chi square test was used, and the p value of 0.0172 indicated a significant difference in the distribution of observed versus expected outcomes across genotypes. [Panel A data by Platon Selemenakis and Mollie Uhrig]

A

Rad51ap1 WT

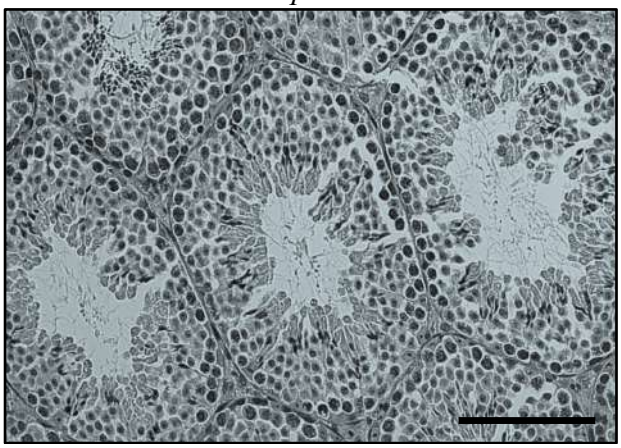

77 days old

Rad51ap1 KO

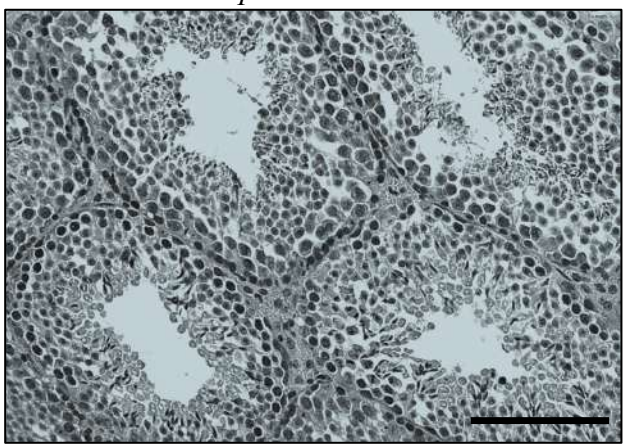

77 days old

B

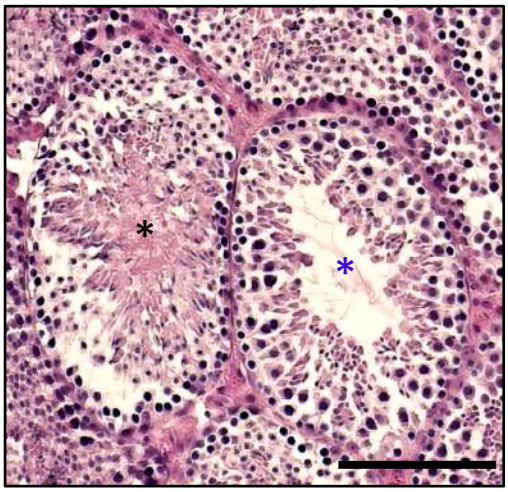

C

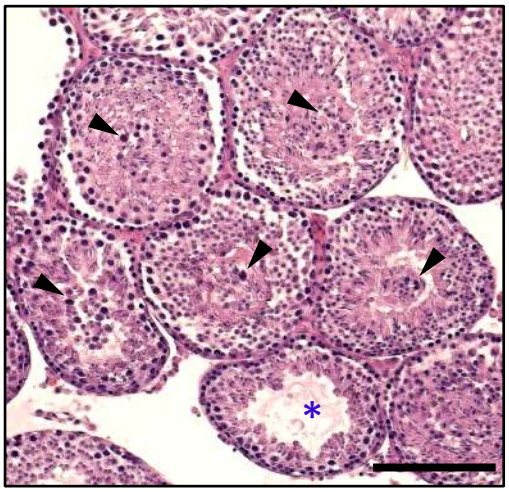

D

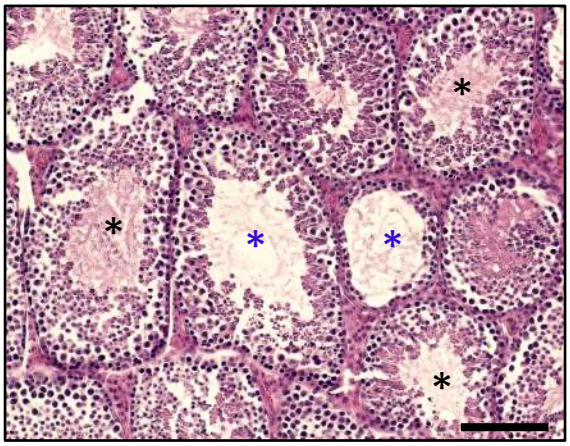

E

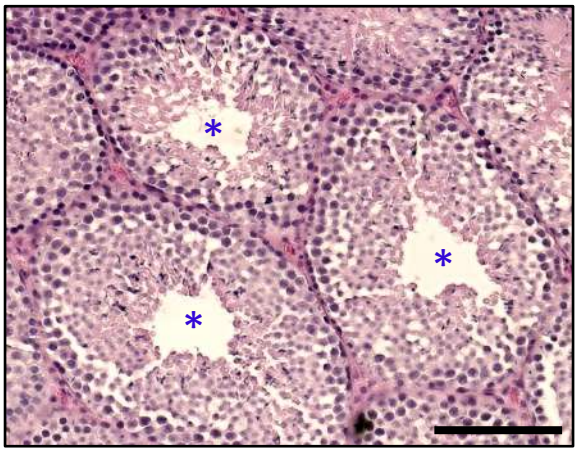

Figure 3.3. Testes of *Rad51ap1*-deficient mice reveal dysplastic spermatogenesis

Shown in panel A are H&E stains (in greyscale) of testes sections from age-matched wild-type and *Rad51ap1* knockout mice (77-days-old). The seminiferous tubules in both groups are lined by germinal epithelium, and evidence of the maturation of these spermatogonia cells to spermatocytes and spermatids is observed from the epithelium towards the tubules' lumens. However, the seminiferous tubules of *Rad51ap1*-deficient mice exhibit distinct morphologic abnormalities (Panels B-E). Abnormalities include marked decrease of elongating spermatids with irregular or lack of tails (blue asterisks), proteinaceous material present in the lumens (black asterisks), and the presence of immature cells in the lumens (black arrowheads). Black bars indicate a scale of 100 microns.

A

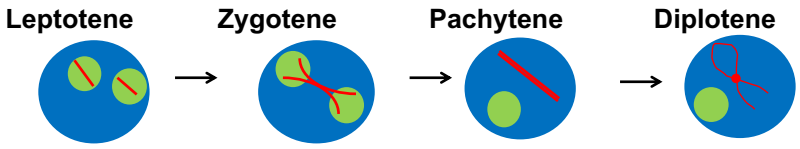

B

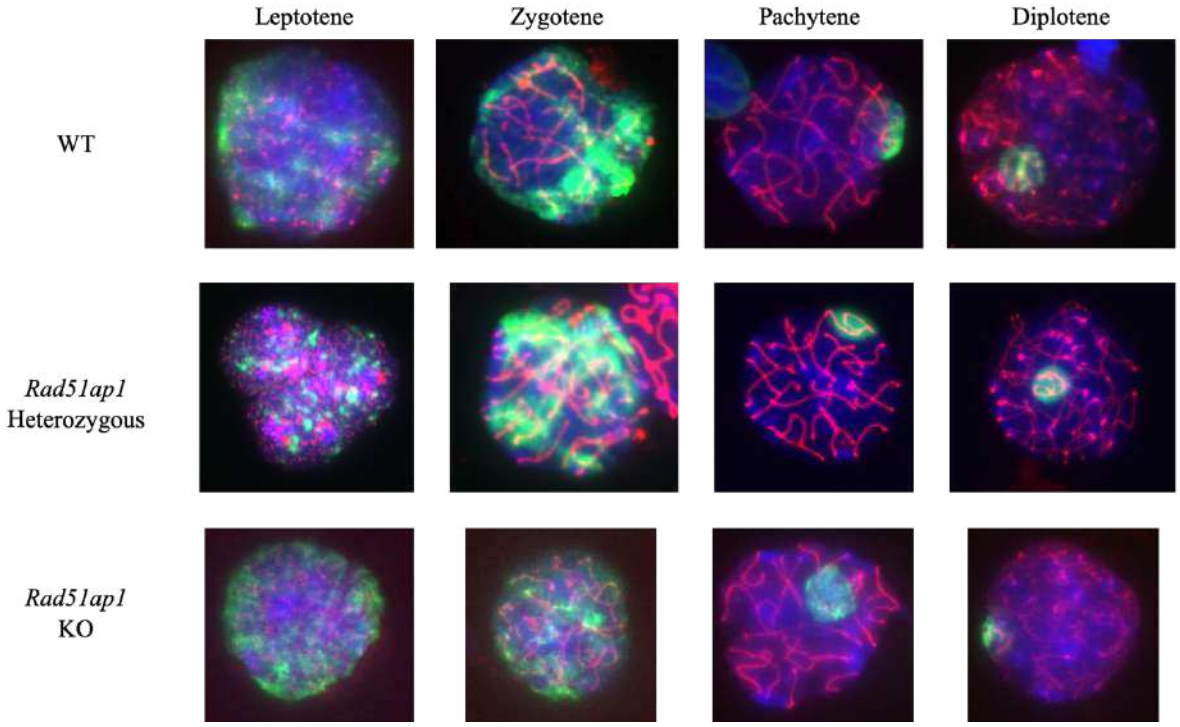

Figure 3.4. *Rad51ap1*-deficient spermatocytes are not defective in assembling the synaptonemal complex during Prophase I

Panel A depicts a schematic of the sub-phases of Prophase I, with synaptonemal complex assembly visualized in meiotic nuclei (blue is representative of DAPI staining). Green signifies γH2AX, sites of DSBs during this process. Red is SCP3, a marker of the axial/lateral element of the synaptonemal complex as homologous chromosomes pair along their lengths. In leptotene, replicated chromosomes begin to condense, and sites of DSBs are abundant. In zygotene, DSBs

remain abundant, but synapsis via the synaptonemal complex between homologous chromosome pairs starts to occur. In pachytene, synapsis is complete, crossover events are possible, and only sex chromosomes sequester in the XY body, which is marked by concentrated γH2AX. During diplotene, the synaptonemal complex starts to disappear, and chiasmata, sites of crossovers, are visible (depicted here as a red circle). Lastly, in diakinesis (not shown here), the nuclear envelope begins to fragment, and the chromosomes are ready for metaphase. In Panel B, analysis of synaptonemal complex assembly and progression was observed in wild-type (n = 2), *Rad51ap1* heterozygous (n = 1), and *Rad51ap1* knockout (n = 8) mice. Localization of γH2AX (green), SCP3 (red), and DAPI (blue) on spread spermatocytes were detected by immunofluorescence. Shown are the chromosome spreads from leptotene, zygotene, pachytene, and diplotene stages of Prophase I.

Tables

Table 3.1. Breeding distribution of mouse litters from this study

Pairings	WT		Het		KO		P-value
	Expected	Observed	Expected	Observed	Expected	Observed	
Het x Het	43 (25%)	37 (21%)	87 (50%)	111 (64%)	43 (25%)	25 (15%)	0.01 (n=173)
WT x Het	13 (50%)	16 (62%)	13 (50%)	10 (38%)	0 (0%)	0 (0%)	n.s. (n=26)
Het x KO	0 (0%)	0 (0%)	5.5 (50%)	5 (45%)	5.5 (50%)	6 (55%)	n.s. (n=11)

Table 3.2. Genotype and age distribution of *Rad51ap1* null, heterozygous, and wild-type animals used in this study for testes isolation and analyses

Genotype	I.D.	Age at euthanization (days)	Littermates/Groups
WT	WT #1	77 days	WT #1-2; littermates
WT	WT #2	77 days	
KO	KO #1	77 days	KO #1-2; littermates
KO	KO #2	77 days	
Het	Het #1	104 days	
KO	KO #3	77 days	KO #3-4; littermates
KO	KO #4	77 days	
KO	KO #5	50 days	KO #5-8; littermates
KO	KO #6	50 days	
KO	KO #7	50 days	
KO	KO #8	50 days	

Table 3.3. Morphological parameters obtained from seminiferous tubules of control wild-type and *Rad51ap1* KO mice

Groups	**Spermatogenesis Index** (Johnson *et al*. 1970)	**Other Abnormalities Observed**
Wild-type (77-days-old)	9.175 ± 0.133	N/A
Rad51ap1 KO (77-days-old)	7.25 ± 0.252****	- Decreased Elongated Spermatids: 126 (63%)**** - Proteinaceous Material in Lumen: 64 (32%)*** - Acaudate Sperm: 60 (30%)*** - Immature Cells in Lumen: 43 (21.5%)** - Hyper-eosinophilic Apoptotic Bodies: 26 (13%)** - Multi-nucleated Cells: 12 (6%)*
Rad51ap1 KO (50-days-old)	6.75 ± 0.234	- Decreased Elongated Spermatids: 138 (69%)**** - Proteinaceous Material in Lumen: 60 (30%)*** - Acaudate Sperm: 47 (23.5%)** - Immature Cells in Lumen: 46 (23%)** - Hyper-eosinophilic Apoptotic Bodies: 13 (6.5%)* - Multi-nucleated Cells: 22 (11%)**

For Spermatogenic Index: n=40 sections per group, values are the means for each group ± SEM; ****, $P < 0.0001$; student's t-test assessing the significance of changes between age-matched control (WT) and experimental (KO) groups at 77-days-old; for 50-days old mice, age-matched controls were unavailable.

For Other Abnormalities Observed: n=200 sections per group. The following histopathology severity grading system by the OECD was used as a guide: *, Grade 1 (minimal); **, Grade 2 (slight); ***, Grade 3 (moderate); ****, Grade 4 (marked).

Table 3.4. Antibodies and concentrations used for immunostaining in this study

Antibody	Species	Brand	Application	Concentration
Anti-γH2AX Ser 139	Mouse	Millipore (cat. 05-636)	Immunofluorescence	1:1000
Anti-SCP3	Rabbit	Abcam (cat. 15093)	Immunofluorescence	1:600
Anti-rabbit Alexa Fluor 594	Goat	Invitrogen (cat. A21121)	Immunofluorescence	1:750
Anti-mouse Alexa Fluor 488	Goat	Invitrogen (cat. A11037)	Immunofluorescence	1:750

CHAPTER FOUR

Conclusions and Future Directions

Summary

DNA repair pathways are important cellular mechanisms for mending DNA damage, maintaining genome integrity, and preventing mutations leading to cancer. Homologous recombination (HR) DNA repair is one of many DNA repair pathways that is vital for relatively error-free repair of especially harmful double-strand breaks (DSBs). Defects in HR are a common cause of cancer, and study of the HR pathway is of great clinical interest due to the sensitivity of HR-deficient cells to a variety of DNA-damaging agents used in cancer therapies. While progress has been made in understanding the HR pathway, questions remain in the field regarding the interplay and mechanistic functions among the multitude of proteins involved.

This thesis examined effects resulting from loss of function of RAD51AP1, an important HR player involved in stimulating the primary HR recombinase RAD51 and in protecting cells from DNA damage. The body of work we have performed for this dissertation addressed existing knowledge gaps regarding the *in vitro* and *in vivo* roles of RAD51AP1 in HR. We examined RAD51AP1 in the context of chromatin and unveiled a novel role in its affinity towards chromatinized DNA. We also investigated two previously reported post translational modifications located within its DNA-binding region and characterized their effects on DNA interaction and in the cellular environment. Additionally, we studied the consequences of *Rad51ap1* loss in an animal system, the mouse, and further unraveled the distinct function of this DNA repair factor in meiotic HR and reproductive biology. Taken together, our findings align with the literature and show that loss or disruption of RAD51AP1 prevents cellular and organismal protection against spontaneous or induced DNA damage.

Conclusions

RAD51AP1 is an important factor involved in HR and interacts with and stimulates the presynaptic RAD51 filament during synapsis and D-loop steps (WIESE *et al*. 2007; MODESTI *et al*. 2007; DUNLOP *et al*. 2012). Evidence of RAD51AP1 interaction towards various DNA substrates has been previously shown (KOVALENKO *et al*. 1997; WIESE *et al*. 2007; MODESTI *et al*. 2007; PARPLYS *et al*. 2014 and 2015; DRAY *et al*. 2010) to occur through two of its DNA-binding domains (DUNLOP *et al*. 2012), and post translational modifications have been identified but not evaluated functionally (ELIA *et al*. 2015; BELI *et al*. 2012; WAGNER *et al*. 2016). We sought to investigate two of these post translational modifications (at S277 and S282) within its C-terminal DNA binding domain as well as the interaction of RAD51AP1 with chromatinized DNA. We encountered a novel interaction between RAD51AP1 and the nucleosome core particle (NCP) that occurs only through its C-terminal DNA binding domain, and phosphorylation of S277 and S282 decreased this interaction. We also found that RAD51AP1 is capable of duplex capture of chromatinized dsDNA. These results expand upon previously characterized functions of the C-terminal domain of RAD51AP1. Our model (**Fig. 4.1**) describes the orientation of the RAD51AP1 protein's C-terminus as a potential means for the protein to interact with RAD51 and chromatinized dsDNA during synaptic complex formation and D-loop steps in HR.

While the biochemical analyses showed reduced affinity by the phosphorylation of S277 and S282 towards NCP, in HeLa cells, we found that the inability to phosphorylate S277 and S282 led to harmful impacts, such as decreased growth, increased sensitivity to DNA damage, and altered RAD51 and RAD51AP1 foci. Nonetheless, our work highlights the importance of these residues' modification status in terms of NCP interaction and in the DNA damage response and

HR activities in cells. We consider that in an un-modified state, RAD51AP1 associates with chromatinized dsDNA, and then upon DNA damage, its phosphorylation at S277 and S282 is optimal for promoting the protein's activities in HR (**Fig. 4.2**). Drawing all of these insights together for accurate modeling of RAD51AP1 functions is important when translating findings from the bench to the bedside. One such application for this knowledge could be in developing therapies against cancer, since RAD51AP1 may be an encouraging target to combat an array of cancers that have high RAD51AP1 expression (see **Chapter 1**, section B).

Limitations of Study

A discrepancy between the biochemical and cellular data appeared, where recombinantly expressed and purified S2D exhibited decreased NCP binding, but S2D expressing RAD51AP1 KO cells behaved much like wild-type and showed no observable phenotype. This difference in the biochemical data and cellular results may be explained by the different environments of the systems utilized, where the mechanistic studies may not mimic the cellular environment in the context of the DNA damage response and may not be as sensitive to represent what is occurring in cells. In terms of our cell work, we only utilized HeLa cell lines, but it would be advantageous to perform our studies in additional cell lines, such as U2OS cells that have previously been employed for insights on RAD51AP1 (DRAY *et al.* 2010; PARPLYS *et al*. 2014 and 2015; WIESE *et al.* 2007; BARROSO-GONZALEZ *et al*. 2019). Non-tumor derived cell lines could also be considered, such as HEK293 cells, that have been used for RAD51AP1 studies (HENSON *et al*. 2006; NGUYEN *et al*. 2018) or MCF10A cells, which were recently used to investigate the functions of classical human RAD51 paralogs (GARCIN *et al*. 2019).

Future Directions

Our results provide new insights into RAD51AP1, in the context of chromatin and two of its post translational modifications (PTMs). There is room for further analysis of RAD51AP1's DNA binding capabilities with additional chromatinized substrates, such as di- and tri-nucleosomes and other higher order chromatin structures. It would also be valuable to identify the kinases and phosphatases responsible for phosphorylating and de-phosphorylating S277 and S282 in RAD51AP1. Potential candidates are CDKs, as this region in RAD51AP1 contains an SP motif recognized by these kinases for phosphorylation of serines. It may also be informative to measure the cellular impacts of these residues in affecting the expression and/or binding of other protein partners, such as RAD52, RAD54, UAF-1, and DMC-1 (in germ cells). Possible techniques in cells for assessing these protein interactions with RAD51AP1 include FRET and PLA methodologies (SEKAR *et al*. 2003; BAHJAT *et al*. 2017). Assessing the potential difference in mobility by WT, S2D, and S2A proteins could also be considered via FRAP (BRAGA *et al*. 2004); such live cell imaging would be helpful in obtaining better insights into the cellular dynamics of RAD51AP1 in un-modified and modified states. Moreover, it is possible that RAD51AP1 functions in other DNA repair pathways, such as Fanconi anemia, hence future studies should investigate the function of these PTMs in the context of other pathways. Such results would offer a more robust understanding of RAD51AP1's mechanistic roles in multiple pathways, which may be important for providing ways to inhibit RAD51AP1's function in cancers with high RAD51AP1 expression, for example.

Effects of *Rad51ap1* loss on murine fertility and spermatogenesis: implications for meiotic HR

Conclusions

RAD51AP1 is highly expressed in human and murine testes (OBAMA *et al*. 2008; MIZUTA *et al*. 1997), and the protein has been shown to interact with and stimulate the meiotic recombinase DMC-1 in the D-loop step of HR (DRAY *et al*. 2011). Very few mouse studies have evaluated RAD51AP1 function, and no mouse studies have evaluated reproductive biology. Hence, we sought to better understand the effects of *Rad51ap1* loss regarding reproductive parameters in male mice. Our findings reveal that loss of *Rad51ap1* has subtle impacts on murine spermatogenesis and fertility. Assessment of 173 mice after heterozygous breeding shows a small, but significant divergence from Mendelian inheritance, with less knockout and wild-type mice produced. Additionally, fewer knockout females were created compared to knockout males. While synaptonemal complex formation and progression through Prophase I of meiosis did not appear affected by *Rad51ap1* loss, evaluation of histological analyses of testes cross sections did reveal subtle defects in male mice that indicated irregularities at spermiogenesis, such as decreased elongated spermatids, lack of spermatozoa tails, and presence of immature cells and abnormal material within seminiferous tubule lumens. Altogether, these findings uncover novel functions of RAD51AP1 at the organismal level.

Limitations of Study

A limitation of this study occurred in regard to breeding, where fewer WT and KO phenotypes were produced after the heterozygous intercrosses. Some litters also produced smaller than average litter sizes, of 4-6 pups instead of the normal 8-12 pups. Despite a significant

difference observed between WT (*n*=2) and KO (*n*=8, 4 age-matched, 4 non-age-matched) male mice in regards to spermiogenesis histologically, our *n* for each cohort is small. It will be valuable to evaluate our findings here with additional mice. Furthermore, our use of an inbred strain here, although the norm, may have offered disadvantages compared to using outbred mice for our studies, where the latter may exhibit a clearer phenotype compared to wild-type mice.

Future Directions

Our findings indicate that loss of *Rad51ap1* in mice showed mild effects on reproductive parameters in male mice at 50- and 77-days old. In this regard, there is room for further characterization of *Rad51ap1* loss through studies that investigate younger-aged male mice, before or during the first wave of spermatogenesis, as a potential role of this gene may be more pronounced earlier in male mice. Inducing DSBs in pre- and/or post-pubertal mice via IR may also provide insights into the role of *Rad51ap1* in protecting germ cells from induced DNA damage; our studies here investigated mice undergoing spontaneous DNA damage. Since the main alteration we observed in *Rad51ap1*-deficient mice occurred during late spermatogenesis in spermiogenesis, future studies on sperm count, morphology, apoptosis via the TUNEL assay, and DNA fragmentation would be reasonable. It would also be invaluable to detect where RAD51AP1 expression is occurring in seminiferous tubules via immunohistochemistry.

Future studies in this model system should also investigate the effects of double knockout mice, which may better highlight the role of *Rad51ap1*; prospective gene targets include *Rad54*, a gene whose product is involved in HR with similar functions to what is known about RAD51AP1 (MAZIN *et al*. 2003; ALEXIADIS *et al*. 2002), and *Atm*, a DNA damage signaling protein (KIRSHNER *et al*. 2009). Studies in our lab show that RAD51AP1 can substitute for RAD54

function in HeLa cells, and we speculate that a double *Rad51ap1*/*Rad54* knockout mouse, if viable, may likely show a more severe phenotype. Likewise, *Atm* knockout mice exhibit hypersensitivity to MMC, which is increased by deletion of either *Rad54* or *Rad54B* (KIRSHNER *et al*. 2009), thus it may be of interest to examine if deletion of *Rad51ap1* in *Atm* mice may also further highlight this phenotype and affect the integrity of germ cells.

Closing Remarks

Our studies characterizing the *in vitro* and *in vivo* roles of RAD51AP1 have both broadened and deepened the field of DNA repair. Firstly, the interaction between RAD51AP1 and chromatin was previously unconnected to its function and has further deepened its potential mechanism of action during the HR reaction. Secondly, post translational modifications have been previously identified in RAD51AP1, but most remain functionally unassessed. Here, we have been able to characterize two additional residues whose proper regulation is essential for HR DNA repair and cellular survival against spontaneous or induced DNA damage. Lastly, the consequences of loss of *Rad51ap1* in an animal system have evaded scientific study until the availability of a recent mouse model, which we have begun to investigate here and were able to reveal a novel role of *Rad51ap1*/RAD51AP1 in regard to spermatogenesis. Further insight into both its mechanistic action and biological function potentiates therapy options that exploit vulnerable targets, such as DNA repair factors like RAD51AP1, in cancer cells. More functional studies and mouse research on *Rad51ap1*/RAD51AP1 are necessary moving forward as we aim to better understand DNA repair. This knowledge can only help in personalizing the treatment of cancers that exploit DNA repair factors or in understanding the mechanisms assuring the fidelity of spermatogenesis.

Figures

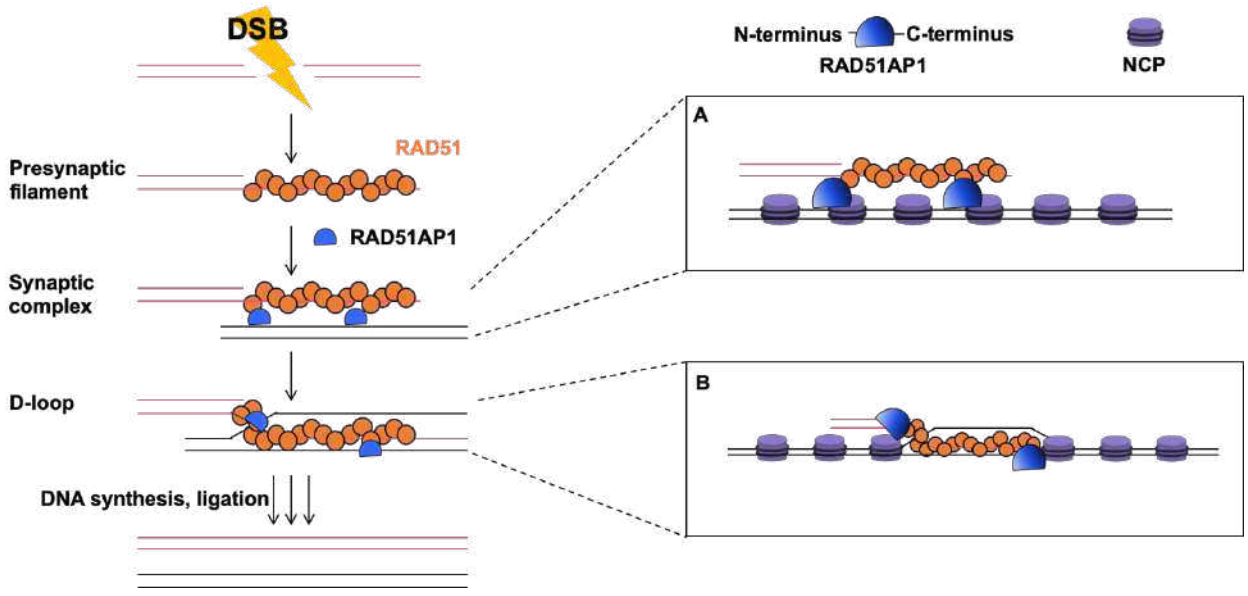

Figure 4.1. Potential mechanisms by which RAD51AP1 may interact with RAD51 and the chromatinized DNA template in HR DNA repair

The findings reported in **Chapter 2** made known that RAD51AP1 interacts with the chromatinized dsDNA substrate, NCP, through its C-terminus. In this model, we depict the RAD51AP1 (blue), with lighter blue as the N-terminus, and darker blue as the C-terminus. In panel A, we propose that the C-terminus of RAD51AP1 is capable of interacting with RAD51 and chromatin during synaptic complex formation (**A**) and D-loop (**B**) steps of HR. The N-terminus, which does not interact with NCP, may associate with ssDNA or dsDNA.

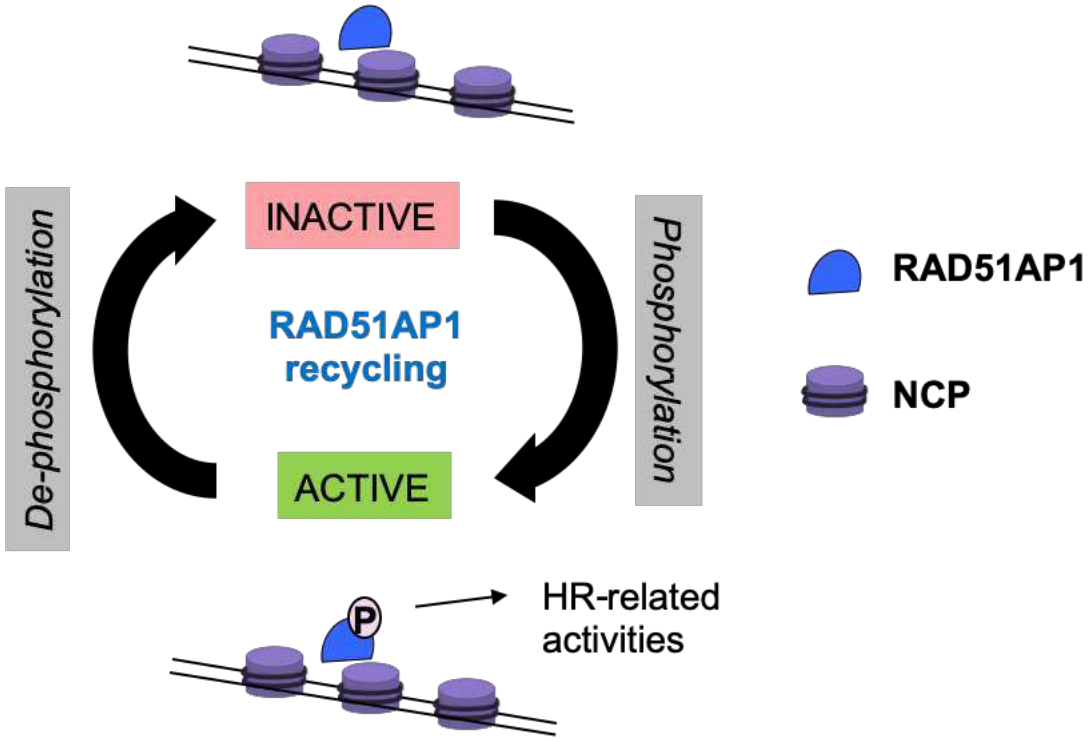

Figure 4.2. Potential model to explain impacts of the phosphorylation status of S277 and S282

We show in **Chapter 2** that RAD51AP1 interacts with NCP, and that phosphorylation at S277 and S282 diminished this association. Additional findings described in **Chapter 2** show that no phosphorylation of S277 and S282 led to detrimental effects in cells in response to DNA damage. From these data, we speculate that in an inactive, un-modified state, RAD51AP1 associates with chromatinized dsDNA, and then upon DNA damage, its phosphorylation at S277 and S282 is optimal for promoting the protein's activities in HR (dissociates from chromatinized dsDNA towards the site of damage).

REFERENCES

AHMED, E.A., H. SCHERTHAN and D.G. DE ROOIJ, 2015 DNA double strand break response and limited repair capacity in mouse elongated spermatids, International Journal of Molecular Sciences (16) 29923-29935.

ALEXEEV, A., A. MAZIN and S.C. KOWALCZYKOWSKI, 2003 Rad54 protein possesses chromatin-remodeling activity stimulated by the Rad51-ssDNA nucleoprotein filament, Nature Structural Biology (10) 182-186.

ALEXIADIS, V. and J.T. KADONAGA, 2002 Strand pairing by Rad54 and Rad51 is enhanced by chromatin, Research Communication Genes & Development (16) 2767-2771.

ALONSO-DE VEGA, I., Y. MARTIN, and V.A. SMITS, 2014 USP7 controls Chk1 protein stability by direct deubiquitination, Cell Cycle 13 (24) 3921–3926.

ASHWOOD-SMITH, M.J. and R.G. EDWARDS, 1996 DNA repair by oocytes, Molecular Human Reproduction (2) 46-51.

AUDEBERT, M., B. SALLES and P. CALSOU, 2004 Involvement of poly(ADP-ribose) polymerase-1 and XRCC1/DNAligase III in an alternative route for DNA double-strand breaks rejoining, Journal of Biological Chemistry (279) 55117-55126.

BAHJAT, M., T.A. BLOEDJES, A. VAN DER VEEN, G. DE WILDE, C. MAAS, *et al*., 2017 Detection and visualization of DNA damaged-induced protein complexes in suspension cell cultures using the proximity ligation assay, Journal of Visualized Experiments (124) e55703.

BARROSO-GONZALEZ, J., L. GARCIA-EXPOSITO, S.M. HOANG, M.L. LYNSKEY, J.L. RONCAIOLI *et al*., 2019 RAD51AP1 is an essential mediator of alternative lengthening of telomeres, Molecular Cell 76 (1) 217.

BARTKOVA, J., Z. HOREJSI, K. KOED, A. KRAMER, F. TORT *et al*., 2005 DNA damage response as a candidate anti-cancer barrier in early human tumorigenesis, Nature 434 (7035) 864–870.

BELI, P., N. LUKASHCHUK, S.A. WAGNER, B.T. WEINERT, J.V. OLSEN *et al*., 2012 Proteomic investigations reveal a role for RNA processing factor THRAP3 in the DNA damage response, Molecular Cell 46 (2) 212–225.

BELLVE, A.R., J.C. CAVICCHIA, C.F. MILLETTE, D.A. O'BRIEN, Y.M. BHATNAGAR *et al*., 1977 Spermatogenic cells of the prepuberal mouse, Journal of Cell Biology (74) 68-85.

BENNETZEN M.V., D.H. LARSEN, J. BUNKENBORG, J. BARTEK, J. LUKAS *et al*., 2010 Site-specific phosphorylation dynamics of the nuclear proteome during the DNA damage response, Molecular & Cellular Proteomics 9 (6) 1314–1323.

BRAGA, J., J.M.P. DESTERRO and M. CARMO-FONSECA, 2004 Intracellular macromolecular mobility measured by fluorescence recovery after photobleaching with confocal laser scanning microscopes, Molecular Biology of the Cell, 15(10) 4749-4760.

BRANDRIFF, B. and R.A. PEDERSEN, 1981 Repair of the ultraviolet-irradiated male genome in fertilized mouse eggs, Science (211) 1431-1433.

BRIDGES, A.E., S. RAMACHANDRAN, R. PATHANIA, U. PARWAL, A. LESTER *et al*., 2020 RAD51AP1 deficiency reduces tumor growth by targeting stem cell self-renewal, Cancer Research, PMID 32665355.

BRYAN, T.M., A. ENGLEZOU, L. DALLA-POZZA, M.A. DUNHAM and R.R. REDDEL, 1997 Evidence for an alternative mechanism for maintaining telomere length in human tumors and tumor-derived cell lines, Nature Medicine (3) 1271-1274.

CAMPEAU, E., V.E. RUHL, F. RODIER, C.L. SMITH, B.L. RAHMBERG *et al.,* 2009, A versatile viral system for expression and depletion of proteins in mammalian cells, PLOS ONE 4(8): e6529.

CHEN, J., D.P. SILVER, D. WALPITA, S.B. CANTOR, A.F. GAZDAR *et al*., 1998 Stable interaction between the products of the BRCA1 and BRCA2 tumor suppressor genes in mitotic and meiotic cells, Molecular Cell 2 (3) 317–328.

CHEN, J.J., D. SILVER, S. CANTOR, D.M. LIVINGSTON, R. SCULLY *et al*., 1999 BRCA1, BRCA2, and Rad51 operate in a common DNA damage response pathway, Cancer Research 59 (7 Suppl) 1752–1756.

CHEN, W., L. LIAO, H. LAI, X. YI and D. WANG, 2020 Identification of core biomarkers associated with pathogenesis and prognostic outcomes of laryngeal squamous-cell cancer using bioinformatics analysis, European Archives of Otorhinolaryngology 277 (5) 1397-1408.

CHI, Y., J.H. CARTER, J. SWANGER, A.V. MAZIN, R.L. MORITZ *et al*., 2020 A novel landscape of nuclear human CDK2 substrates revealed by in situ phosphorylation, Science Advances (6) eaaz9899.

CHUDASAMA, D., V. BO, M. HALL, V. ANIKIN, J. JEYANEETHI, *et al*., 2018 Identification of cancer biomarkers of prognostic value using specific gene regulatory networks (GRN): a novel role of RAD51AP1 for ovarian and lung cancers, Carcinogenesis 39 (3) 407-417.

COHN, M.A., P. KOWAL, K. YANG, W. HAAS, T.T. HUANG *et al*., 2007 A UAF1-containing multisubunit protein complex regulates the Fanconi anemia pathway, Molecular Cell 28 (5) 786–797.

CUKRAS, S., E. LEE, E. PALUMBO, P. BENAVIDEZ, G.L. MOLDOVAN *et al.*, 2016 The USP1-

UAF1 complex interacts with RAD51AP1 to promote homologous recombination repair, Cell Cycle 15 (19) 2636–2646.

DALEY J.M., Y. KWON, H. NIU and P. SUNG, 2013 Investigations of homologous recombination pathways and their regulation, Yale Journal of Biology and Medicine 86 (4) 453–461.

DALEY, J.M., W.A. GAINES, Y. KWON and P. SUNG, 2014 Regulation of DNA pairing in homologous recombination, Cold Spring Harbor Perspective Biology 6 (11) a017954.

DAVIES, A.A., J.Y. MASSON, M.J. MCILWRAITH, A.Z. STASIAK, A. STASIAK *et al*., 2001 Role of BRCA2 in control of the RAD51 recombination and DNA repair protein, Molecular Cell 7 (2) 273–282.

DIA, F. T. STRANGE, J. LIANG, J. HAMILTON and K.M. BERKOWITZ, 2017 Preparation of meiotic chromosome spreads from mouse spermatocytes, Journal of Visualized Experiments (129) e55378.

DRAY, E., J. ETCHIN, C. WIESE, D. SARO, G.J. WILLIAMS *et al*., 2010 Enhancement of RAD51 recombinase activity by the tumor suppressor PALB2, Nature Structural and Molecular Biology 17 (10) 1255–1259.

DRAY, E., M.H. DUNLOP, L. KAUPPI, J. SAN FILIPPO, C. WIESE *et al*., 2011 Molecular basis for enhancement of the meiotic DMC1 recombinase by RAD51 associated protein 1 (RAD51AP1), Proceedings of the National Academy of Sciences of the United States of America 108 (9) 3560–3565.

DUNLOP, M.H., E. DRAY, W. ZHAO, M.S. TSAI, C. WIESE *et al*., 2011 RAD51-associated protein 1 (RAD51AP1) interacts with the meiotic recombinase DMC1 through a conserved motif, Journal of Biological Chemistry 286 (43) 37328–37334.

DUNLOP M.H., E. DRAY, W. ZHAO, J. SAN FILIPPO, M.S. TSAI *et al*., 2012 Mechanistic insights into RAD51-associated protein 1 (RAD51AP1) action in homologous DNA repair, Journal of Biological Chemistry 287 (15) 12343–12347.

DURRBAUM, M. and Z. STORCHOVA, 2015 Effects of aneuploidy on gene expression: implications for cancer, The FEBS Journal (283) 791-802.

DYER, P.N., R.S. EDAYATHUMANGALAM, C.L. WHITE, Y. BAO, S. CHAKRAVARTHY *et al*., 2004 Reconstitution of nucleosome core particles from recombinant histones and DNA, Methods in Enzymology (375) 23-44.

ELIA, A.E., A.P. BOARDMAN, D.C. WANG, E.L. HUTTLIN, R.A. EVERLEY *et al*., 2015 Quantitative proteomic atlas of ubiquitination and acetylation in the DNA damage response, Molecular Cell 59 (5) 867–881.

ESSERS, J., R.W. HENDRIKS, S.M.A. SWAGEMAKERS, C. TROELSTRA, J. DE WIT *et al*., 1997

Disruption of mouse RAD54 reduces ionizing radiation resistance and homologous recombination, Cell (89) 195-204.

FANG, M., F. XIA, M. MAHALINGAM, C.M. VIRBASIUS, N. WAJAPEYEE *et al*., 2013 MEN1 is a melanoma tumor suppressor that preserves genomic integrity by stimulating transcription of genes that promote homologous re- combination-directed DNA repair, Molecular and Cellular Biology 33 (13) 2635–2647.

FAUSTRUP, H., S. BEKKER-JENSEN, J. BARTEK, J. LUKAS, and N. MAILAND, 2009 USP7 counteracts SCFbetaTrCP- but not APCCdh1-mediated proteolysis of Claspin, Journal of Cell Biology 184 (1) 13–19.

GARCIN, E.B., S. GON, M.R. SULLIVAN, G.J. BRUNETTE, A. DE CLAN *et al*., 2019 Differential requirements for the RAD51 paralogs in genome repair and maintenance in human cells, PLOS Genetics 15(10) e1008355.

GOMEZ-MONTOTO, L., L. ARREGUI, N. MEDINA-SANCHEZ, M. GOMENDIO and E.R.S. ROLDAN, 2012 Postnatal testicular development in mouse species with different levels of sperm competition, Reproduction (143) 333-346.

GORDON, D.J., B. RESIO, and D. PELLMAN, 2012 Causes and consequences of aneuploidy in cancer, Nature Review Genetics (13) 189-203.

GORGOULIS, V.G., L.V. VASSILIOU, P. KARAKAIDOS, P. ZACHARATOS, A. KOTSINAS *et al*., 2005 Activation of the DNA damage checkpoint and genomic in- stability in human precancerous lesions, Nature 434 (7035) 907–913.

GOTTESFELD, J.M. and K. LUGER, 2001 Energetics and affinity of the histone octamer for defined DNA sequences, Biochemistry 40 (37) 10927-33.

GOYAL, N., M.J. ROSSI, O.M. MAZINA, Y. CHI, R.L. MORITZ *et al*., 2018 RAD54 N-terminal domain is a DNA sensor that couples ATP hydrolysis with branch migration of Holliday junctions, Nature Communications 34 (9) 1-10.

GROTH, P., M.L. ORTA, I. ELVERS, M.M. MAJUMDER, A. LAGERQVIST *et al*., 2012 Homologous recombination repairs secondary replication induced DNA double-strand breaks after ionizing radiation, Nucleic Acids Research 40 (14) 6585–6594.

GUNES, S., M. AL-SADAAN, and A. AGARWAL, 2015 Spermatogenesis, DNA damage and DNA repair mechanisms in male infertility. Reproductive BioMedicine Online (31) 309-319.

GUPTA, R.C., E. FOLTA-STOGNIEW, S. O'MALLEY, M. TAKAHASHI and C.M. RADDING, 1999 Rapid exchange of A:T base pairs is essential for recognition of DNA homology by human Rad51 recombination protein, Molecular Cell 4 (5) 705–714.

HALAZONETIS, T.D., V.G. GORGOULIS and J. BARTEK, 2008 An oncogene-induced DNA damage model for cancer development, Science 319 (5868) 1352–1355.

HANDKIEWICZ-JUNAK, D., M. SWIERNIAK, D. RUSINEK, M. OCZKO-WOJCIECHOWSKA, G. DOM *et al*., 2016 Gene signature of the post-chernobyl papillary thyroid cancer, European Journal of Nuclear Medicine and Molecular Imaging 43 (7) 1267–1277.

HAUER, M.H. and S.M. GASSER, 2020 Chromatin and nucleosome dynamics in DNA damage and repair, Genes & Development (31) 2204-2221.

HELLEDAY, T., 2010 Homologous recombination in cancer development, treatment and development of drug resistance, Carcinogenesis 31 (6) 955–960.

HENSON, S.E., S.C. TSAI, C.S. MALONE, S.V. SOGHOMONIAN, Y. OUYANG *et al*., 2006 Pir51, a Rad51-interacting protein with high expression in aggressive lymphoma, controls mitomycin C sensitivity and prevents chromosomal breaks, Mutation Research 601 (1–2) 113–124.

HOLLAND, A.J., and D.W. CLEVELAND, 2012 Losing balance: the origin and impact of aneuploidy in cancer, EMBO Reports (13) 501-514.

HU, J., S.S. HWANG, M. LIESA, B. GAN, E. SAHIN *et al*., 2012 Antitelomerase therapy provokes ALT and mitochondrial adaptive mechanisms in cancer, Cell (148) 651-663.

HUNTER, N., 2006 Meiotic recombination. In: AGUILERA, A., R. ROTHSTEIN, editors. Molecular Genetics of Recombination. Heidelberg: Springer-Verlag. 381-442.

IWANAGA, R., H. KOMORI, S. ISHIDA, N. OKAMURA, K. NAKAYAMA *et al*., 2006 Identification of novel E2F1 target genes regulated in cell cycle- dependent and independent manners, Oncogene 25 (12) 1786–1798.

JACKSON, D.A. and A. POMBO, 1998 Replicon clusters are stable units of chromosome structure: evidence that nuclear organization contributes to the efficient activation and propagation of S phase in human cells, Journal of Cell Biology 140(6): 1285-1295.

JACKSON, S.P., and J. BARTEK, 2009 The DNA-damage response in human biology and disease, Nature (461) 1071-1078.

JAMSAI, D., A.E. O'CONNOR, L. O'DONNELL, J.C.Y. LO, and M.K. O'BRYAN, 2015 Uncoupling of transcription and translation of Fanconi anemia (FANC) complex proteins during spermatogenesis, Spermatogenesis (5) 1, e979061.

JASKELIOFF, M., S. VAN KOMEN, J.E. KREBS, P. SUNG and C.L. PETERSON Rad54p is a chromatin remodeling enzyme required for heteroduplex DNA joint formation with chromatin, Journal of Biological Chemistry (278) 9212-9218.

JOHNSON, N., Y. LI, Z.E. WALTON, K.A. CHENG, D. LI *et al*., 2012 Compromised CDK1 activity sensitizes BRCA-proficient cancers to PARP inhibition, Nature Medicine 17 (7) 875-882.

KAUFFMANN, A., F. ROSSELLI, V. LAZAR, V. WINNEPENNINCKX, A. MANSUET-LUPO *et al*., 2008 High expression of DNA repair pathways is associated with metastasis in melanoma patients, Oncogene 27 (5) 565–573.

KEE, Y. and A.D. D'ANDREA, 2010 Expanded roles of the Fanconi anemia pathway in preserving genomic stability, Genes & Development (16) 24, 1680-94.

KEENEY, S., C.N. GIROUX, and N. KLECKNER, 1997 Meiosis-specific DNA double-strand breaks are catalyzed by Spo11, a member of a widely conserved protein family. Cell (88) 375-384.

KIRSHNER, M., M. RATHAVS, A. NIZAN, J. ESSERS, R. KANAAR *et al*., 2009 Analysis of the relationships between ATM and the Rad54 paralogs involved in homologous recombination repair, DNA Repair (8) 253-261.

KOVALENKO, O.V., E.I. GOLUB, P. BRAY-WARD, D.C. WARD and C.M. RADDING, 1997 A novel nucleic acid-binding protein that interacts with human rad51 recombinase, Nucleic Acids Research 25 (24) 4946–4953.

KOVALENKO O.V., C. WIESE and D. SCHILD, 2006 RAD51AP2, a novel vertebrate- and meiotic-specific protein, shares a conserved RAD51-interacting C-terminal domain with RAD51AP1/PIR51, Nucleic Acids Research 34 (18) 5081–5092.

KREJCI, L., V. ALTMANNOVA, M. SPIREK, and X. ZHAO, 2012 Homologous recombination and its regulation, Nucleic Acids Research 40 (13) 5795-5818.

LAMB, N.E., S.L. SHERMAN, and T.J. HASSOLD, 2005 Effect of meiotic recombination on the production of aneuploid gametes in humans. Cytogenetetic and Genome Research (111) 250–255.

LAURINI, E., D. MARSON, A. FERMEGLIA, S. AULIC, M. FERMEGLIA *et al*., 2020 Role of Rad51 and DNA repair in cancer: a molecular perspective, Pharmacology & Therapeutics (208) 107492.

LE, K., H. GUO, Q. ZHANG, X. HUANG, M. XU *et al*., 2019 Gene and lncRNA co-expression network analysis reveals novel ceRNA network for triple-negative breast cancer, Scientific Reports (1) 15122.

LEDUC, F., V. MAQUENNEHAN, G.B. NKOMA, and G. BOISSONNEAULT, 2008a DNA damage response during chromatin remodeling in elongating spermatids of mice, Biology of Reproduction (78) 324-332.

LEDUC, F., G.B. NKOMA and G. BOISSONNEAULT, 2008b Spermiogenesis and DNA repair: a possible etiology of human infertility and genetic disorders, Systems Biology in Reproductive Medicine (54) 1, 3-10.

LEHRAIKI, A., M. CEREZO, F. ROUAUD, P. ABBE, M. ALLEGRA *et al*., 2015 Increased CD271 expression by the NF-kB pathway promotes melanoma cell survival and drives acquired resistance to BRAF inhibitor vemurafenib, Cell Discovery (1) 15030.

LI, S., Y. XUAN, B. GAO, X. SUN, S. MIAO *et al*., 2018 Identification of an eight-gene prognostic signature for lung adenocarcinoma, Cancer Management and Research (10) 3383-3392.

LIANG, F., S. LONGERICH, A.S. MILLER, C. TANG, O. BUZOVETSKY *et al*., 2016 Promotion of RAD51-mediated homologous DNA pairing by the RAD51AP1-UAF1 complex, Cell Reports 15 (10) 2118–2126.

LIANG, F. A.S. MILLER, S. LONGERICH, C. TANG, D. MARANON *et al*., 2019 DNA requirement in FANCD2 deubiquitination by USP1-UAF1-RAD51AP1 in the fanconi anemia DNA damage response, Nature Communications 10 (1) 2849.

LIANG, F. A.S. MILLER, C. TANG, D. MARANON, E.A. WILLIAMSON *et al*., 2020 The DNA-binding activity of USP1-associated factor 1 is required for efficient RAD51-mediated homologous DNA pairing and homology-directed DNA repair, Journal of Biological Chemistry Jbc.RA120.013714.

LIM, G., Y. CHANG and W. HUH, 2020 Phosphoregulation of Rad51/Rad52 by CDK1 functions as a molecular switch for cell cycle-specific activation of homologous recombination, Science Advances (6) eaay2669.

LONGERICH, S., J. LI, Y. XIONG, P. SUNG, and G.M. KUPFER, 2014 Stress and DNA repair biology of the Fanconi anemia pathway, Blood (18) 124, 2812-9.

LORD, C.J. and A. ASHWORTH, 2013 Mechanisms of resistance to therapies targeting BRCA-mutant cancers, Nature Medicine 19 (11) 1381–1388.

LORD, C.J. and A. ASHWORTH, 2017 PARP inhibitors: synthetic lethality in the clinic, Science 355 (6330) (2017) 1152–1158.

LOWARY, P.T. and J. WIDOM, 1998 New DNA sequence rules for high affinity binding to histone octamer and sequence-directed nucleosome positioning, Journal of Molecular Biology (276) 19-42.

LUGER, K., AW. MADER, R.K RICHMOND, D.F. SARGENT and T.J. RICHMOND, 1997 Crystal structure of the nucleosome core particle at 2.8 A resolution, Nature (389) 251-260.

MARCHETTI, F. and A.J. WYROBEK, 2005 Mechanisms and consequences of paternally-

transmitted chromosomal abnormalities, Birth Defects Research Part C Embryo Today (75) 112-129.

MARCHETTI, F. and A.J. WYROBEK, 2008 DNA repair decline during mouse spermiogenesis results in the accumulation of heritable DNA damage. DNA Repair (Amst) (7) 572-581.

MARTIN, R.W., B.J. ORELLI, M. YAMAZOE, A.J. MINN, S. TAKEDA *et al*., 2007 RAD51 up-regulation bypasses BRCA1 function and is a common feature of BRCA1-deficient breast tumors, Cancer Research 67 (20) 9658–9665.

MARTINEZ, I., J. WANG, K.F. HOBSON, R.L. FERRIS and S.A. KHAN, 2007 Identification of differentially expressed genes in HPV-positive and HPV-negative oropharyngeal squamous cell carcinomas, European Journal of Cancer 43 (2) 415–432.

MARTINEZ-PEREZ, E. and M.P. COLAIACOVO, 2009 Distribution of meiosis recombination events: talking to your neighbors, Current Opinion in Genetics & Development (2) 105-112.

MATHE, A., M. WONG-BROWN, B. MORTEN, J.F. FORBES, S.G. BRAYE *et al*., 2015 Novel genes associated with lymph node metastasis in triple negative breast cancer, Scientific Reports (5) 15832.

MATSUOKA, S., B.A. BALLIF, A. SMOGORZEWSKA, E.R. MCDONALD III, K.E. HUROV *et al*., 2007 ATM and ATR substrate analysis reveals extensive protein networks responsive to DNA damage, Science 316 (5828) 1160–1166.

MAZIN, A.V., A.A. ALEXEEV and S.C. KOWALCZYKOWSKI, 2003 A novel function of Rad54 protein – stabilization of the Rad51 nucleoprotein filament, Journal of Biological Chemistry, (278) 14029-14036.

MESSLAEN, S., A. LE BRAS, C. DUQUENNE, V. BARROCA, D. MOISON *et al*., 2013 Rad54 is required for the normal development of male and female germ cells and contributes to the maintenance of their genome integrity after genotoxic stress, Citation: Cell Death and Disease (4) e774.

MEYER-FICCA, M.L., J.D. LONCHAR, I. MOTOMASA, M.L. MEISTRICH, C.A. AUSTIN *et al*. 2011 Poly(ADP-Ribose) Polymerases PARP1 and PARP2 modulate topoisomerase II beta (TOP2B) function during chromatin condensation in mouse spermiogenesis, Biology of Reproduction (84) 900-909.

MILES, G.D., M. SEILER, L. RODRIGUEZ, G. RAJAGOPAL and G. BHANOT, 2012 Identifying microRNA/mRNA dysregulations in ovarian cancer, BMC Research Notes (5) 164.

MIZUTA, R., J.M. LASALLE, H.L. CHENG, A. SHINOHARA, H. OGAWA *et al*., 1997 RAB22 and

RAB163/mouse BRCA2: proteins that specifically interact with the RAD51 protein, Proceedings of the National Academy of Sciences of the United States of America 94 (13) 6927-6932.

MODESTI M., M. BUDZOWSKA, C. BALDEYRON, J.A. DEMMERS, R. GHIRLANDO *et al*., 2007 RAD51AP1 is a structure-specific DNA binding protein that stimulates joint molecule formation during RAD51-mediated homologous recombination, Molecular Cell 28 (3) 468–481.

MOYNAHAN, M.E., A.J. PIERCE and M. JASIN, 2001a BRCA2 is required for homology-directed repair of chromosomal breaks, Molecular Cell 7 (2) 263–272.

MOYNAHAN, M.E., T.Y. CUI and M. JASIN, 2001b Homology-directed dna repair: mitomycin-c resistance, and chromosome stability is restored with correction of a Brca1 mutation, Cancer Research 61 (12) 4842–4850.

MOYNAHAN M.E. and M. JASIN, 2010 Mitotic homologous recombination maintains genomic stability and suppresses tumorigenesis, Nature Reviews Molecular Cell Biology 11 (3) 196–207.

MULLER, A., E. BOITIER, T. HU, G.J. CARR, A.C. LE FEVRE *et al*., 2005 Laboratory variability does not preclude identification of biological functions impacted by hydroxyurea, Environmental and Molecular Mutagenesis 46 (4) 221–235.

NGUYEN, T.T.T., E.M. PARK, Y.S. LIM and S.B. HWANG, 2018 Nonstructural protein 5A impairs DNA damage repair: implications for hepatitis C virus-mediated hepatocarcinogenesis, Journal of Virology 92 (11) e00178-18.

NIJMAN, S.M., T.T. HUANG, A.M. DIRAC, T.R. BRUMMELKAMP, R.M. KERKHOVEN *et al*., 2005 The deubiquitinating enzyme USP1 regulates the Fanconi anemia pathway, Molecular Cell 17 (3) 331 –339.

OBAMA, K., S. SATOH, R. HAMAMOTO, Y. SAKAI, Y. NAKAMURA *et al*., 2008 Enhanced expression of RAD51 associating protein-1 is involved in the growth of intrahepatic cholangiocarcinoma cells, Clinical Cancer Research 14 (5) 1333–1339.

PAGE, S.L., and R.S. HAWLEY, 2003 Chromosome choreography: the meiotic ballet. Science (301) 785–789.

PARPLYS, A.C., K. KRATZ, M.C. SPEED, S.G. LEUNG, D. SCHILD *et al*., 2014 RAD51AP1-deficiency in vertebrate cells impairs DNA replication, DNA Repair (Amst.) 24 87–97.

PARPLYS, A.C., W. ZHAO, N. SHARMA, T. GROESSER, F. LIANG *et al*., 2015 NUCKS1 is a novel RAD51AP1 paralog important for homologous recombination and genome stability, Nucleic Acids Research 43 (20) 9817–9834.

PATHANIA, R., S. RAMACHANDRAN, G. MARIAPPAN, P. THAKUR, H. SHI *et al*., 2016 Combined inhibition of DNMT and HDAC blocks the tumorigenicity of cancer stem-like cells and attenuates mammary tumor growth, Cancer Research 76 (11) 3224–3235.

PEREZ-HERNANDEZ, M., A. ARIAS, D. MARTINEZ-GARCIA, R. PEREZ-TOMAS, R. QUESADA *et al*., 2019 Targeting autophagy for cancer treatment and tumor chemosensitization, Cancers 11 (10) 1599.

QIAO, H., J.K. CHEN, A. REYNOLDS, C. HOOG, M. PADDY *et al*. 2012 Interplay between synaptonemal complex, homologous recombination, and centromeres during mammalian meiosis, PLOS Genetics (8) 6, e1002790.

REDMER, T., I. WALZ, B. KLINGER, S. KHOUJA, Y. WELTE *et al*., 2017 The role of the cancer stem cell marker CD271 in DNA damage response and drug resistance of melanoma cells, Oncogenesis 6 (1) e291.

RICHARDON C., 2005 RAD51, genomic stability, and tumorigenesis, Cancer Letters 218 (2) 127–139.

RUSSO, A., E. CORDELLI, T. SALVITTI, E. PALUMBO and F. PACCHIEROTTI, 2018 Rad54/Rad54B deficiency is associated to increased chromosome breakage in mouse spermatocytes, Mutagenesis (33) 323-332.

SANKARANARAYANAN, P., T.E. SCHOMAY, K.A. AIELLO and O. ALTER, 2015 Tensor GSVD of patient- and platform-matched tumor and normal DNA copy-number profiles uncovers chromosome arm-wide patterns of tumor-exclusive platform-consistent alterations encoding for cell transformation and predicting ovarian cancer survival, PLOS One 10 (4) e0121396.

SARASIN, A., and A. KAUFFMANN, 2008 Overexpression of DNA repair genes is associated with metastasis: a new hypothesis, Mutation Research 659 (1–2) 49–55.

SCULLY, R., A. PANDAY, R. ELANGO and N.A. WILLIS, 2019 DNA double-strand break repair-pathway choice in somatic mammalian cells, Nature Reviews Molecular Cell Biology (20) 698-714.

SEEBER, A. M. HAUER and S.M. GASSER, 2013 Nucleosome remodelers in double-strand break repair. Current Opinion in Genetics & Development (23) 1-11.

SEKAR, R.B. and A. PERIASAMY, 2003 Fluorescence resonance energy transfer (FRET) microscopy imaging of live cell protein localizations, Journal of Cell Biology 160 (5) 629-633.

SHRIVASTAV, M., L.P. DE HARO and J.A. NICKOLOFF, 2008 Regulation of DNA double-strand break repair pathway choice, Cell Research 18 (1) 134–147.

SIMHADRI, S., S. PETERSON, D. PATEL, Y. HUO, H. CAI *et al*., 2014 Male fertility defect associated with disrupted BRCA1-PALB2 interaction in mice, Journal of Biological Chemistry (289) 24617-24629.

SONG, H., S.L. XIA, C. LIAO, Y.L. LI, Y.F. WANG, *et al*., 2004 Genes encoding Pir51, Beclin 1, RbAp48 and aldolase b are up or down-regulated in human primary hepatocellular carcinoma, World Journal of Gastroenterology 10 (4) 509–513.

SONG, H., F. WU, S. LI, Z. WANG, X. LIU *et al*., 2017 Microarray expression analysis of MYCN-amplified neuroblastoma cells after inhibition of CDK2, Neoplasma 64 (3) 351-357.

SONG, M., M.N. KUMARAN, M. GOUNDER, D.G. GIBBON, W. NIEVES-NEIRA *et al*., 2018 Phase I trial of selenium plus chemotherapy in gynecologic cancers, Gynecologic Oncology 150 (3) 478-486.

SORIA, G., S.E. POLO and G. ALMOUZNI, 2012 Primer, repair, restore: the active role of chromatin in the DNA damage response, Molecular Cell (46) 722-743.

SOWA, M.E., E.J. BENNETT, S.P. GYGI and J.W. HARPER, 2009 Defining the human deubiquitinating enzyme interaction landscape, Cell 138 (2) 389–403.

SUNG, P., L. KREJCI, S. VAN KOMEN and M.G. SEHORN, 2003 Rad51 recombinase and recombination mediators, Journal of Biological Chemistry 278 (44) 42729–42732.

THORSLUND, T., F. ESASHI and S.C. WEST, 2007 Interactions between human BRCA2 protein and the meiosis-specific recombinase DMC1, EMBO Journal 26 (12) 2915–2922.

TOWERS, C.G., D. WODETZKI and A. THORBURN, 2020 Autophagy and cancer: modulation of cell death pathways and cancer cell adaptations, Journal of Cell Biology 219 (1) e201909033.

TUBBS, A. and A. NUSSENZWEIG, 2017 Endogenous DNA damage as a source of genomic instability in cancer, Cell 168 (4) 644–656.

UEDA, J., A. HARADA, T. URAHAMA, Y. OHKAWA, H. KURUMIZAKA *et al.* 2017 Testis-specific histone variant H3t gene is essential for entry into spermatogenesis, Cell Reports (18) 593-600.

WAGNER, S.A., H. OEHLER, A. VOIGT, D. DALIC, A. FREIWALD *et al*., 2016 ATR inhibition rewires cellular signaling networks induced by replication stress, Proteomics 16 (3) 402–416.

WANG, H., B. ROSIDI, R. PERRAULT, M. WANG, L. ZHANG *et al*., 2005a DNA ligase III as a candidate component of backup pathways of nonhomologous end joining, Cancer Research (65) 4020-4030.

WANG, Q., Y. TAN, C. FANG, J. ZHOU, Y. WANG *et al*., 2019 Single-cell RNA-seq reveals RAD51AP1 as a potent mediator of EGFRvIII in human glioblastomas, Aging (18) 7707-7722.

WANG, Y., Q. YU, A.H. CHO, G. RONDEAU, J. WELSH *et al*., 2005b Survey of differentially methylated promoters in prostate cancer cell lines, Neoplasia 7 (8) 748–760.

WESOLY, J., S. AGARWAL, S. SIGURDSSON, W. BUSSEN, S. VAN KOMEN *et al*., 2006 Differential contributions of mammalian Rad54 paralogs to recombination, DNA damage repair, and meiosis, Molecular and Cellular Biology (26; 3) 976-989.

WIESE, C., E. DRAY, T. GROESSER, J. SAN FILLIPPO, I. SHI *et al*., 2007 Promotion of homologous recombination and genomic stability by RAD51AP1 via RAD51 recombinase enhancement, Molecular Cell 28 (3) 482–490.

WILTSHIRE, T.D., C.A. LOVEJOY, T. WANG, F. XIA, M.J. O'CONNOR *et al*., 2010 Sensitivity to poly(ADP-ribose) polymerase (PARP) inhibition identifies ubiquitin-specific peptidase 11 (USP11) as a regulator of DNA double- strand break repair, Journal of Biological Chemistry 285 (19) 14565–14571.

WU, Y., H. WANG, L. QIAO, X. JIN, H. DONG *et al*., 2019 Silencing of RAD51AP1 suppresses epithelial-mesenchymal transition and metastasis in non-small cell lung cancer, Thoracic Cancer 10 (9) 1748-1763.

XIA, B., Q. SHENG, K. NAKANISHI, A. OHASHI, J. WU *et al*., 2006 Control of BRCA2 cellular and clinical functions by a nuclear partner, PALB2, Molecular Cell 22 (6) 719–729.

XIE, S., X. JIANG, J. ZHANG, S. XIE, Y. HUA *et al*., 2019 Identification of significant gene and pathways involved in HBV-related hepatocellular carcinoma by bioinformatics analysis, PeerJ (7) e7408.

YANG, F., and P.J. WANG, 2009 The mammalian synaptonemal complex: a scaffold and beyond, Genome Dynamics (5) 69-80.

ZEMAN, M.K. and K.A. CIMPRICH, 2014 Causes and consequences of replication stress, Nature Cell Biology 16 (1) 2–9.

ZHANG, Z., H.Y. FAN, J.A. GOLDMAN and R.E. KINGSTON, 2007 Homology-driven chromatin remodeling by human RAD54, Nature Structural & Molecular Biology (14) 397-405.

ZHAO, W., S. VAITHIYALINGAM, J. SAN FILIPPO, D.G. MARANON, J. JIMENEZ-SAINZ *et al.*, 2015 Promotion of BRCA2-dependent homologous recombination by DSS1 via RPA targeting and DNA mimicry, Molecular Cell 59 (2) 176–187.

ZICKLER, D., 2006 From early homologue recognition to synaptonemal complex formation, Chromosoma (115) 158-174.

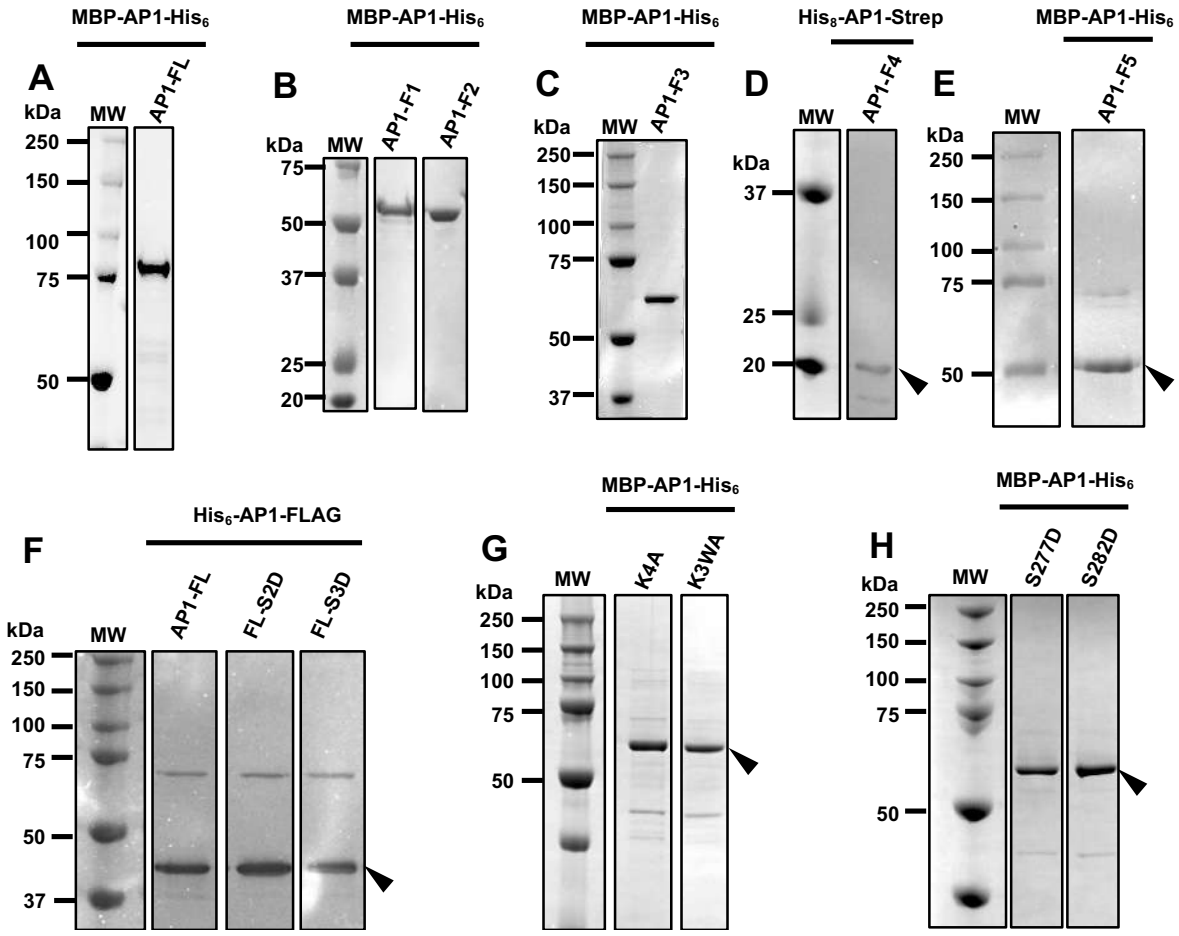

Figure S2.1 SDS-PAGE gels of purified human RAD51AP1 protein and RAD51AP1 fragments used in this study for EMSA, PD, and duplex capture assays

(A-C) MBP-RAD51AP1-His_6-tagged F.L., F1, F2, F3 (each loaded at 200 ng)

(D) His_8-RAD51AP1-Strep-tagged F4 (loaded 80 ng)

(E) MBP-RAD51AP1-His_6-tagged F5 (loaded 100 ng)

(F) His_6-RAD51AP1-FLAG-tagged F.L., F.L.-S2D, and F.L.-S3D (loaded 200 ng)

(G-H) MBP-RAD51AP1-His_6-tagged F3-K4A, F3-K3WA, F3-S277D, and F3-S282D (each loaded at 200 ng)

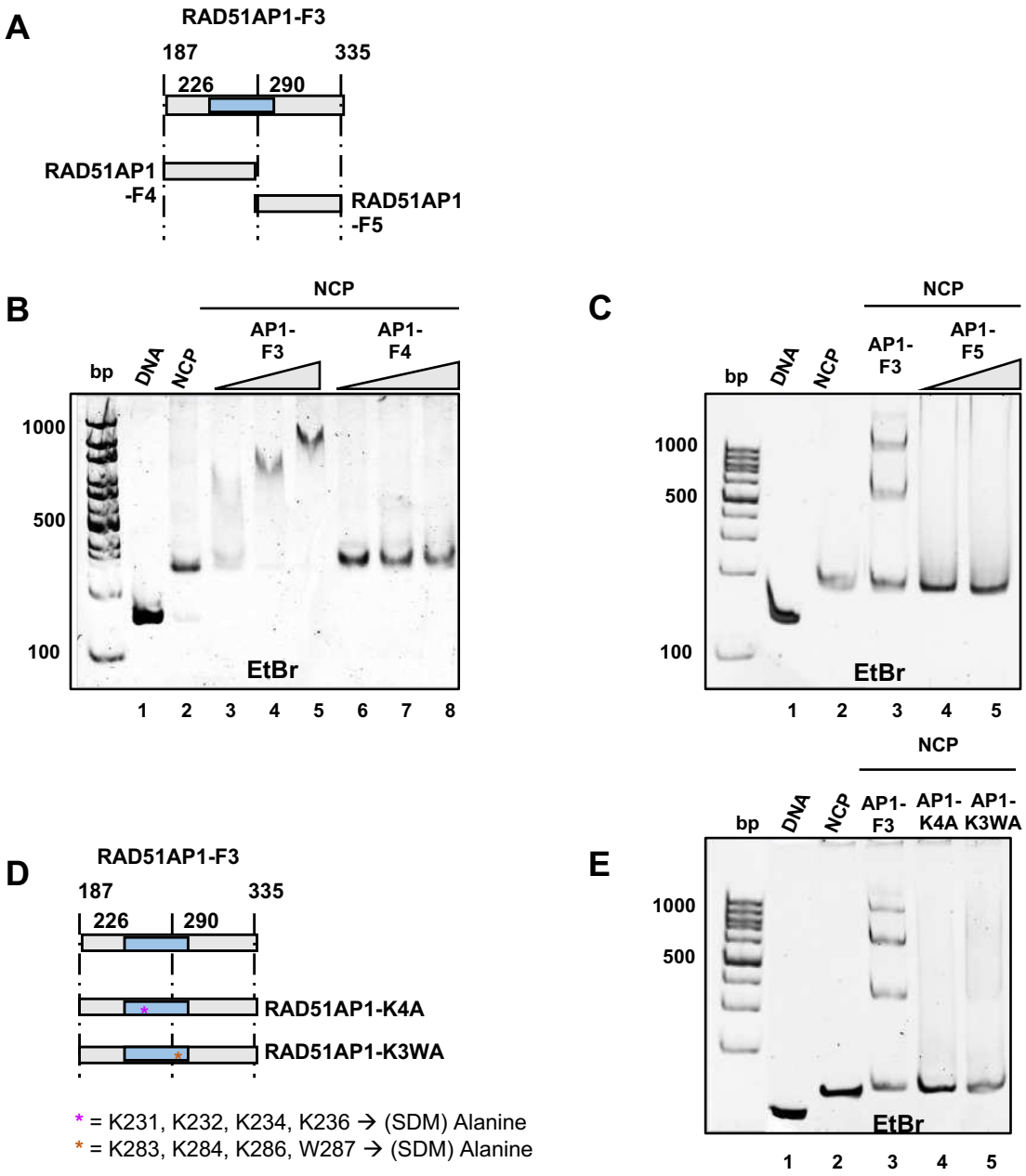

Figure S2.2 Analysis of RAD51AP1 DNA binding defective mutants for NCP binding

(A-C) Panel A is a schematic of RAD51AP1-F3, -F4, and -F5 fragments used. Panels B and C are EMSAs of these fragments after incubation with NCP. (D-E) Panel D is a schematic of RAD51AP1-F3 and mutant versions with crucial DNA-binding residues mutagenized. Panel E is EMSA of these mutants after incubation with NCP.

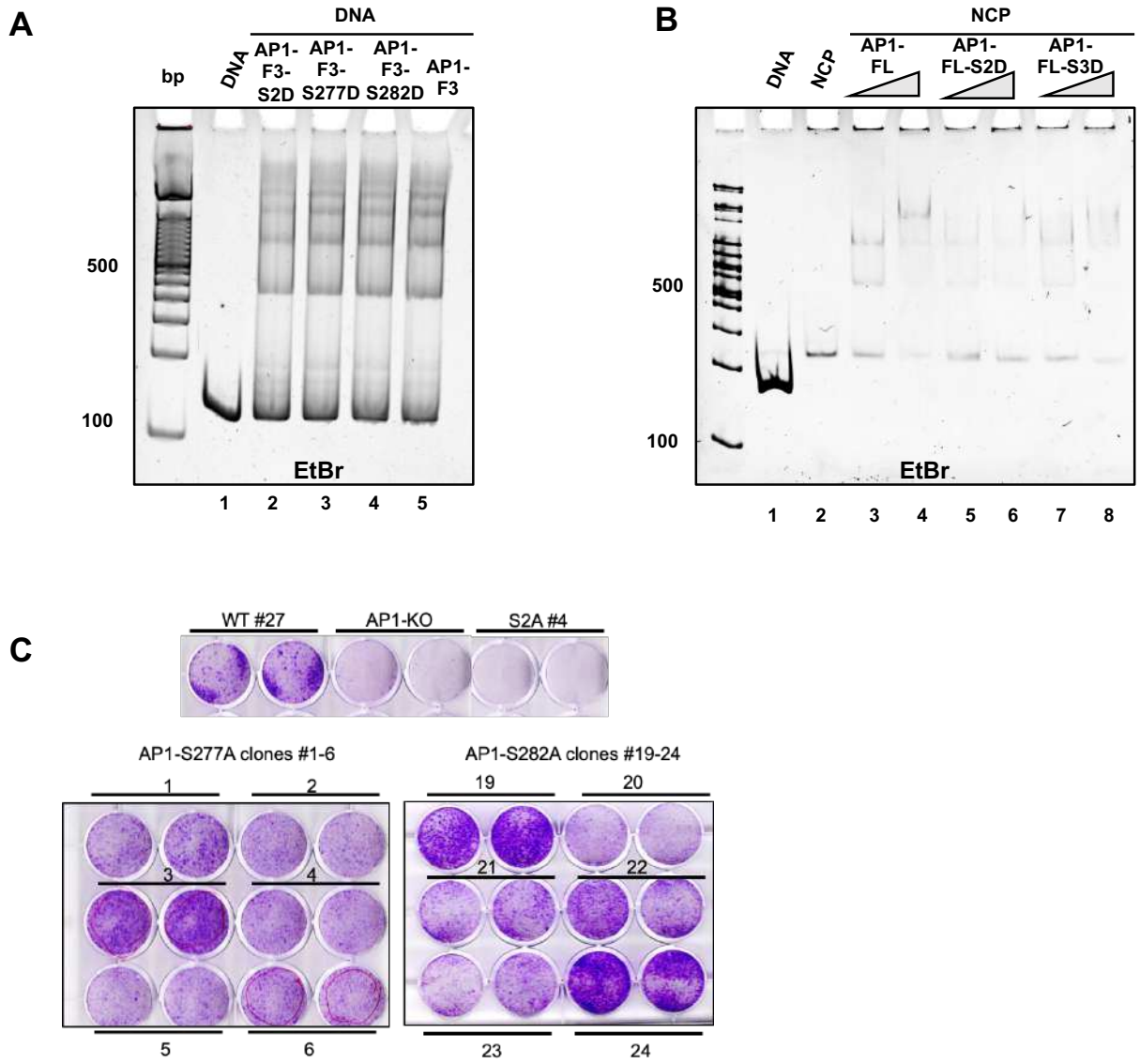

Figure S2.3 Characterization of RAD51AP1 S277 and S282 for DNA binding and cell survival

(A) EMSA of 147bp dsDNA mobility shifts after incubation with RAD51AP1 fragments: F3, F3-S2D, F3-S277D, and F3-S282D. (B) EMSA of NCP mobility shift after incubation with RAD51AP1 fragments: F3, F3-S2D, and F3-S3D. (C) Representative images of the results from colony formation assays after 30 uM MMC chronic treatment of RAD51AP1 KO cells (AP1-KO) and derivative cell lines expressing RAD51AP1-S277A or -S282A mutants or RAD51AP1 wild-type protein (WT #27). [Panel C data by Neelam Sharma]

A

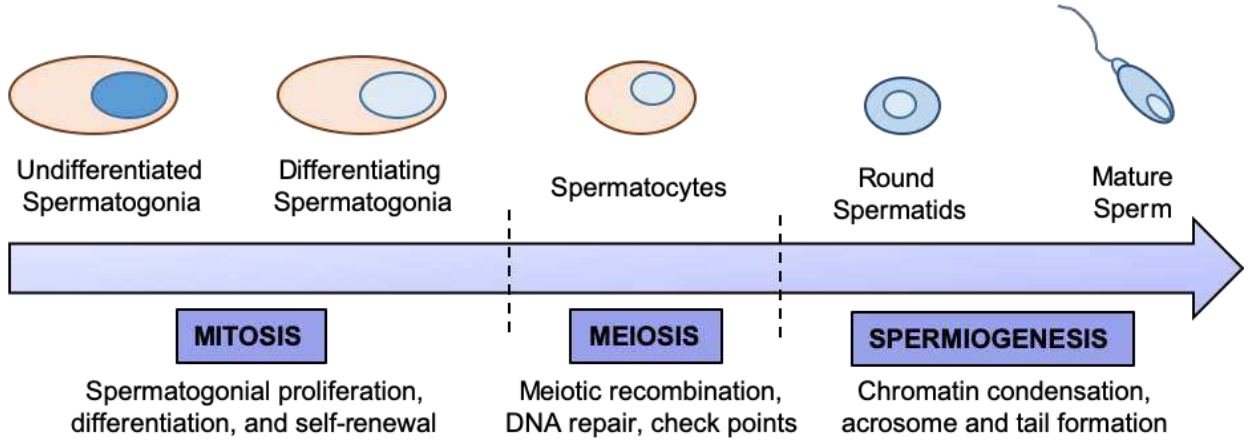

B

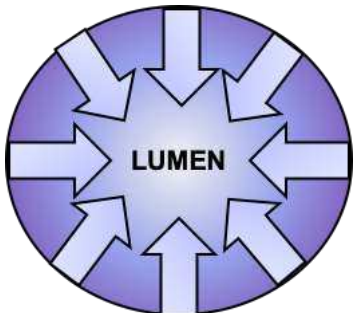

Figure S3.1 Schematic representation of the orderly maturation of germ cells during spermatogenesis (adapted from UEDA *et al.* 2017 and JAMSAI *et al*. 2015)

In panel A, a depiction of male germ cell differentiation (spermatogenesis) is shown. All pre-meiotic cells are called spermatogonia, which are stem cells that either regenerate or differentiate towards maturation. Germ cells are called spermatocytes, and these cells undergo meiosis and utilize HR during this stage. After meiosis, these haploid cells are referred to as spermatids. During spermiogenesis (the final stage of spermatogenesis), spermatids undergo morphologic changes into the mature product called spermatozoa. Panel B shows a simple depiction of a cross section of a seminiferous tubule. All stages of spermatogenesis as described in A occur in these tubules, and arrows dictate the directional progression of spermatogenesis. Mature spermatozoa are released into the lumen.

LIST OF PUBLICATIONS

I. Articles:

1. **Pires, E.**, Sung, P., Wiese, C. *Role of RAD51AP1 in DNA repair and carcinogenesis* (2017). DNA Repair. 51(1):e6822

II. Abstracts:

National:

1. **Elena Pires**, Neelam Sharma, Wilson Zhao, Patrick Sung, and Claudia Wiese. *Investigating the role of RAD51AP1 in homologous recombination repair*. 65th Radiation Research Society Annual Meeting. San Diego, CA. November 2019. (Poster).

2. **Elena Pires**, Neelam Sharma, Wilson Zhao, Patrick Sung, and Claudia Wiese. *Investigating the role of RAD51AP1 in homologous recombination repair*. American Association for Cancer Research Annual Meeting. Atlanta, GA. April 2019. (Poster).

3. **Elena Pires**. *Characterization of homologous recombination DNA repair in canine tumor cell lines*. Veterinary Cancer Society Mid-Year Meeting. Anchorage, AK. March 2018. (Oral).

4. **Elena Pires**, David Maranon, Douglas Thamm, and Claudia Wiese. *Characterization of homologous recombination DNA repair in canine tumor cell lines*. 63rd Radiation Research Society Annual Meeting. Cancún, Mexico. October 2017. (Poster).

5. **Elena Pires**, Neelam Sharma, David Maranon, and Claudia Wiese. *Investigating the function of RAD51AP1 in double-strand break repair*. 62nd Radiation Research Society Annual Meeting. Waikoloa, HI. October 2016. (Poster).

6. **Elena Pires**, Neelam Sharma, David Maranon, Douglas Thamm, and Claudia Wiese. *Insights into homologous recombination DNA repair in mammals*. NIH-Merial Symposium. Columbus, OH. July 2016. (Poster).

Local:

1. **Elena Pires**. *Investigating the role of RAD51AP1 in homologous recombination repair*. CVMBS Annual Research Day, Colorado State University. Fort Collins, CO. January 2020. (Oral).

2. **Elena Pires**, Neelam Sharma, Wilson Zhao, Patrick Sung, and Claudia Wiese. *Investigating the role of RAD51AP1 in homologous recombination repair*. CMB-MCIN-BMB Poster Symposium, Colorado State University. Fort Collins, CO. February 2019. (Poster).

3. **Elena Pires**, Neelam Sharma, Wilson Zhao, Patrick Sung, and Claudia Wiese. *Investigating the role of RAD51AP1 in homologous recombination repair*. CVMBS Annual Research Day, Colorado State University. Fort Collins, CO. January 2019. (Poster).

4. **Elena Pires**, Neelam Sharma, Wilson Zhao, Patrick Sung, and Claudia Wiese. *Investigating the role of RAD51AP1 in homologous recombination repair*. Graduate Student Showcase, Colorado State University. Fort Collins, CO. November 2018. (Poster).

5. **Elena Pires**, Neelam Sharma, David Maranon, Douglas Thamm, and Claudia Wiese. *Characterization of homologous recombination DNA repair in canine tumor cell lines*. CVMBS Annual Research Day, Colorado State University. Fort Collins, CO. January 2018. (Poster).

6. **Elena Pires**, Neelam Sharma, David Maranon, Douglas Thamm, and Claudia Wiese. *Investigating the function of RAD51AP1 in double-strand break repair*. CVMBS Annual Research Day, Colorado State University. Fort Collins, CO. January 2017. (Poster).